A. I. ALIKHANIAN NATIONAL SCIENTIFIC LABORATORY
YEREVAN PHYSICS INSTITUTE

Koryun Beglar Oganesyan

COMPARATIVE ANALYSIS OF FREE ELECTRON LASERS

A THESIS

submitted for the degree of Doctor of Physical-Mathematical Science in division 01.04.20 – "Physics of Charged Particle Beams and Accelerator Technics"

Yerevan – 2016

Contents

INTRODUCTION

In the middle of the 1970s John Madey [1] and colleagues constructed the first free electron laser operating in the infrared wavelength range.

JOURNAL OF APPLIED PHYSICS VOLUME 42, NUMBER 5 APRIL 1971

Stimulated Emission of Bremsstrahlung in a Periodic Magnetic Field

JOHN M. J. MADEY
Physics Department, Stanford University, Stanford, California 94305
(Received 20 February 1970; in final form 21 August 1970)

The Weizsäcker–Williams method is used to calculate the gain due to the induced emission of radiation into a single electromagnetic mode parallel to the motion of a relativistic electron through a periodic transverse dc magnetic field. Finite gain is available from the far-infrared through the visible region raising the possibility of continuously tunable amplifiers and oscillators at these frequencies with the further possibility of partially coherent radiation sources in the ultraviolet and x-ray regions to beyond 10 keV. Several numerical examples are considered.

Todd Smith, John Madey, Luis Elias and Dave Deacon

Since that time tremendous progress has been made in the FEL technique and free electron lasers now occupy an appropriate place among other sources of coherent radiation.

When the first operating free electron laser was constructed, it seemed that FELs would form only a small supplement to a long list of available at that time quantum laser. Actually, the appearance of FELs led to a new direction for sources of coherent radiation: they embodied the type of coherent source to which all experimenters have aspired since the invention of the laser. It is relevant to note that despite the FEL being referred to as a laser, the principle of its operation is similar to that of conventional vacuum-tube devices: it is based on the interaction of electron beams with radiation in vacuum. From this point of view FELs form a separate class of vacuum-tube devices capable of generating powerful coherent radiation at any wavelength from the millimeter to the X-ray part of the spectrum similar to the vacuumtube devices which generate coherent radiation at any wavelength, from the kilometer to the millimeter range. Also, free electron lasers possess all the attractive features of vacuum-tube devices. FEL radiation is always totally polarized and has ideal, i.e. diffraction, dispersion. FELs are capable of providing a high efficiency of transformation of the electron beam power into radiation power. Remembering that electron accelerators of driving beams for FELs can provide high average and peak power with an effective transformation of electric power into electron beam power, one can expect to reach a high level of total FEL efficiency and high peak and average output radiation power.

Despite strong competition from conventional lasers, the FEL is recognized nowadays as a unique tool for scientific applications requiring tunable coherent radiation from the far-infrared or VUV to X-ray ranges. Taking into account the future perspectives of the FEL, many industrial firms undertake intensive investigations into FEL technology, aiming at

constructing powerful UV FELs for industrial applications such as material processing, lithography, isotope separation, and chemical applications. Significant effort of scientists and enengineers working in the field of conventional quantum lasers are directed towards the construction of X-ray lasers.

Brawn Future X FELs

The last years have seen an exceptionally fast progress in the development of a novel photon source with unprecedented performance figures, the X-ray FEL.

A milestone of paramount importance for these developments was the first lasing of LCLS in self amplified stimulated emission mode (SASE) at 1.5 Å in 2009 [2], just three years ago. Before this it was not at all certain if the SASE operation mode can be achieved at such short wavelength. Now LCLS is a well established user facility with an exciting experimental program [3].

The importance of SASE stems from two key features. Firstly it allows FEL operation in single pass mode, i.e. without mirrors. Secondly the amplification process uses the shot noise of the electron beam as input, i.e. no external seeding source is required. These two features allow application of the SASE FEL mode over an extremely large wavelength range, spanning more than five orders of magnitude from infrared light to hard X rays. More important, SASE holds presently a monopoly for the production of intense laser radiation for the EUV to hard X-rays wavelength domain. An excellent overview of the theory of SASE and the theoretical, technical and experimental developments towards its realization can be found in [4]. The first implementation of SASE for a photon-science user facility is FLASH at DESY [5-6], an EUV/soft X-ray FEL.

In June 2011 the second hard X-ray FEL, SACLA, saw its first SASE photon beam with a wavelength of 1.2 Å [7]. SACLA uses technical solutions quite different from LCLS featuring C-band RF for the linac, in-vacuum undulators and a unique diode electron gun design with thermionic cathode. In particular the linac and undulator technology of SACLA allows for a total facility length as short as 800m, which is less than half the length of LCLS.

The biggest and most powerful amongst presently funded FEL projects is the European XFEL presently under construction [8]. Its 17 GeV superconducting linac will distribute ten times per second a train of 2200 electron bunches into three FEL lines and produce FEL radiation with wavelength as short as 0.5 Å. Future X-ray FELs are listed in [9].

SEEDING

Although SASE has paved the way for X-ray FELs and is the baseline mode of operation for most facilities in operation or under construction it has disadvantages inherent to the stochastic nature of the shot noise starting the FEL amplification process. Since different time slices of the electron pulse start the lasing process independently SASE FEL pulses consist of a number of radiation spikes with a time and spectral distribution which changes randomly from pulse to pulse. The duration of the spikes is of the order of the FEL cooperation length. As a consequence pulse energy and spectral shape fluctuates from pulse to pulse no matter how stable the initial electron beam is. Even though the transverse coherence of SASE FELs is very good, the longitudinal coherence is limited to the time of individual spikes. These inherent drawbacks of SASE can be overcome either by seeding the FEL process with a coherent external radiation source, i.e. a laser, or by "selfseeding" with a spectral filter introduced in the SASE gain process.

The initial step for seeding a short wavelength FEL by an external laser is the modulation of the electron beam energy by overlapping laser and electron beam inside an undulator magnet called modulator. For direct seeding at the nominal FEL wavelength the initial laser has to be equipped with a high harmonic generation (HHG) frequency conversion in a gas cell. In this case the modulator has the same period as the FEL modulators. Alternatively the electron beam is energy modulated at the wavelength of the laser in a long period modulator and the longitudinal micro-bunching is generated by an *R56* element downstream of the modulator. The harmonic content of the micro-bunching at the laser wavelength starts the FEL process at the nominal FEL wavelength in the undulators downstream of the *R56* element. This scheme is called High Gain Harmonic Generation (HGHG) process.

Free-Electron Lasers are powerful, tunable, coherent sources of radiation, which are used in scientific research, plasma heating, condensed matter physics, atomic, molecular and optical physics, biophysics, biochemistry, biomedicine etc. FELs today produce radiation ranging from millimeter wavelengths to ultraviolet and X rays, including parts of spectrum in which no other intense, tunable sources are available. This field of modern science is interesting from the point of view of fundamental research and very promising for further applications.

There are many alternative ways for FEL operation: Compton FEL, Cherenkov FEL, FEL with media with periodically modulated refractive indexes, Smith-Purcell FEL, Surface Plasmon FEL, FEL without inversion et al. We will review here some types of FEL.

An important direction in the development of free electron lasers is a search for methods that will permit construction of a small-size FEL operating at high frequencies. One of the ways to achieve this goal consists of using small-period periodic structures and, in particular, media with periodically modulated refractive indexes (MPMRI) [10-19]. Such media can be constructed by using a solid-state superlattice [10,11], a structure working in the construction material absorption edge frequency domain [12,13], periodically spaced foil strips [14,15], an ion-acoustic wave in a plasma [16], a gas-plasma medium with a periodically modulated degree of ionization [17], etc.

To be more specific, let us discuss briefly the problem of preparation of a gas-plasma medium. Such a medium can consist of a series of breakdowns in a gas produced, e .g, by a train of pulses of an external laser. Such a train can be focused by a mirror that is turned around an axis perpendicular to the laser beam direction of propagaion. Subsequent laser pulses are focused into spots equally separated from each other. As a result, a gas-plasma medium with periodically modulated degree of ionization is formed [17]. Some other possibilities to create a series of breakdowns in a gas consist of using a sinusoidal transparent diffraction grating as a focusing system or using a standing microwave in a waveguide filled with a gas, or employing a gas discharge formed by a net-shaped electrode.

An important direction in the development of free electron lasers is a search for methods that will permit construction of a small-size FEL operating at high frequencies. Creation of compact inexpensive sources of radiation operating effciently in visible, UV, or soft X-ray domains is one of the most important directions in the development and investigation of Free-

Electron Lasers. A short-wavelength radiation can be generated by a FEL using either a high-energy (multy-GeV) electron beam or a short period undulator. One of the ideas often mentioned and discussed in the proposal context is that of a FEL using (MPMRI). MPMRI can be considered as a kind of a volume diffraction grating. The following two types of MPMRI have been proposed: (1) a gas-plasma medium with periodically varied density or degree of ionization [10] and references therein and (2) a spatially periodical solid-state superlattice-like (SLL) structure, which can be composed, e.g., of a series of layers of different materials with different refractive indices [11] and references therein. The experimental feasibility of a transition radiation FEL was shown recently [12].

Smith-Purcell FEL

There is currently substantial interest in the development of THz sources for applications to biophysics, medical and industrial imaging, nanostructures, and materials science [20] (Mickan,Zhang). At the present time, available THz sources fall into three categories: gas lasers, solid-state devices, and electron-beam driven devices. Optically and electrically pumped molecular gas lasers provide hundreds of lines between 40 and 1000 μ m, but they are inherently not tunable. Solid-state THz sources include p-type germanium lasers, quantum-cascade lasers, and excitation of numerous materials with subpicosecond optical laser pulses. p-type Ge lasers can be continuously tunable from 1 to 4 THz, but require a large (1-T) external magnetic field, and must be operated at 20 K [21] (Brundermann, Chamberin, Haller). Electron-beam driven sources of THz radiation include backward-wave oscillators (BWOs), synchrotrons, and free-electron lasers (FELs). BWOs are commercially available, compact devices that operate from 30–1000 GHz

and produce milliwatts of average power [22](Pierce), [2, 23] (Dobroiu et al). Modern synchrotrons with short electron bunches, such as BESSY II in Berlin [24] (Abo-Bakr et al.) and the recirculating linac at Jefferson Laboratory [25] (Williams), produce broadband radiation out to about 1 THz with tens of watts of average power. Conventional FELs have also been operated in the THz region at several laboratories, with average power as high as hundreds of Watts [26-29] (Ramian; Vinokurov, et al.; Koike et al.; Jeong et al.). Coherently enhanced THz emission from relativistic electrons in an undulator has been observed at ENEA-Frascati [30] (Doria et al.). However, synchrotrons and conventional FELs require large facilities.

Another source of radiation in the THz region is Smith-Purcell (SP) radiation. The effect discovered in 1953 by Smith and Purcell [31] and called then by their names consists in emission of light by electrons moving above a grating. Later, after the advent of Free Electron Lasers (FEL), it was suggested to use the Smith-Purcell effect to create a new type of FEL – the Smith-Purcell Free Electron Laser (SP FEL). From the very beginning, SP FEL seemed to be very perspective to make a small-size FEL operate efficiently in visible and UV frequency regions. In several papers [32] SP FEL were investigated both theoretically and (to some extent) experimentally. Recently, there has been a renewed interest in the SP system related to both a possibility of using it to generate intense radiation from the millimeter to optical region [33] and to implement it in nondestructive beam diagnostics [34]. The experiments at Dartmouth College [35,36] have stimulated new investigations concerning the SP FEL [37] (experimental) and [38] (theoretical and particle-in-cell simulations).

Unfortunately, these papers altogether indicate a lack of common understanding even in such a basic problem as the main physical mechanisms of efficient amplification in SP FEL. One of the open questions is how high is the light frequency that can be expected to be produced by SP FEL? Another important problem is: do electrons in the SP FEL interact only with the surface grating or also with the whole bulk of the crystal whose surface has a grating? This problem emerges, in particular, from the results and calculations of [32] (Chang, McDaniel), in which the electron-crystal interaction is assumed to give rise to some quantum interference effects increasing drastically the SP FEL gain.

Surface Plasmon

Creation of compact inexpensive sources of radiation operating effciently in visible, UV, or soft X-ray domains is one of the most important directions in the development and investigation of Free-Electron Lasers.

A theory of stimulated radiation from relativistic electrons moving above a two dimensional lattice of microscopic bumps has been developed. It has been shown that the excitation of resonant electron-plasma oscillations inside the bumps leads to intense monochromatic UV, visible or IR radiation, A novel type of FEL, based on the interaction of electron beam with the two-dimensional lattice, has been discussed. As reported in refs. [39-41], a new kind of electromagnetic radiation may occur when a fast electron moves close to a surface on which microscopic roughnesses exist. The radiation is caused by the excitation of the collective resonance oscillations of electrons of the material inside the roughnesses. As pointed out in ref. [39], this kind of radiation was probably first observed in the UV region under the

bombardment of metal foils by electrons at grazing incidence. For FEL purposes a regular grid of identical microbumps may be used as a source of coherent radiation . On the other hand, the Smith-Purcell radiation from diffraction gratings is often considered from this point of view. The objectives of the present proposal are to discuss the relationship between the two kinds of electromagnetic radiation from electrons and to clearify the advantages which the radiation from local plasmons (RLP) may have.

Our calculations show that, the main difference between the RLP and the Smith-Purcell radiation lies in the resonance condition when the polarizability of the bumps may be increased by several decimal orders. It should be noted, however, that a linear diffraction grating with deep enough grooves may have resonance properties similar to the resonance properties of the isolated bumps, especially for the plasma oscillations perpendicular to the grooves.

The radiation from the local plasmons has an evident advantage over the familiar Smith-Purcell radiation due to the much higher intensity and the gain which may be achieved in FEL devices. However, the resonance conditions for the plasmons excitation may exist at definite frequencies dependent on the bump shape, the dimension (if the higher multipoles are excited) and the dielectric susceptibility of the material.

FELWI

Usually FEL [42,43] use the kinetic energy of relativistic electrons moving through a spatially modulated magnetic field (wiggler) to produce coherent radiation. The frequency of radiation is determined by the energy of electrons, the spatial period of magnetic field and the magnetic field

strength of the wiggler. This permits tuning a FEL in a wide range unlike atomic or molecular lasers. However for purposes of achievement of short-wavelength region of generation there are important possible limitations of the FEL gain.

The idea of inversionless FEL or FELWI (FEL without inversion) was formulated and discussed by one of the collaborators of this project M.O. Scully and coworkers [44-48] and continued [50-55]. In the usual FEL the gain is an anti-symmetric function of the detuning $\Delta = E - E_{res}$, where E and E_{res} are the electron energy and its resonance value in the undulator. The integral of such a gain over Δ (or E) is zero. By definition, in FELWI $\int G(E)dE \neq 0$ and mainly, G>0. Moreover, if in the usual FEL in the "hot-beam" regime (i.e., in the case of a broad electron energy distribution) the averaged gain is proportional to the squared inverse width of the distribution function, $(\delta E)^{-2}$, in FELWI $G(E) \propto (\delta E)^{-1}$. Hence, in the case of energetically wide beams the FELWI gain can exceed significantly the gain of the usual FEL. This advantage of FELWI (compared to usual FELs) makes such devices particularly interesting and potentially perspective in short-wave-length regions.

The conditions $\int G(E)dE \neq 0$ and G>0 imply that amplification of light can take place almost at any position of the resonance energy E_{res} with respect the energy $E = E_0$, at which the electron distribution function $f(E)$ is maximal. In FELWI amplification can take place both at positive and negative slopes of the function $f(E_{res})$, as well as its peak. This feature of FEWI is in a great contrast with that of FEL, where amplification can take place only at

the positive slope $f(E_{res})>0$. This last condition is easily interpreted as the condition of inversion: in FEL the number of electrons with $E>E_{res}$ must be larger than with $E<E_{res}$. In FELWI amplification can occur independently of the relation between E_{res} and $E=E_0$. This means that for amplification in FELWI it does not matter whether the number of particles with energy $E>E_{res}$ is larger than with energy $E<E_{res}$ or not. This explains an origin of the concept "without inversion" for the kind of FEL to be considered.

A concept of FELWI is related to that of Lasing Without Inversion (LWI) [49] in atomic systems – three-level systems or systems with autoionizing atomic levels. In both cases effects of amplification without inversion are explained by interference. But specific kinds of interference in FELWI and atomic systems are significantly different. In atomic systems amplification without inversion is attributed to interference of different channels of transitions between the same initial and final atomic states. In contrast, interference in FELWI has a purely classical character. A typical scheme of FELWI involves two wigglers and a dispersion zone between them. Field-induce corrections to classical electron trajectories acquired in the first and second wigglers interfere with each other. A proper construction of the dispersion zone can give rise to such a form of interference which provides the described above spectral features of the FELWI gain. So, the characteristic features of FELWI allow to distinguish it as a novel FEL mechanism which has fundamental as well as applied value.

The materials of this dissertation have been extensively discussed with experts in this area, and presented in several International scientifc centers

such as University of New Mexico (Albuquerque, NM, USA) , Texas A&M University (Colledge Station, TX, USA), Thomas Jefferson Lab (Newport News, VA, USA), University of North Texas (Denton, TX, USA), Brookhaven National Lab (New York, NY, USA) etc.

They are reported in Conferences, Workshops and Meetings, such as:

- Physics of Quantum Electronics , 2009; 2010
- Central European Workshop on Quantum Optics Belgrade 2009; Turku 2010
- International Laser Physics Workshops Trieste 2004; Kyoto 2005; Lousanne 2006; Trondheim 2008; Barcelona 2009; Sarajevo; Calgary 2012; Prague 2013; Sofia 2014; Shanghai 2015
- FEL New York 2013
- IPAC, New Orlean 2012; Shanghai 2012; Kyoto 2011;
- NAPAC , Pasadena, 2014
- SPIE & Photonics, San Diego 2014

These results also have been reported on YerPhI seminars.

This dissertation is based on 23 publications in journals (IEEE J. of Quant. Electr.[79], Appl.Phys. Lett.[116], ЖЭТФ(JHEP)[117], ЖТФ(ZhTP)[114,171], Квантовая Электроника (Sov.J.Quant.Electr.) [66], NIM A [165], Physica Scripta [55,166], Laser Physics [54], Laser Physics Lett. [164,167,169], J. of Modern Optics [126,161,162,168,157,170], Известия НАН Армении, Физика [163,172,173], J. of Physics, Conf. Series [174].

Single author publications are NIM A [165], Laser Phys. Lett. [167], J.of Modern Optics [161,162,170].

There are several scientic goals and aspects which were initiated these studies, and this dissertation.

We will defend in this dissertation:

1. Investigation of spectral intensity of a spontaneous emission and the gain of an external wave in the strophotron. The main resonance frequency is shown to depend on the initial conditions of the electron, and in particular on its initial transversal coordinate x_0. The spectral intensity of a spontaneous emission and the gain are averaged over x_0. The averaged spectral intensity is showh to have only a very weakly expressed resonance structure, whereas in the averaged gain, the resonance peaks are shown to be much higher than the nonresonant background. A physical nature of these resonances remaining after averaging is discussed. The maximum achieveable averaged gain and frequency of the strophotron FEL are estimated.

2. We propose and describe an FEL in which an electron beam interacts with a strong standing wave and the conditions are favorable for the channeling of electrons between constant-phase planes. We describe the equations of motion of electrons moving along the wiggler axis, the magnetic field in which is spacially inhomogeneous.

3. A relativistic electron motion in a transversally inhomogeneous magnetic field of a wiggler is shown to consist of fast (undulator) and slow (strophotron) components. By separating fast and slow motions and by averaging equations of motion over fast undulator oscillations, we find spectral intensity of strophotron spontaneous emission in such a system. The

strophotron intensity of spontaneous emission is shown to be well separated spectrally from the usual undulator parts.

4. A threshold condition for amplification without inversion in a free-electron laser without inversion (FELWI) is determined. This condition is found to be too severe for the effect to be observed in an earlier suggested scheme because a threshold intensity of the field to be amplified appears to be too high. This indicates that alternative schemes have to be found for making the creation of an FELWI realistic.

The interaction between noncolinear laser and relativistic electron beams in a static magnetic undulator has been studied within the framework of dispersion equations. For a free-electron laser without inversion (FELWI), the threshold parameters are found. The large-amplification regime should be used to bring an FELWI above the threshold laser power.

5. We have used the framework of the dispersion equation to study coherent Smith-Purcell (SP) radiation induced by a relativistic magnetized electron beam in the absence of a resonator. We have found that the dispersion equation describing the induced SP instability is a quadratic equation for frequency; and the zero-order approximation for solution of the equation, which gives the SP spectrum of frequency, corresponds to the mirror boundary case, when the electron beam propagates above plane metal surface (mirror). It was found that the conditions for both the Thompson and the Raman regimes of excitation do not depend on beam current and depend on the height of the beam above the grating surface. The growth rate of the instability in both cases is proportional to the square root of the electron beam current.

6. A possibility of channeling of low-energy relativistic positrons in some ionic crystals with axial symmetry with coaxial symmetry around separate crystal axes of negative ions in some types of crystals, is shown. The annihilation processes of positrons with medium electrons are investigated in details. The lifetime of a positron in the regime of channeling is estimated; the existence of long relaxation lifetime has been shown.

This dissertation consists of introduction, six chapters, summary and Bibliography. The format will be as follows:

Introduction. In Introduction the topical character of problem is justified and the preceding works on the subject are reviewed.

Chapter 1. Relativistic strophotron is a system in which fast electrons move along a potential "trough" produced hy quadrupole magnetic or electric lenses. Spectral intensity of a spontaneous emission and the gain of an external wave in the strophotron are given by a superposition of contributions from emission or amplification at different (odd) harmonics of the main resonance frequency $\omega_{res}(x_0)$. The main resonance frequency is shown to depend on the initial conditions of the electron, and in particular on its initial transversal coordinate x_0. This dependence $\omega_{res}(x_0)$ is shown to give rise to a very strong inhomogeneous broadening of the spectral lines. The broadening can become large enough for the spectral lines to overlap with each other. The spectral intensity of a spontaneous emission is averaged over x_0. The averaged spectral intensity is showh to have only a very weakly expressed resonance structure, whereas in the averaged gain,

the resonance peaks are shown to be much higher than the nonresonant background. A physical nature of these resonances remaining after averaging is discussed. The maximum achieveable averaged gain and frequency of the strophotron FEL are estimated.

Chapter 2. The gain of an external wave in the strophotron is given by a superposition of contributions from amplification at different (odd) harmonics of the main resonance frequency $\omega_{res}(x_0)$.The gain is averaged over x_0. In the averaged gain, the resonance peaks are shown to be much higher than the nonresonant background. A physical nature of these resonances remaining after averaging is discussed. The maximum achieveable averaged gain and frequency of the strophotron FEL are estimated.

The nonlinear and quantum mechanical theories of amplification in plane parabolic through are developed.

Chapter 3. A free-electron laser based on the channeling of a strong standing electromagnetic wave crossing a beam of weakly relativistic electrons is proposed and described. Allowance is made for the standing-wave-field spatial inhomogeneity governing the unusual spectral structure of the gain of a wave propagating parallel to the electron beam. Estimates indicate that the gain should be sufficient for the construction of a free-electron laser operating in the infrared range.

The spectral distribution of spontaneous emission and the gain for electrons moving in a plane wiggler (an undulator) with inhomogeneous

magnetic field are calculated. It is shown that electrons perform composite motion, consisted of a slow (strophotron) and fast (undulator) components. The equations of coupled motion of electrons is obtained by averaging the equations of undulator motion. It is shown that the allowance for the magnetic field inhomogeneity leads to an appearance of additional peaks both in the spectral distribution of spontaneous radiation and in the gain.

Chapter 4. The spatial amplification of a wave in a magnetostatic undulator with noncollinear electron and laser beams is studied in the framework of the dispersion relation for single-frequency and collective regimes. The dependence of the gain on the electron beam width is estimated with regard to the spatial boundedness of the beams. The laser power threshold at which the selection with respect to the transverse velocity is possible is obtained for a free-electron laser without inversion.

A threshold condition for amplification without inversion in a free-electron laser without inversion (FELWI) is determined. This condition is found to be too severe for the effect to be observed in an earlier suggested scheme because a threshold intensity of the field to be amplified appears to be too high. This indicates that alternative schemes have to be found for making the creation of an FELWI realistic.

Chapter 5. We have used the framework of the dispersion equation to study coherent Smith-Purcell (SP) radiation induced by a relativistic magnetized electron beam in the absence of a resonator. We have found that the

dispersion equation describing the induced SP instability is a quadratic equation for frequency; and the zero-order approximation for solution of the equation, which gives the SP spectrum of frequency, corresponds to the mirror boundary case, when the electron beam propagates above plane metal surface (mirror). It was found that the conditions for both the Thompson and the Raman regimes of excitation do not depend on beam current and depend on the height of the beam above the grating surface. The growth rate of the instability in both cases is proportional to the square root of the electron beam current.

Chapter 6. A possibility of channeling of low-energy relativistic positrons in some ionic crystals with axial symmetry with coaxial symmetry around separate crystal axes of negative ions in some types of crystals, is shown. The annihilation processes of positrons with medium electrons are investigated in details. The lifetime of a positron in the regime of channeling is estimated; the existence of long relaxation lifetime has been shown.

Chapter 1. Relativistic Strophotron

The Chapter based on 3 publications [79,171]

1.1. Overview

ORIGINALLY the name "strophotron" had been used [57,58] for a nonrelativistic device with electrons injected and oscillating along the x axis, the oscillations arising under the action of a constant electric field with a scalar potential Φ parabolically depending on x. The electron drift along the z axis has been providebdy the y component of the same electric field and by a constant homogeneous magnetic field $\mathbf{B} \perp Ox$.

In the relativistic strophotron [59], a relativistic electron beam is supposed to be injected at the (x,z) plane under some small angle $\alpha << 1$ to the z axis. As the motion along the z axis is the main motion of the electron beam itself in this case, there is no need in the *y* component of the electric field and in the magnetic field $\mathbf{B} \parallel Ox$. In accordance with [59], we will consider here a relativistic electron beam moving in the potential "trough" produced by electric or magnetic quadrupole lenses. The corresponding static potentials are supposed to depend parabolically on x and to be independent on *y* and z.

There were some publications earlier than [59] where the idea about quadrupole lenses was mentioned (see some references below). But probably the paper by Zaretsky and Nersesov [59] was the first one in which this idea was formulated explicitly as a suggestion of a new type of a FEL.

The paper [59] gives a correct description of ampiification at the main resonance frequency ores which itself **(as** well as the gain) is found correctly under the condition that the electron energy ***E*** is not too high (see below).

An attempt to describe amplification at higher harmonics in the paper [59] was unsuccessful. In the relativistic strophotron, there is a small but not negligible connection between the longitudinal and transversal electron motions. This connection was not taken into account carefully enough in the paper [59]. This is the reason why, for example, the paper [59] does not contain a description of amplification at higher harmonics in the most important case when the electromagnetic wave propagates along the *z* axis and its amplification is most efficient.

The resonance frequency of the strophotron ω_{res} has been found correctly for any ε by Bessonov [60] when he considered some features of a spontaneous emission of electrons channeling in a crystal. It should be mentioned in this context that the geometry of a static field described above corresponds to one. of the models which are often used [61,62] for a description of the electron channeling in crystals. For this reason, sometimes the strophotron is characterized by the term “macroscopic channeling.”

Sometimes [63], vice versa, a crystal with electrons channeling in it is called the “solid-state strophotron.” But, of course, there is a large difference between the strophotron and the crystal. The electron channeling in crystals is accompanied by many other processes such as dechanneling, bremsstrahlung, interaction with phonons, heating and damage of a crystal,

absorption of radiation in the volume of a crystal, etc. All of these processes require a careful analysis in a problem of channeling, but they have no analogy in the scheme with external fields (the strophotron). Besides, there is a very pronounced difference in the scales of dimensions and energies: if the diameter of a channel in a crystal is $d = 10^{-8} cm$ and the electron energy ε can vary from 2 MeV to *5* GeV [62], in the strophotron $d = 1 cm$ and $\varepsilon = 10 - 50 MeV$ (see the estimates below in Summary). This quantitative difference will be shown to give rise to a very appreciable qualitative difference in a physics of processes which can occur in these two schemes.

The resonance frequency ω_{res} found in the paper [60] depends on the initial condition of the electron: on the angle α and on the initial transversal electron coordinate x. This conclusion is confirmed by the derivation of the present paper. The dependence $\omega_{res}(x_0)$ will be shown to be very important for the strophotron FEL. Due to this dependence, there appears a very strong inhomogeneous broadening of the spectral lines of emission and amplification .

This broadening can become large enough for the spectral lines to overlap with each other. Under these conditions, averaging over x becomes very important and can essentially change the results. We will find both the spectral intensity of a spontaneous emission and the gain of an external wave averaged over x_0, i.e., over the distribution of electrons in the cross section of the beam. The averaged spectral intensity of a spontaneous emission will be shown to have only a very weakly expressed resonance structure with a dominating nonresonant background. The averaged gain

will be shown to have a more noticeable resonance structure exceeding the nonresonant background. The maximum achieveable averaged gain and frequency of the strophotron FEL will be estimated.

Sometimes [62] the strophotron emission is considered as analogous to the undulator emission, i.e., the emission from the system with a transversal magnetic field periodically depending on z. Sometimes [64] the strophotrons are not separated from the undulators at all, being called "the undulators of the second class." We will not use this name here. Of course, this is a purely terminological question. But the main idea permitting the joining of strophotrons and undulators [64] is based on a similarity of the solutions of corresponding equations. Such a similarity does exist for a single electron. A detailed comparison will be given in paragraph 1.2. But the above-mentioned strong dependence $\omega_{res}(x_0)$ exists only in the strophotron and does not exist in the undulator. For this reason, a very pronounced difference between the strophotron and the undulator emission can appear when the results are averaged over x_0, i.e., when one considers not a single electron, but the beam as a whole.

In the paper [65], the systems with quadrupole lenses have been criticized because of a possible instability in the y direction (in the plane geometry described above).

It is difficult to say now how important this difficulty is. We will not dwell upon this problem here. We hope to consider later the geometry with an axial symmetry in which we hope the problem of instability will be obviated,

but the main results of the present consideration will hold well, at any rate, qualitatively.

1.2. Classical Theory of Emission and Amplification at Higher Harmonics in the Relativistic Strophotron FEL

1.2.1. Electron Motion in Static Fields of The Strophotron

We will consider separately two possible realizations of the strophotron corresponding to the use of electric or magnetic quadrupole lenses.

A. Electric Field

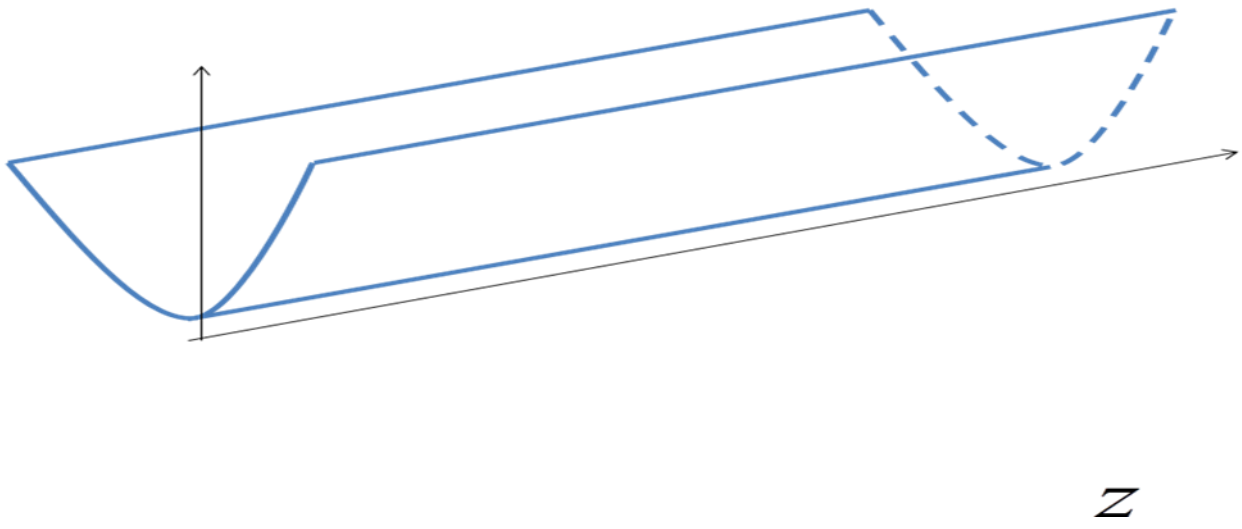

Fig.1. Model of plane parabolic through for FEL .

Let the scalar potential $\Phi(x)$ have the form $\Phi(x)=\Phi_0(x/d)^2$ where Φ_0 and $2d$ are the height and the width of the potential "trough." The equations of electron motion are

$$\frac{dp_x}{dt}=-\frac{2e\Phi_0}{d^2}x, \qquad \frac{dp_z}{dt}=0 \tag{1.2.1}$$

where $p_{x,z}$ are the components of the electron momentum along the x and z axes.

In accordance with the second equation (1.2.I), the longitudinal momentum and energy are conserved: $p_z=const$, $\varepsilon_z=\left(p_z^2+m^2\right)^{1/2}=const$ (we use the system of units in which $c = 1$). The first equation (1) can be transformed into an equation for the transversal coordinate:

$$\ddot{x}+x\Omega^2\left(1-\dot{x}^2\right)^{3/2}=0, \quad \Omega^2=\frac{2e\Phi_0}{\varepsilon_z d^2}. \tag{1.2.2}$$

If $|\dot{x}|<<1$, (1.2.1) for *x(t)* turns into the equation of a harmonic oscillator having the solution

$$x(t)=x_0\cos\Omega t+\frac{\dot{x}_0}{\Omega}\sin\Omega t \tag{1.2.3}$$

where x_0 and $\dot{x}_0\approx\alpha$ are the initial transversal coordinate and speed of the electron. The condition $|\dot{x}|<<1$ is satisfied if $|\alpha|<<1$ and $|x_0|\Omega<<1=2\pi|x_0|/\lambda_0<<1$ where $\lambda_0=2\pi c/\Omega$ is the spatial period (along the *z* axis) of transversal oscillations of the electron. These conditions and the solution (1.2.3) will be referred to later as the "harmonic approximation."

Although $p_z = const$, the longitudinal speed *u,* depends on time *t* because the total kinetic energy $\varepsilon_{kin} \neq const$. Under the condition $|\dot{x}| << 1$,

$$v_z \equiv \dot{z} = p_z / \varepsilon_{kin} \approx \frac{p_z}{\varepsilon_z}\left(1 - \frac{\dot{x}^2}{2}\right) \tag{1.2.4}$$

where

$$\begin{aligned} &\frac{p_z}{\varepsilon_z} = const = \frac{\dot{z}_0}{\left(1 - \dot{x}_0^2\right)^{1/2}}, \\ &\dot{z}_0 = v_0 \cos\alpha \approx 1 - \frac{1}{2\gamma^2} - \frac{\alpha^2}{2} \end{aligned} \tag{1.2.5}$$

where v_0 is the total initial electron speed, $\gamma = \varepsilon_0 / mc^2 >> 1$ is the relativistic factor, and ε_0 is the initial electron kinetic energy.

Under the condition $|\dot{x}| << 1$, the anharmonicity of (1.2.2) ($\propto \dot{x}^2$) is small and can be ignoreads responsible for small corrections only. On the other hand, the small correction to v_z (1.2.4), proportional to $\dot{x}^2$, may not be ignored because the coordinate *z* appears often in the combination *z* – *t* (see below) in which the main term of expansion (1.2.4) almost completely cancels. Equations (1.2.3) and (1.2.4) immediately yield

$$\begin{aligned} z(t) &= \dot{z}_0 \left\{ \left(1 + \frac{\alpha^2 + x_0^2\Omega^2}{4}\right) t + \frac{\alpha^2 + x_0^2\Omega^2}{8\Omega} \left[\sin(2\Omega t + \varphi_0) - \sin\varphi_0\right] \right\} \\ &\approx t + \left\{ -\left(\frac{1}{2\gamma^2} + \frac{\alpha^2 + x_0^2\Omega^2}{4}\right) t + \frac{\alpha^2 + x_0^2\Omega^2}{8\Omega} \left[\sin(2\Omega t + \varphi_0) - \sin\varphi_0\right] \right\} \end{aligned} \tag{1.2.6}$$

where φ_0 = constant.

$$\sin\varphi_0 = \frac{2x_0\Omega\alpha}{\alpha^2 + x_0^2\Omega^2}, \qquad \cos\varphi_0 = -\frac{\alpha^2 - x_0^2\Omega^2}{\alpha^2 + x_0^2\Omega^2}. \tag{1.2.7}$$

In the harmonic approximation (1.2.3), the amplitude of transversal oscillation of the electron is equal to $a=\left(x_0^2+\alpha^2/\Omega^2\right)^{1/2}$. Depending on the time transversal kinetic energy, $\varepsilon_{kin}(t)$ is given by

$$\varepsilon_{\perp kin}(t)\equiv\varepsilon-\varepsilon_z=\sqrt{\varepsilon_z^2+p_x^2}-\varepsilon_z\approx\frac{p_x^2}{2\varepsilon_z}\approx\varepsilon\frac{v_x^{\,2}}{2}. \tag{1.2.8}$$

In the static potential $\Phi(x)$, the electron also has the potential transversal energy

$$\varepsilon_{\perp pot}=e\Phi_0\frac{x^2}{d^2}=\varepsilon\frac{x^2\Omega^2}{2}. \tag{1.2.9}$$

In the harmonic approximation (1.2.3), the total transversal energy is conserved (as well as ε_z*):*

$$\varepsilon_{\perp pot}(t)\equiv\varepsilon_{\perp kin}-\varepsilon_{\perp pot}=\frac{\varepsilon}{2}\left(\alpha^2+x_0^2\Omega^2\right)=const. \tag{1.2.10}$$

All the solutions described above (1.2.3)-(1.2.10*)* are correct under the assumption about a suddenly switching-on interaction which is applicable if $\Delta t<<2\pi/\Omega$ where Δt is the switching-on time or the time it takes for the electron to traverse the transitional layer $\Delta L<<c/\Delta t$**.** The condition $\Delta t\Omega<<2\pi$ can be written as $\Delta L<<\lambda_0$. This inequality is satisfied if, e.g., $\Delta L=.2-3cm$ and $\lambda_0=.10cm$.

Under the assumption about a suddenly switching-on interaction, the electron's transversal energy jumps up at ***t*** = 0 to be increased by the term $\varepsilon\left(x_0^2\Omega^2/2\right)$. However, the total energy ε is conserved because at the same moment ***t*** = 0, the electron's longitudinal energy ε_z has a jump equal to

$\Delta\varepsilon_z = -\varepsilon\left(x_0^2\Omega^2/2\right)$. This last conclusion can be confirmed by an analysis of the equations of motion in the transitional layer where the scalar potential $\Phi(x,z)$ can be taken, e.g., in the form $\Phi(x,z) = \Phi_0\left(x^2 z/d^2\Delta L\right),\ 0 \le z \le \Delta L$. Writing down these equations explicitly and taking in them the limit $\Delta L \to 0$ one can check that the change of the momentum in this transitional layer is equal to $\Delta p_x = 0$ and $\Delta p_z = -\varepsilon\left(x_0^2\Omega^2/2\right)$ to confirm the formulated above conclusion about the jump in $\Delta\varepsilon$. Of course, $|\Delta\varepsilon_z| << \varepsilon$, and this jump almost does not change the angle α (its change is $=.\alpha x_0^2\Omega^2 << \alpha$).

B. Magnetic Field

Let the vector potential $\mathbf{A} \perp Oz$ be equal to $A_x = -A_0(x^2/d^2)$. The corresponding magnetic field $\mathbf{H} \| Oy$ is given by $H(x) = 2A_0 x/d^2$. The equations of motion of the electron have the form

$$\frac{dp_x}{dt} = -\frac{2eA_0}{d^2}xv_z, \qquad \frac{dp_z}{dt} = \frac{2eA_0}{d^2}xv_x. \tag{1.2.11}$$

In this case, the total energy of the electron is constant $\varepsilon = \sqrt{p_x^2 + p_y^2 + m^2} = const$. Equations (1.2.11) can be reduced to the form of equations for the coordinates x, z because $\mathbf{p} = \varepsilon\mathbf{v}$

$$\ddot{x} \equiv \dot{v}_x = -\frac{2eA_0}{\varepsilon d^2}x\dot{z}, \qquad \ddot{z} \equiv \dot{v}_z = \frac{2eA_0}{\varepsilon d^2}x\dot{x}. \tag{1.2.12}$$

The second equation (1.2.12) is immediately integrated to give

$$\dot{z} = \frac{eA_0}{\varepsilon d^2}\left(x^2 - x_0^2\right) + v_0\cos\alpha \equiv \frac{\Omega^2}{2}\left(x^2 - x_0^2\right) + v_0\cos\alpha \tag{1.2.13}$$

where $\Omega = \left(2e\Phi_0 / \varepsilon d^2\right)^{1/2}$

Substituting $\dot{z}$ (1.2.13) in the first equation (1.2.12), we find the nonlinear equation for x(t):

$$\ddot{x} + x\Omega^2\left(v_0\cos\alpha + \frac{1}{2}\Omega^2\left(x^2 - x_0^2\right)\right) = 0. \qquad (1.2.14)$$

Equation (1.2.14) differs from the corresponding equation (1.2.2) in the electric field. But in (1.2.14), again the anharmonicity is small if $\alpha << 1$, $|x_0|\Omega << 1$. In the harmonic approximation equation, (1.2.14) has the same solution (1.2.3) as (1.2.2). The longitudinal speed and coordinate can be easily found in the harmonic approximation from (1.2.3) and (1.2.13), and they can be shown to be given by the previous expression (1.2.6). Hence, although the equations of motion of the electron in the electric and magnetic fields (1.2. 1) and (1.2.1 1) do not coincide, their solutions in the harmonic approximation $\dot{x} << 1$ do coincide. This is the reason why both spontaneous and stimulated emission in the strophotron do not depend on the kind of the field (electric or magnetic) creating a potential “trough” for electrons.

Differing from the case of the electrostatic field in the magnetic strophotron, both longitudinal and transversal energies of the electron are continuous at the boundary, i.e., they have no jump at *t* = 0 even in the approximation of a suddenly switching-on interaction.

Inside the strophotron, the transversal energy is determined similarly to that given by (1.2.4):

$$\varepsilon_\perp(t) \equiv \varepsilon - \sqrt{m^2 + p_z^2} = \varepsilon - \sqrt{\varepsilon^2 - p_x^2} \approx \varepsilon\frac{v_x^2}{2} \neq \text{const}.$$

$\varepsilon_\perp$ depends on time ***t*** and $\varepsilon_\perp(t=0)=\varepsilon\alpha^2/2$. In the harmonic approximation, there is an integral of motion (additional to the total energy $\varepsilon_\perp$***)*** given by the sum

$$\varepsilon_{\perp eff}=\varepsilon_\perp+\varepsilon\frac{\Omega^2x^2}{2}=\frac{\varepsilon}{2}\left(\alpha^2+x_0^2\Omega^2\right)=const \qquad (1.2.15)$$

In a quantum-mechanical description [59,66] this sum plays the role of the effective transversal energy having the eigenvalues $l\hbar\Omega$ where ***l*** is an integer. This is the reason why for the sum (1.2.15), we use the notation $\varepsilon_{\perp eff}$ It is necessary to emphasize that $\varepsilon_{\perp eff}$ not the real transversal energy, and hence it is not surprising that $\varepsilon_{\perp eff}\neq\varepsilon_\perp(t=0)=\varepsilon\alpha^2/2$.

1.3. Quadrupole lenses scheme and equations of electron motion in strophotron static fields

Usually the concept FEL is associated with undulator the magnetic field of which is periodical function of longitudinal coordinate z. There exist other systems too allowing transverse oscillations of electrons, and consequently, there are other possibilities for creation FELs. In one of such system movement of electrons was considered in plane parabolic potential , i.e. in the field whose potential do not depend on one of the transverse coordinates (for example, y) and on the longitudinal z and has square dependence on the other transverse coordinate x. For the systems of this type sometimes the term strophotron is used.

Single quadrupole lens, as it was well known, does not satisfy the above mentioned conditions: his potential square depends on both transverse

coordinates x and y (near axis Oz), if dependence on x is potential through then the dependence on y is inverted through. So, in the direction Ox there is focusing and there are possible oscillations, and in the direction Oy movement is aperiodic and the beam decay occurs. This means, that for beam stability needed correction.

Here is described self consistent scheme of correction by use of additional quadrupole lenses providing electron beam stability and oscillation periodicity in both transverse coordinates.

A scheme is presented in Fig.2. Its base is long electrostatic or magnetic quadrupole lens focusing electrons in direction Ox and defocusing in direction Oy.

Let scalar potential $\phi(x,y)$ of long electrostatic quadrupole lens has a form $\phi = \frac{\phi_0}{d^2}\left(x^2 - y^2\right)$, where ϕ_0 and 2d height and width of potential through in direction Ox. The equations of electron motion in this through have a form

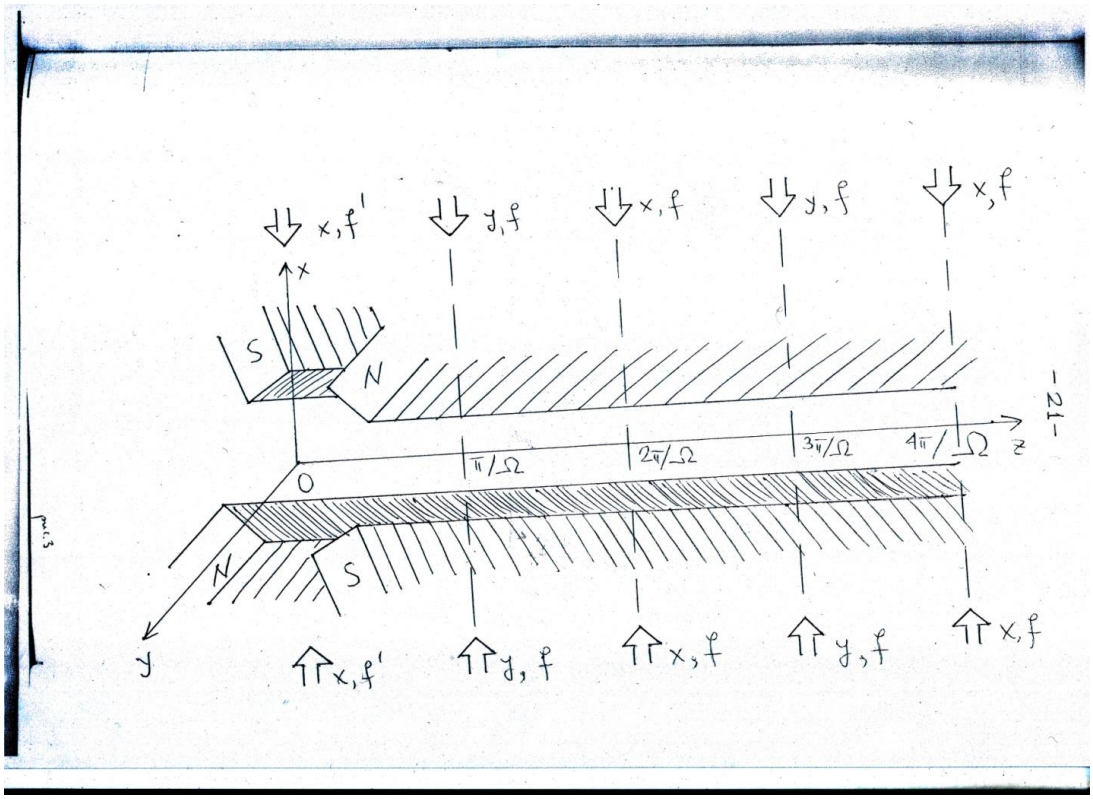

Fig. 2. Basic and corrective lenses layout.

$$\frac{dp_x}{dt} = -\frac{2e\phi_0}{d^2}x, \quad \frac{dp_y}{dt} = \frac{2e\phi_0}{d^2}y, \quad \frac{dp_z}{dt} = 0, \tag{1.3.1}$$

where $p_{x,y,z}$ are components of electron momentum along axes Ox,Oy, Oz.

According to third Eq. of (1.3.1) the longitudinal momentum and energy are conserved $p_z = const$, $\varepsilon_z = \left(p_z^2 + m^2\right)^{1/2} = const$ (here the system is used where c=1). Taking into account $\dot{p}_x = \dot{x}\left(\varepsilon_z^2 + p_z^2 + p_y^2\right)^{1/2}$, $\dot{p}_y = \dot{y}\left(\varepsilon_z^2 + p_z^2 + p_y^2\right)^{1/2}$ the second and third Eqs. Give

$$\ddot{x} + \Omega^2 x\left(1 - \dot{x}^2\right)^{3/2} = 0, \quad \Omega^2 = \frac{2e\phi_0}{d^2\varepsilon_z} \tag{1.3.2}$$

$$\ddot{y} - \Omega^2 x\left(1-\dot{y}^2\right)^{3/2} = 0. \qquad (1.3.3)$$

At $|\dot{x}| << 1$ Eq. (1.3.2) for x(t) turns to equation of harmonic oscillator having a solution

$$x(t) = x_0 \cos \Omega t + \frac{\dot{x}_0}{\Omega} \sin \Omega t, \qquad (1.3.4)$$

where x_0 and $\dot{x}_0 \approx \alpha$ initial coordinate and velocity along Ox axis, $\alpha = \sin\alpha = p_\perp / p$ electron entry angle in strophotron.

At $|\dot{y}| << 1$ Eq. (1.3.3) gives exponential growing solution

$$y(t) = y_0 \,\mathrm{ch}\, \Omega t + \frac{\dot{y}_0}{\Omega} \,\mathrm{sh}\, \Omega t, \qquad (1.3.5)$$

where now y_0 and $\dot{y}_0$ initial coordinate and velocity along Oy axis.

In the case of magnetic lens with vector potential $\mathbf{A} \| Oz$, $A_z = -\frac{A_0}{d^2}\left(x^2 - y^2\right)$ (the corresponding magnetic field $H_y = -\frac{2A_0}{d^2} y$, $H_x = \frac{2A_0}{d^2} x$) the equations of electron motion are

$$\frac{dp_x}{dt} = -\frac{2eA_0}{d^2} x v_z, \quad \frac{dp_y}{dt} = \frac{2eA_0}{d^2} y v_z, \quad \frac{dp_z}{dt} = \frac{2eA_0}{d^2}\left(x\dot{x} - y\dot{y}\right). \qquad (1.3.6)$$

In this case total energy of electron is conserved

$\varepsilon = \left(p_x^2 + p_y^2 + p_z^2 + m^2\right)^{1/2} = const$.

Equations (1.3.6) can be written as equations for x, y, z, because of $\mathbf{p} = \varepsilon \mathbf{v}$

$$\ddot{x} \equiv v_x = -\frac{2eA_0}{d^2 \varepsilon} x\dot{z}, \quad \ddot{y} \equiv v_y = \frac{2eA_0}{d^2 \varepsilon} y\dot{z}, \quad \ddot{z} \equiv v_z = \frac{2eA_0}{d^2 \varepsilon}(x\dot{x} - y\dot{y}). \qquad (1.3.7)$$

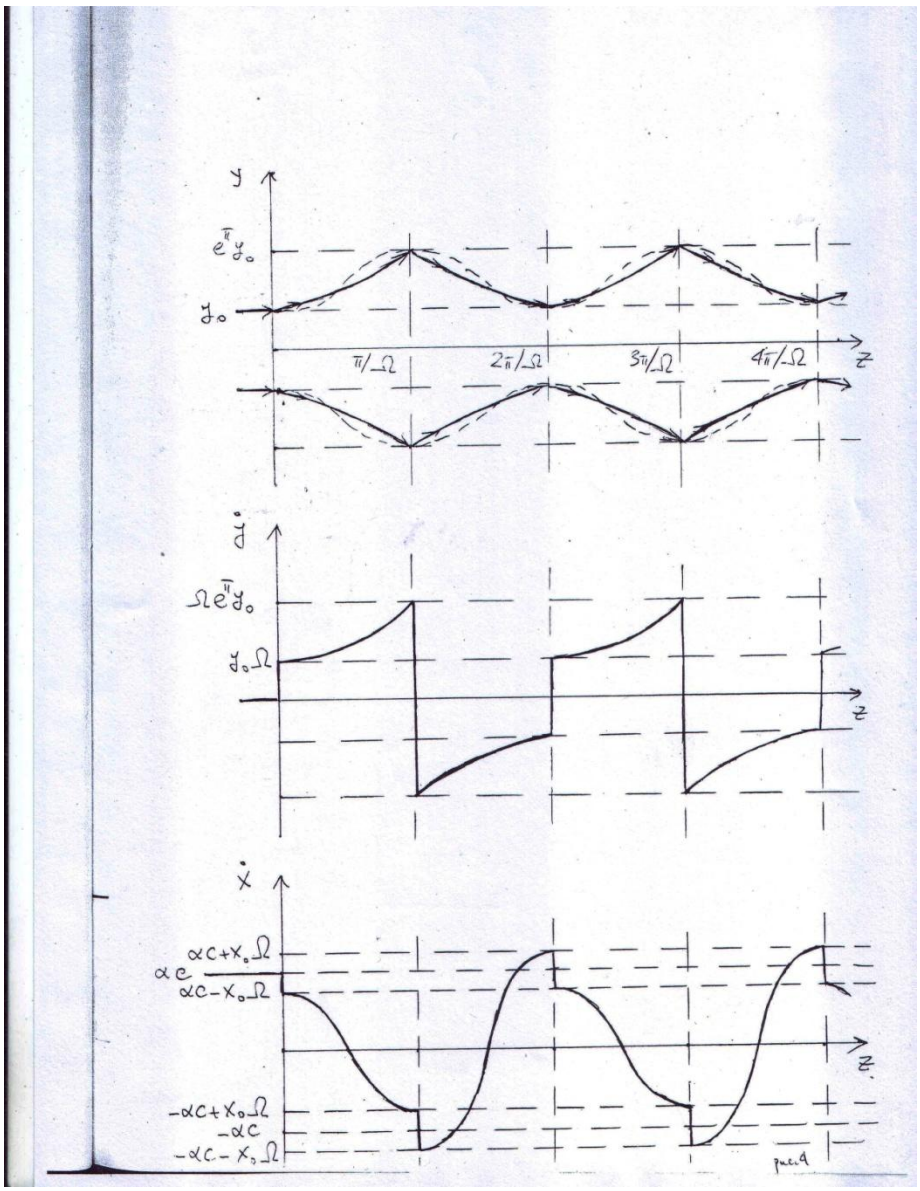

Fig.3. Electron trajectories in relativistic strophotron.

The third equation of (1.3.6) is <u>immediately</u> integrated giving

$$\dot{z} = \frac{eA_0}{d^2\varepsilon}\left\{\left(x^2 - x_0^2\right) - \left(y^2 - y_0^2\right)\right\} + v_0\cos\alpha$$

$$\equiv \frac{\Omega^2}{2}\left\{\left(x^2 - x_0^2\right) - \left(y^2 - y_0^2\right)\right\} + v_0\cos\alpha, \quad where \quad \Omega = \left(\frac{2eA_0}{\varepsilon d^2}\right)^{1/2}.$$

(1.3.8)

Putting $\dot{z}$ (1.3.8) into first and second equations of (1.3.7) we find nonlinear equations for x(t) and y(t)

$$\ddot{x}+\Omega^2 x\left[v_0\cos\alpha+\frac{1}{2}\Omega^2\left(x^2-x_0^2\right)-\frac{1}{2}\Omega^2\left(y^2-y_0^2\right)\right]=0 \qquad (1.3.9)$$

$$\ddot{y}-\Omega^2 y\left[v_0\cos\alpha+\frac{1}{2}\Omega^2\left(x^2-x_0^2\right)-\frac{1}{2}\Omega^2\left(y^2-y_0^2\right)\right]=0. \qquad (1.3.10)$$

Equations (1.3.9) and (1.3.10) differ from corresponding equations (1.3.2) and (1.3.3) for electric field. But as before in equations (1.3.9) and (1.3.10) small anharmonicity can be neglected if $|\alpha|\ll 1$, $|x_0|\Omega\ll 1$, $|y_0|\Omega\ll 1$. In the harmonic approximation equations (1.3.9), (1.3.10) have the same solutions (1.3.4) and (1.3.5). Those equations show that there is a focusing in Ox direction and there are possible electron oscillations, and there is defocusing in direction Oy and occurs beam decay of the beam. This means that for beam stabilization its correction is needed.

The well known hard focusing with crossed quadrupole lenses is used for beam stabilization. Arrows in the figure indicate the positions of corrective lenses along the Oz axis of the system at a distance π/Ω from each other. Indexes x and y show those transverse directions in which corresponding lens is focusing. The corrected lenses are assumed to be short, so that their length l is much less than focal length f. This assumption allows us to not analyze in detail the electron motion in the corrective lenses, describing their action instantaneous change in a component of the electron velocity on $\pm x_i f$, $\mp y_i f$, where x_i and y_i values of the transverse coordinate at the intersection of electron i-th corrected lens.

Focal lengths of all corrected lenses (except first) we accept to be

$$f=\frac{1}{2\Omega}=\frac{f'}{2}=\frac{f_0}{\pi}, \qquad (1.3.11)$$

where $f' = 2f$ is focal length of first lens located at the entrance (z=0), and f_0 is focal length of basic quadrupole lens $f_0 = \pi / 2\Omega << L$. This choice provides the electron motion periodicity on both transverse coordinates (see Fig.). Electron velocity in direction Oy , $\dot{y}$ changes his direction(sign) during every correction (Fig.3. a,b), electron velocity in direction Ox , $\dot{x}$ at the intersection of corrective lenses abruptly changed to $\pm 2x_0\Omega$, and $\pm x_0\Omega$ at intersection first lens (see Fig.3.). These abrupt changes in speed $\dot{x}$ are small in comparison with its initial value $\dot{x} \approx \alpha$ if the condition holds

$$\Omega \Delta x_0 << \alpha \qquad (1.3.12)$$

where Δx_0 is transverse size of the beam in the Ox direction corresponding to the electrons fly in the vicinity of the Oz axis and giving an effective contribution to the resonant radiation and equal $\frac{4}{\Omega}\sqrt{\frac{\lambda}{\pi L}}$, where L is system length, λ - radiation wavelength (see (2.2.2)).

If the necessity of correction and focusing of the beam in the Oy direction is evident, the need for focus adjustment in the Ox direction is associated with the requirements of periodicity of the oscillations and the absence of accumulated change of velocity $\dot{x}$.

Under condition (1.3.12) jumps of velocity $\dot{x}$ are small and do not essentially affect the nature of the oscillations x(t), Fourier expansion of which has a form

$$x(t) = x_0 \cos\Omega t + \frac{\alpha}{\Omega}\sin\Omega t - \frac{2x_0}{\pi}\left(1 - 2\sum_{k=1}^{\infty}\frac{1}{4k^2 - 1}\cos 2k\Omega t\right). \qquad (1.3.13)$$

Under the selected installation scheme of corrective lenses movement in a second transverse coordinate y is also periodic with the same period $2\pi/\Omega$ if $\dot{y}_0 = 0$. Condition $\dot{y}_0 \neq 0$ violates periodicity. During one period $2\pi/\Omega$, y increases on $\dot{y}_0/\Omega$. The deviation from the strict periodic motion in y means that for $\dot{y}_0 \neq 0$ is a certain degree of instability. This instability is small under condition

$$\frac{L}{\lambda}\frac{\dot{y}_0}{\Omega} = \frac{L\dot{y}_0}{2\pi} << d_{ey} \tag{1.3.14}$$

where L is the system length, $\lambda = 2\pi/\Omega$. The condition (1.3.14) means that the increase of y independence on $\dot{y}_0 \neq 0$ on the whole length L should be less than transverse dimension of the beam in the y direction d_{ey}.

With values L=300cm, d_{ey}=1cm the condition (1.3.14) gives

$$\dot{y}_0 << \frac{2\pi d_{ey}}{L} = 2\times 10^{-2} \tag{1.3.15}$$

The condition of used approximation has a form

$$e^{\pi} d_{ey} < D_y,\ 1/\Omega, \tag{1.3.16}$$

where D_y is a lens aperture in the Oy direction.

From the above it can be seen, that the movement of the electron beam in the system of quadrupole lenses of the type described has a two-dimensional character, and in each of them many harmonics of transverse oscillation frequencies are essential. The problems of investigation spontaneous and stimulated radiation in such a system on a higher harmonics of resonant frequency are very complicated. Therefore below the simplified

mathematical model will be considered – model of plane parabolic through. It will be shown that in this simplified model, there are a number of physical factors that were not previously taken into account, but are essential for the correct evaluation of the real possibilities of amplification in FEL, based on macroscopic channeling effect in the quadrupole lenses .

Note finally the stability of the motion of electrons in the system with a quadrupole lenses. A small deviation of the focal distance $\delta f << f$ does not lead to instability in the movement in the x direction. In the direction y it leads to increase of y coordinate, so that $\delta y_0 / y_0 = . N \frac{\delta f}{f}$, where y_0 is coordinate y at the entrance in system, δy_0 is increase on the system length, N- number of periods, and f is lens focal length. The condition of small deviation along y is $\delta y_0 / y_0 < 1$, which is equivalent to the requirement $\frac{\delta f}{f} < \frac{1}{N}$.

1.4. SPONTANEOUS EMISSIION OF THE STROPHOTRON

Using the solutions (1.2.3) and (1.2.6), we can find the spectral intensity of a spontaneous emission of the electron. The spectral intensity of emission in the most interesting case, along the *z* axis, is determined by the well-known formula [67]

$$\frac{d\mathrm{E}_{\omega}}{d\omega do}=\frac{e^2\omega^2}{4\pi^2}\left|\int_0^T dt\ \dot{x}e^{i\omega(t-z)}\right|^2 \tag{1.4.16}$$

where *do* is an infinitely small solid angle in the direction *0z,* and .T is the time it takes for the electron to traverse through the strophotrori.

Substituting x(t) (1.2.3) and z(t) (1.2.6) into (1.4.16) and expanding the periodical integrand in the Fourier series, we obtain

$$\frac{d\mathrm{E}_{\omega}}{d\omega do}=\frac{T^2e^2\omega^2}{16\pi^2}\left(\alpha^2+x_0^2\Omega^2\right)\sum_{s=0}^{\infty}\frac{\sin^2 u_s}{u_s^2}\left(J_s(\mathrm{Z})-J_s(\mathrm{Z})\right)^2 \tag{1.4.17}$$

where $J_{s,s+1}(\mathrm{Z})$ are the Bessel functions,

$$u_s=\frac{T}{4\gamma^2}\left[\omega\left(1+\frac{\gamma^2}{2}\left(\alpha^2+x_0^2\Omega^2\right)\right)-2\gamma^2\Omega(2\mathrm{s}+1)\right] \tag{1.4.18}$$

$$Z=\frac{\omega}{8\Omega}\left(\alpha^2+x_0^2\Omega^2\right). \tag{1.4.19}$$

Equation (1.4.17) describes the spectrum of emission consisting of a superposition of the spectral lines located at the odd harmonic $(2\mathrm{s}+1)\omega_{res}(\mathrm{s}=0,1,2,...)$ of the main resonance frequency

$$\omega_{res}=\frac{2\gamma^2\Omega}{1+\frac{\gamma^2}{2}\left(\alpha^2+x_0^2\Omega^2\right)}. \tag{1.4.20}$$

These lines are separated each from other by the term $2\omega_{res}$ and their width is found from the condition $u_s=1$ to be on the order of $2\omega_{res}/\Omega T$. If the number $N_0=\Omega T=(L/\lambda_0)$ of electron oscillations at thel ength of the

strophotron *L* **is** large erlough $N_0 >> 1$, the spectral lines in'(1.4.17) for a single electron do not overlap. A relative intensity of emission at the harmonics with a number (2s + 1) is determined by the factor $\left(J_s(\mathrm{Z}) - J_s(\mathrm{Z})\right)^2$. If $\alpha\gamma << 1$ and $|x_0|\Omega\gamma << 1$, $Z = (2\mathrm{s}+1)/4\gamma^2\left(\alpha^2 + x_0^2\Omega^2\right) << s$. In this case of rather small γ, α, and $|x_0|$, only the main frequency ω_{res} (1.4.20) is emitted with an appreciable intensity. Emission at higher harmonics s >> 1 becomes possible only when $\alpha\gamma >> 1$ or $|x_0|\Omega\gamma >> 1$. But, of course, in this case, the main resonance frequency ω_{res} (1.4.20) falls down.

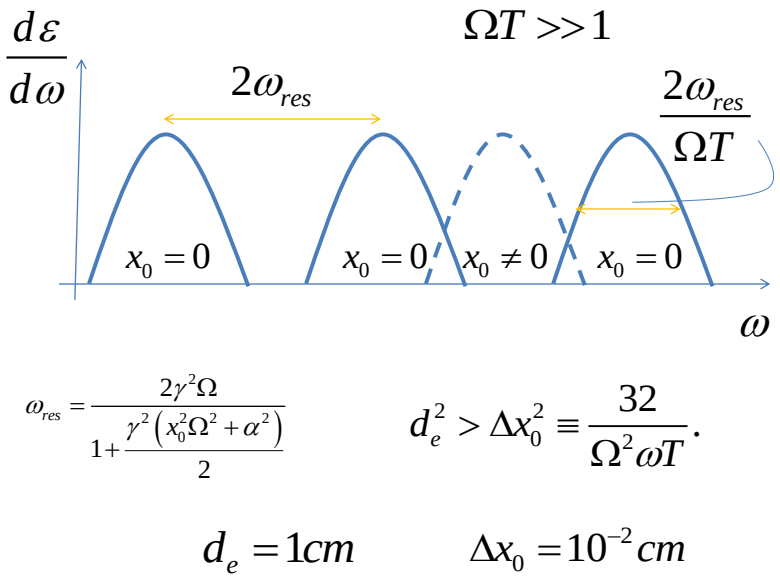

Рис.4. Зависимость спектрального распределения спонтанного излучения электронов в релятивистском строфотроне от частоты.

In accordance with the' remark made in the Introduction, the resonance frequency ω_{res} (1.4.20) has been obtained correctly in the paper [60] (see also [62]).

It is interesting to compare the results (1.4.17)-(1.4.20) to the corresponding results for the plane undulator [65,68]. These formulas can be reduced to the same form being expressed in terms of the "undulator parameter" $K_{und} = eB_0\lambda_0 / 2\pi mc^2$ (B_0 and λ_0. are the magnetic field strength and the period of the undulator) which, in the case of a strophotron, is replaced by $K_{str} = \alpha\left(\alpha^2 + x_0^2\Omega^2\right)^{1/2} = \lambda(\Omega a / c)$. Now (1.4.17)-(1.4.20) take the form

(1.4.21)

where $r_0 = e^2 / mc^2 2$ is the classical electron radius,

(1.4.22)

$$\omega_{res} = \frac{2\gamma^2\Omega}{1+\frac{1}{2}K^2}. \qquad (1.4.23)$$

and the argument of the Bessel function Z (1.4.19) calculated at $(2s+1)\omega_{res}$ is given by

$$Z = \frac{2s+1}{4}\frac{K^2}{1+\frac{1}{2}K^2}. \qquad (1.4.24)$$

Formally, these results completely coincide with the results of the papers [65,68]. Hence, for a single electron, the spectral intensity of a spontaneous emission can be reduced to the coinciding forms in the cases of the strophotron and of the plane undulator. But this coincidence will be shown to disappear when, instead of a single electron, one considers the electron beam as a whole. And the reason is in a different definition and

parametrical dependence of the *K* parameter in the undulator and in the strophotron.

1.5. AVERAGING OVER ELECTRON DISTRIBUTION

Although for a single electron, the spectral lines of emission (1.4.17) do not overlap as long as $\Omega T \gg 1$, they can overlap for different electrons, i.e., for different values of x_0. This possibility results from a strong dependence of ω_{res} (1.4.20) on x_0, which means that there is a strong inhomogeneous broadening of the spectral lines. To take this broadening into account, we must average (1.4.17) over x_0. This averaging will be ddone with the use of the Gaussian distribution function

$$f(x_0) = \frac{1}{\tilde{d}_e \sqrt{\pi}} e^{-x_0^2/\tilde{d}_e^2}, \tag{1.5.25}$$

where $\tilde{d}_e = d_e / 2\sqrt{\ln 2}$, d_e is t he diameter of the electron beam, $d_e < d$.

But first we will qualitatively estimate the conditions under which the inhomogeneous broadening exceeds the homogeneous width of the lines $2\omega_{res}/\Omega T$. Let, for example, the diameter d_e not be too large and $x_0 = x_0^{(s)}$, Then the shift of ω_{res}(1.4.20) which occurs when x_0 grows from 0 to $d_e/2$ is equal t $\delta\omega_{res} = (1/16) d_e^2 \Omega \omega_{res}^2$. The corresponding shift of the line $(2s+1)\omega_{res}$ is $\delta\omega_s (1/16) d_e^2 \Omega \omega_{res}$. The shift $\delta\omega_s$ is larger than the homogeneous width $2\omega_{res}/\Omega T$ if

$$d_e^2 > \Delta x_0^2 \equiv \frac{32}{\Omega^2 \omega T}. \tag{1.5.26}$$

If $d_e^2 > \Delta x_1^2 \equiv 32/\Omega\omega$, the shift $\delta\omega_s$ also exceeds the distance between' the adjacent lines $2\omega_{res}$ and the lines overlap. In the strophotron with external fields, the typical

values are: $d_e = 1cm$, $\Delta x_0 = 10^{-2} cm$, $\Delta x_1 = 3\times 10^{-2} cm$ (see the Conclusion), and $d_e >> \Delta x_0, \Delta x_1$ i.e., there is a strong inhomogeneous broadening and the lines overlap.

In the process of channeling in crystal, this effect can be less important because of a very small *d* ($d = 10^{-8} cm$), e.g., for $\gamma = 10^3$ and $\omega = 2\gamma^2\Omega$, $\Omega = 10^{14} s^{-1}$ and A $\Delta x_1 = 3\times 10^{-7} cm > d_e$. Broadening of spectral lines can be connected in this case with anharmonicity, but this effect is different from that resulting from the dependence $2\omega_{res}$ in (1.4.20). At lower energy, ε=10-50 MeV, there is an even more pronounced difference between real and "macroscopic" channeling. For such energies, the number of levels in the potential pit ($e\Phi_0/\hbar\Omega$) in the case of a crystal is rather small ($\leq$10 [62]). Hence, the anharmonicity is rather strong, and transitions between the levels can have an essentially quantum mechanical nature.

Vice versa, in the strophotron, the number of levels can be extremely large (up to 10^{12}). In this case, the anharmonicity is very weak and well applicable.

Averaging (1.4.17) under the condition (1.5.26), we can replace the factor $\sin^2 u_s / u_s^2$ by δu_s (some exclusions will be indicated below). From the condition $u_s = 0$, we find

$$\left(x_0^{(s)}\right)^2 = \frac{4}{\Omega\omega}(2s+1) - \frac{\alpha^2}{\Omega^2} - \frac{2}{\gamma^2\Omega^2} \equiv \frac{8}{\Omega\omega}\left(s - s_{\min}\right) \geq 0 \qquad (1.5.27)$$

where

$$s_{\min} = \frac{\alpha^2 \omega}{8\Omega} + \frac{\omega}{4\gamma^2\Omega^2} - \frac{1}{2}. \tag{1.5.28}$$

The argument of the Bessel functions Z (1.4.19) is now equal to

$$Z\left(x_0 = x_0^{(s)}\right) \equiv Z_s = s + \frac{1}{2} - \frac{\omega}{4\gamma^2\Omega^2}. \tag{1.5.29}$$

To simplify the formulas, we will use the following assumptions

$$\alpha\gamma >> 1, \quad \omega >> 2\gamma^2\Omega \tag{1.5.30}$$

from which it follows, in particular, that $s_{\min} >> 1$. Under these conditions, $Z_s < s$ (1.5.29) and both the index **s** of the Bessel function and its argument Z_s are large $Z_s, s >> 1$. Hence, the Bessel functions may be approximated by the McDonald functions [102]

$$J_s(Z_s) - J_{s+1}(Z_s) \approx \frac{2(s - Z_s)}{\pi\sqrt{3}\, s} K_{2/3}\left[\frac{2(s - Z_s)^{3/2}}{3\sqrt{s}}\right] \approx \frac{\omega K_{2/3}\left[\frac{\omega}{\omega_{\max}}\sqrt{\frac{s_{\min}}{s}}\right]}{2\gamma^2\Omega\pi\sqrt{3}} \tag{1.5.31}$$

Where

$$\omega_{\max} = 3\gamma^3\alpha\,\Omega \tag{1.5.32}$$

A similar approximation also has been used in the theory of a spontaneous emission in the plane undulator [68]. Now the averaged spectral intensity takes the form

$$\frac{\overline{d\mathrm{E}_\omega}}{d\omega do} = \frac{e^2 T \omega^{5/2}}{2\sqrt{2}\, 3\pi^{3/2}\tilde{d}_e \Omega^{5/2}\gamma^4} \sum_{s - s_{\min} \geq 1}^{\infty} \frac{s - s_{\min} + \frac{\alpha^2\omega}{8\Omega}}{s^2\sqrt{s - s_{\min}}} \times K_{2/3}\left[\frac{\omega}{\omega_{\max}}\sqrt{\frac{s_{\min}}{s}}\right] \exp\left[-\frac{8(s - s_{\min})}{\Omega\omega\tilde{d}_e^2}\right]. \tag{1.5.33}$$

If $\omega \sim \omega_{\max}$ the McDonald function $K_{2/3}(u)$ may be approximated by

$$K_{2/3}(u) \approx \frac{\Gamma(2/3)}{2^{1/3}u^{2/3}}, \quad |u| << 1 \text{ (34)} \tag{1.5.34}$$

to give

$$\frac{\overline{d\mathrm{E}}\omega}{d\omega do}=\frac{3^{1/3}\Gamma^2\left(\frac{2}{3}\right)e^2T\left(\frac{\omega}{\Omega}\right)^{1/2}}{2^{1/6}\,\pi^{7/2}\tilde{d}_e}$$
$$\times\sum_{s-s_{\min}\geq 1}^{\infty}\frac{s-s_{\min}+\frac{\alpha^2\omega}{8\Omega}}{s^{4/3}\sqrt{s-s_{\min}}}\exp\left[-\frac{8\left(s-s_{\min}\right)}{\Omega\omega\tilde{d}_e^2}\right]. \qquad (1.5.35)$$

All the terms of this series are well defined if $s_{\min}$ is not close to an integer. In this case, the sum over s (1.5.35) may be replaced by the integral over the new variable $x=\left(8/\Omega\omega\tilde{d}_e^2\right)(s-s_{\min})$ to yield

$$\frac{\overline{d\mathrm{E}}\omega}{d\omega do}=\frac{3^{1/3}\Gamma^2\left(\frac{2}{3}\right)e^2T\omega^{2/3}}{2^{2/3}\,\pi^{7/2}\alpha^{2/3}}$$
$$\times\int_0^{\infty}dx\,e^{-x}\frac{\frac{1}{\sqrt{x}}+\frac{\Omega^2\tilde{d}_e^2}{\alpha^2}\sqrt{x}}{\left(1+\frac{\Omega^2\tilde{d}_e^2}{\alpha^2}x^2\right)^{4/3}}. \qquad (1.5.36)$$

Rigorously, the lower limit of this integral is not zero $x_{\min}=\left(\Delta x_0/\tilde{d}_e\right)^2<<1$ (what corresponds to the condition $s-s_{\min}\geq 1$**)**. But approximately $x_{\min}$ may be replaced by 0. It gives an error $=\sqrt{x_{\min}}<<1$ because the integrand of (1.2.36) only has a root singularity at the point x = 0 which is easily integrated.

Equation (1.5.31) describes the nonresonant background of a spontaneous emission of the electron beam in the strophotron. When $s_{\min}$ is not close to an integer, the resonance structure of a spontaneous emission is completely smoothed out after averaging over x_0.

As a function of ω, the spectral intensity (1.5.36) grows $\omega^{2/3}$ as long as $\omega<\omega_{\max}$ When $\omega>\omega_{\max}$ the M CDonald function $K_{2/3}(u)$ in (1.5.33) becomes exponentially small for s not too far from $s_{\min}$ This behavior of $K_{2/3}(u)$ cuts

the sum over s from the region of small s by a condition stronger than $s > s_{\min}$ Hence, in the integral over *x* (1.5.36), the lower limit does not become small, $\tilde{x}_{\min} = \left(\alpha / \tilde{d}_e \Omega\right)\left(\omega / \omega_{\max}\right)^2$.

If $\alpha >> \tilde{d}_e \Omega$ the integral (1.5.36) itself becomes exponentially small. Thus, $\omega_{\max}$ (1.5.32) is the frequency at which the spectral intensity $\left(\overline{d\mathrm{E}}\omega / d\omega do\right)_{n.r.}$, has its maximum which, for $\alpha = \tilde{d}_e \Omega$, is on the order of

$$\left[\left(\frac{\overline{d\mathrm{E}}\omega}{d\omega do}\right)_{n.r.}\right]_{\max} = .e^2 \Omega T \gamma^2. \qquad (1.5.37)$$

Now let $s_{\min}$ be close to some integer $|s_{\min} - N| << 11$ where $N = [s_{\min}]$ or $N = [s_{\min}] + 1$; [u] denotes the integer closest to u but less than u. In this case, the term with s = N in the sum (1.5.33) becomes anomalously large and tends to infinity when $s_{\min} \to N$. This result indicates now that the factor $\sin^2 u_s / u_s^2$ in (1.4.17) may not be replaced by δu_s because it has a singularity stronger than the δ function. This is the reason why the term with s = N can have a resonance character even after averaging over x_0. Taking separately only the resonance term s = N in the sum (1.4.17), we can average this term over x_0 directly:

$$\left(\frac{\overline{d\mathrm{E}_\omega}}{d\omega do}\right)_{res} = \frac{2\sqrt{2} e^2 T^{3/2} \omega_N^{5/2}}{3\pi^{9/2} \tilde{d}_e \Omega \alpha^2 \gamma^4} K_{2/3}^2\left[\frac{\omega_N}{\omega_{\max}}\right] F_{res}(\omega) \qquad (1.5.38)$$

where, under the conditions (1.5.30), $\omega_N = \left(4\Omega / \alpha^2\right)(2\mathrm{N}+1)$ and $F_{res}(\omega)$ is the resonance form factor

$$F_{res}(\omega)=\int d\xi \frac{\sin^2\left[\xi^2+\frac{\alpha^2 T}{8}\left(\omega-\omega_N\right)\right]}{\left[\xi^2+\frac{\alpha^2 T}{8}\left(\omega-\omega_N\right)\right]^2}. \qquad (1.5.39)$$

Here we took into account that the interval Δx_0 giving the main contribution to the integral over *x*. is determined by (1.5.26) and according to the given assumption $\Delta x_0 << d_e$. For this reason, the exponential factor in the Gaussian distribution function $f(x_0)$ (1.5.25) was replaced by the unity.

When $\omega < \omega_{\max}$ (1.5.38) with the aid of approximation (1.5.34) is reduced to

$$\left(\frac{\overline{d\mathrm{E}}_\omega}{d\omega do}\right)_{res}=\frac{3^{1/3}2^{5/6}\Gamma^2\left(\frac{2}{3}\right)}{\pi^{9/2}\tilde{d}_e}\frac{e^2T^{3/2}\omega_N{}^{1/6}\Omega^{1/3}}{\alpha^{2/3}}F_{res}(\omega). \qquad (1.5.40)$$

The resonances are located at $\omega \approx \omega_N = (2\mathrm{N}+1)\omega_{res}$. In a general case, the given frequency of radiation ω can be realized by different electrons with different values of x_0. The larger x_0 is the smaller ω_{res} (1.4.20) is and the larger s are necessary to provide the given ω. When $x_0 = 0$, ω_{res} is maximum and the necessary s is minimum. Hence, there is the threshold number s (equal to $N = [s_{\min}]$ *or* $N = [s_{\min}]+1$), and this threshold number is realized by the electrons with $x_0 = 0$. At the threshold, the intensity of each harmonic has its maximum because the factor $\sin^2 u_s / u_s^2$ has, in this case, a stronger singularity than the δ function. This anomalously large contribution of the *(2N* + 1) st harmonic at the threshold of its appearance means that even the averaged intensity of a spontaneous emission

concerns a resonance structure to some extent. The physical meaning of the parameter Δx_0 (1.5.26) is that not all the electrons contribute to the resonance part of emission, but only those which enter the strophotron near the axis ($x_0 = 0$) in a small interval of values of x_0, $x_0, |x_0| \le \Delta x_0$. This is the reason why the height of these resonance peaks is not too large. From (1.5.36) and (1.5.40), we find

$$\left(\overline{d\mathrm{E}} / d\omega do\right)_{res} / \left(\overline{d\mathrm{E}} / d\omega do\right)_{n.r.} = . \frac{T^{1/2}}{d_e \omega^{1/2}} << 1. \qquad (1.5.41)$$

Hence, in a spontaneous emission, the nonresonant background is much higher than the resonance peaks when $N \ge N_0$.

The spectral width of the resonances is equal to the width of the curve $F_{res}(\omega)$ (1.5.39) $\Delta\omega = 8/\alpha^2 T = 2\omega_{res}(x_0 = 0)/\Omega T << 2\omega_{res}(x_0 = 0)$. This width is small. For this reason, remembering Madey's theorem [70], one can expect that in a stimulated emission, the role of resonances can be more important because the derivative from the narrow function $F_{res}(\omega)$ (1.5.39) can be large enough. This conclusion is confirmed by the following consideration.

1.6. Summary

Relativistic strophotron is a system in which fast electrons move along a potential "trough" produced hy quadrupole magnetic or electric lenses. Spectral intensity of a spontaneous emission and the gain of an external wave in the strophotron are given by a superposition of contributions from emission or amplification at different (odd) harmonics of the main resonance frequency $\omega_{res}(x_0)$. The main resonance frequency is shown to depend on the initial conditions of the electron, and in particular on its initial

transversal coordinate x_0. This dependence $\omega_{res}(x_0)$ is shown to give rise to a very strong inhomogeneous broadening of the spectral lines. The broadening can become large enough for the spectral lines to overlap with each other. The spectral intensity of a spontaneous emission is averaged over x_0. The averaged spectral intensity is showh to have only a very weakly expressed resonance structure, whereas in the averaged gain, the resonance peaks are shown to be much higher than the nonresonant background. A physical nature of these resonances remaining after averaging is discussed. The maximum achieveable averaged gain and frequency of the strophotron FEL are estimated.

2. Chapter 2.

The Gain, Nonlinear and Quantum Theories of Amplification RS

The chapter is based on publication [79,66,114]

2.1 THE GAIN

In principle, the gain in the strophotron can be found from the above derived spectral intensityo f a spontaneous emission with the aid of Madey's theorem in one of its versions [70-72]. But, unfortunately, as a rule, in a derivation of these general relations between spontaneous and stimulated processes, some assumptions are used. They require a check in any new case. For this reason, we prefer a direct derivation of the gain from the equations of motion.

We start from the following equations of motion of the electron in the electrostatic field with the scalar potential $\Phi(x) = \Phi_0 (x/d)^2$ and in the

electromagnetic wave propagating along the z axis with frequency ω and electric field strength amplitude E_0:

$$\begin{aligned}\frac{dp_z}{dt} &= ev_x E_0 \cos\omega(t-z),\\ \frac{dp_x}{dt} &= eE_0(1-v_z)\cos\omega(t-z)-\frac{2e\Phi_0}{d^2}x.\end{aligned} \tag{2.1.42}$$

The total (kinetic + potential) energy of the electron is

$$\varepsilon_{tot} = \left(m^2 + p_x^2 + p_y^2\right)^{1/2} + e\,\Phi_0\frac{x^2}{d^2} \tag{2.1.43}$$

and the rate of its change is equal to [67]

$$\frac{d\varepsilon_{tot}}{dt} = eE_0 v_x \cos\omega(t - z). \tag{2.1.44}$$

In this paper, we will only investigate the linear gain to find which is sufficient to obtain the first-order corrections $x^{(1)}$ and $z^{(1)}(t)$ to $x^{(0)}(t)$ and $z^{(0)}(t)$

given by (1.2.3) and (1.2.6). These first-order corrections obey the equations

$$\begin{cases}\dfrac{dp_x^{(1)}}{dt} = -\varepsilon_0\Omega^2 x^{(1)} + eE_0\cos\omega\left(t - z^{(0)}\right),\\ \dfrac{dp_z^{(1)}}{dt} = eE_0 v_x^{(0)}\cos\omega\left(t - z^{(0)}\right).\end{cases} \tag{2.1.45}$$

The linear (field-independent) gain is determinedb y the second-order $\left(\propto E_0^{\,2}\right)$ part of $\frac{d\varepsilon_{tot}}{dt}$(2.1.44) which can be expressed in terms of $x^{(1)}$, $z^{(1)}$

$$\frac{d\varepsilon_{tot}}{dt} = eE_0\left\{\dot{x}^{(1)}\cos\omega(t - z^{(0)}) + \omega v_x^{(0)} z^{(1)}\sin\omega(t - z)\right\}. \tag{2.1.46}$$

The energy emitted by the electron during the time T is given by

$$\Delta\varepsilon = -\int_0^T \frac{d\varepsilon_{tot}}{dt}\,dt. \tag{2.1.47}$$

On the right-hand side of the first equation (2.1.45), the cosine of the periodical function in $z^{(0)}(t)$ (1.2.6) can be expanded in the Fourier series to give the Bessel functions with the argument Z (1.4.19). Then the first equation (2.1.45) is easily integrated to give $p_z^{(1)}$.

To integrate the second equation (2.1.43), we first use the relations

$$p_x = v_x \frac{\sqrt{p_z^2 + m^2}}{\sqrt{1 - v_x^2}},$$
$$\frac{dp_x}{dt} = \frac{dv_x}{dt} \frac{\sqrt{p_z^2 + m^2}}{\left(1 - v_x^2\right)^{3/2}} + v_x \frac{p_z dp_z / dt}{\sqrt{1 - v_x^2}\sqrt{p_z^2 + m^2}}. \tag{2.1.48}$$

Finding from the second equation (2.1.48) $\frac{dp_x^{(1)}}{dt}$ and then using the condition $v_x << 1$, we reduce the second equation (2.1.45) to the form

$$\ddot{x}^{(1)} + \Omega^2 x^{(1)} = \frac{eE_0}{\varepsilon_0}\left(1 - v_z^{(0)}\right)\cos\omega\left(t - z^{(0)}\right) - \frac{1}{\varepsilon_0}\frac{d}{dt}\left(v_x^{(0)} p_z^{(1)}\right). \tag{2.1.49}$$

Using $p_z^{(1)}$ found from the first equation (2.1.45), we can integrate (2.1.49) to find $x^{(1)}$. Now the correction $v_z^{(1)}$ to $\dot{z}^{(0)}(t)$(1.2.6) can be found from the relation (1.2.4)

$$v_z = \frac{p_z}{\varepsilon_z}\left(1 - \frac{1}{2}v_x^2\right)$$

which, in the first order, takes the form

$$v_z^{(1)} \approx \frac{p_z^{(1)}}{\varepsilon_0 \gamma^2} - v_x^{(0)} v_x^{(1)}. \tag{2.1.50}$$

In principle, all of these calculations are simple, although rather cumbersome. They will be described in detail elsewhere. Here we will present only the found result:

$$\Delta\varepsilon = \frac{e^2 E_0^2 T^3 \omega}{64\varepsilon_0}\left(\alpha^2 + x_0^2\Omega^2\right)\left(\frac{1}{\gamma^2} + \frac{\alpha^2 + x_0^2\Omega^2}{4}\right)$$
$$\times \sum_s \frac{d}{du_s}\frac{\sin^2 u_s}{u_s^2}\left(J_s(Z) - J_{s+1}(Z)\right)^2. \tag{2.1.51}$$

The same result in the same manner can be derived from the classical equations of motion in the case of the strophotron with a magnetic "trough." We have also derived (2.1.51) using a different approach in the framework of a quantum-mechanical description of electron motion [66].

To compare $\Delta\varepsilon$ (2.1.51) in the strophotron to the corresponding result for FEL with the plane undulator [73-78], we will rewrite (2.1.51) in a different form using the effective "undulator parameter" $K = K_{str} = \gamma\,\Omega a$:

$$\Delta\varepsilon = \frac{e^2 E_0^2 T^3 \Omega}{32\varepsilon_0 \gamma^2} K^2 \frac{1+\frac{1}{4}K^2}{1+\frac{1}{2}K^2} \times \sum_s (2s+1) \frac{d}{du_s} \frac{\sin^2 u_s}{u_s^2} \left(J_s(Z) - J_{s+1}(Z)\right)^2 . \tag{2.1.52}$$

In the case of the plane undulator, the results derived by Becker [73] and Colson [75] written in the same form are given by

$$\Delta\varepsilon = \frac{e^2 E_0^2 T^3 \Omega}{16\varepsilon_0 \gamma^2} K^2 \sum_s (2s+1) \frac{d}{du_s} \frac{\sin^2 u_s}{u_s^2} \left(J_s(Z) - J_{s+1}(Z)\right)^2 . \tag{2.1.53}$$

Where

$$K = K_{und} = \frac{eB_0\lambda_0}{2\pi mc^2} .$$

The result (2.1.53) also can be derived from the expressionfor the spectral intensity of a spontaneous emission of [65] [coinciding with our (1.4.21)] by the use of the relation between the characteristics of the spontaneous and stimulated processes of [72].

A comparison of (2.1.52) and (2.1.53) shows that there is a difference determined by the factor

$$\frac{1}{2}\frac{1+\frac{1}{4}K^2}{1+\frac{1}{2}K^2} \equiv \xi$$

Numerically, this difference is not too important because $\frac{1}{2} \le \xi \le \frac{1}{4}$. But, on the other hand, this result shows that there is not a complete coincidence between the strophotron and the undulator, even at the single-electron level. This difference becomes much more pronounced when we consider the beam as a whole because of a difference in the definitions of the *K* parameter in the undulator and in the strophotron. In the latter case, the parameter *K* depends on x_0, whereas in the case of the undulator, the *K* parameter is x_0 independent.

Each term of the sums (2.1.51), (2.1.52) describes a stimulated emission in the vicinity of the 2s + 1-st harmonic of the main resonance frequency ω_{res}(1.4.20). Again, if α and x_0 are fixed, i.e., for a single electron, the lines of stimulated emission do not overlap because they are separated by the term ω_{res} exceeding their homogeneous width $\omega_{res}/\Omega T$ where $\Omega T >> 1$. The gain at higher harmonics is determined by the factor $\left(J_s(Z) - J_{s+1}(Z)\right)^2$. which is not small only if $\gamma^2\left(\alpha^2 + x_0^2\Omega^2\right) \equiv K_{str} >> 1$. In this case, the resonance frequency ω_{res} (1.4.20) differs essentially from the resonance frequency 27% found in [59]. This difference indicates once more that the results of [59] are correct only for $K < 1$, and hence they are applicable only for a description of amplification at the main frequency ω_{res}(1.4.20).

The expression of [59] for the gain at the main frequency ω_{res}, is correct under the conditions $K < 1$ and $d_e < \Delta x_0$ where Δx_0 is determined by

the right-hand side of inequality (1.5.26). Otherwise, under the condition (1.5.26)

($d_e > \Delta x_0$), the gain must be averaged over x_0, and this procedure can essentially change the result of [59].

For the beam as a whole, under the condition (1.5.26), again there is a strong inhomogeneous broadening. It means that in a general case, after averaging over x_0 many terms of the sum over s give their contribution to the energy $\Delta\varepsilon$ emitted at a given frequency ω. The nonresonance part of the averaged emitted energy is found similarly $\left(\overline{\left(\frac{d\mathrm{E}\omega}{d\omega do}\right)}_{n.r.}\right.$ (2.1.33), (2.1.35) and has the form

$$\overline{\Delta\varepsilon}_{n.r.} = \frac{\sqrt{3}Te^2E_0^2\omega^{1/2}}{32\sqrt{2^{1/2}\varepsilon_0\tilde{d}_e\pi^{5/2}}}\sum_{s-s_{\min}\geq 1}\left(s-s_{\min}\right)^{-3/2}\left\{\varphi\left(x_0^{(s)}\right)-x_0^{(s)}\varphi\left(x_0^{(s)}\right)\right\} \tag{2.1.54}$$

where $x_0^{(s)}$ and $s_{\min}$ are given by (1.5.27) and (1.5.28):

$$\begin{aligned}\varphi\left(x_0^{(s)}\right) &= \exp\left(-\frac{x_0^2}{\tilde{d}_e^2}\right)\left(\alpha^2+x_0^2\Omega^2\right)\\ &\times\left(\frac{1}{2\gamma^2}+\frac{\alpha^2+x_0^2\Omega^2}{4}\right)\left[J_s\left(Z\left(x_0\right)\right)-J_{s+1}\left(Z\left(x_0\right)\right)\right]^2.\end{aligned} \tag{2.1.55}$$

Similar to a transition from (1.5.35) to (1.5.36), the sum over s (2.1.54) can be replaced by the integral over $x=\left(8/\Omega\omega\tilde{d}_e^2\right)\left(s-s_{\min}\right)$ Under the conditions (1.5.30), and if $\omega<\omega_{\max}$, the result is given by

$$\begin{aligned}\overline{\Delta\varepsilon}_{n.r.} &= \frac{3^{1/3}\Gamma^2\left(\frac{1}{3}\right)}{16\cdot 2^{1/6}\pi^{3/2}}\frac{Te^2E_0^2\omega^{1/2}}{\varepsilon_0\tilde{d}_e\Omega^{7/6}\omega^{5/6}}\\ &\cdot\frac{\Delta x_0}{\tilde{d}_e}\int_{x_{\min}}^{\infty}\frac{dx}{x^{3/2}}\left(\tilde{\varphi}(x)-2x\tilde{\varphi}'(x)\right)\end{aligned} \tag{2.1.56}$$

where

$$x_{\min} = .\left(\Delta x_0 / \tilde{d}_e\right)^2 << 1$$

and

$$\tilde{\varphi}(x) = e^{-x}\left(1 + \frac{\Omega^2 \tilde{d}_e^2}{\alpha^2} x\right)^{2/3}. \qquad (2.1.57)$$

Now the lower limit of integration in (2.1.56) may not be replaced by 0 because the integrand has too strong a singularity at the point x = 0. These are small x around $x_{\min}$ which give the main contribution to the integral (2.1.56). For this reason, the nonresonance emitted energy (2.1.56) can be estimated as

$$\overline{\Delta\varepsilon}_{n.r.} = \frac{Te^2 E_0^2 \alpha^{4/3}}{\varepsilon_0 d_e \Omega^{7/6} \omega^{5/6}} \qquad (2.1.58)$$

This is an estimate of the nonresonant background in an amplification of the external wave.

Again the resonances in the emitted energy $\overline{\Delta\varepsilon}$ appear when $s_{\min}$ (1.5.28) is close to some integer $|s_{\min} - N| << 1$, $N = [s_{\min}]$ or $N = [s_{\min}] + 1$. A physical nature of these resonances is the same as previously: they correspond to the threshold of appearance of a new channel of amplification. The threshold corresponds to $x_0 \approx 0$. The factor $(d / du_s)\left(\sin^2 u_s / u_s^2\right)$ in the sums (2.1.51), (2.1.52) has a stronger singularity at the threshold than $\delta'(x_0)$. This is why this threshold term being averaged over x_0 gives an anomalously large contribution to $\overline{\Delta\varepsilon}$. Th e result has the form

$$\overline{\Delta\varepsilon}_{res} = \frac{T^{5/2} e^2 E_0^2 \alpha^{1/2}}{3\pi^{5/2} 8\sqrt{2}\varepsilon_0 \tilde{d}_e \Omega \gamma^4} K_{2/3}^2\left(\frac{\omega_N}{\omega_{\max}}\right) \tilde{F}_{res}(\omega) \qquad (2.1.59)$$

where again $\omega_N = \left(4\Omega/\alpha^2\right)(2\mathrm{N}+1)$, $\omega_{\max} = 3\gamma^3\alpha\,\Omega$ .The factor of the resonance curve $\tilde{F}_{res}(\omega)$ is given by

$$\tilde{F}_{res}(\omega) = \int \frac{d\xi}{\xi}\frac{d}{d\xi}\frac{\sin^2\left[\xi^2 + \frac{\alpha^2 T}{8}\left(\omega-\omega_N\right)\right]}{\left[\xi^2 + \frac{\alpha^2 T}{8}\left(\omega-\omega_N\right)\right]^2} = \frac{\alpha^2 T}{8}\frac{d}{d\omega}F_{res}(\omega) \qquad (2.1.60)$$

where $F_{res}(\omega)$ (1.5.39) is the form factor of the resonance curve in a spontaneous emission.

If $\omega < \omega_{\max}$, with the aid of the approximation (1.5.34), (2.1.59) is reduced to

$$\overline{\Delta\varepsilon}_{n.r.} = \frac{3^{1/3}\Gamma^2\left(\frac{2}{3}\right)}{16\cdot 2^{1/6}\pi^{5/2}}\frac{T^{5/2}e^2E_0^2\Omega^{1/3}\alpha^{4/3}}{\varepsilon_0\tilde{d}_e\omega_N{}^{5/6}}\tilde{F}_{res}(\omega). \qquad (2.1.61)$$

Comparison with $\overline{\Delta\varepsilon}_{n.r.}$(58) gives an estimate

$$\overline{\Delta\varepsilon}_{res} / \overline{\Delta\varepsilon}_{n.r.} = .(\Omega T)^{3/2} >> 1. \qquad (2.1.62)$$

In a stimulated emission, the relation between the height of the resonance peaks and the nonresonant backgrounisd inverse as compared to a spontaneous emission. The nonresonant background (2.1.58) gives only a negligibly small contribution to the gain which is determined mainly by the resonance emitted energy $\overline{\Delta\varepsilon}_{res}$(2.1.59), (2.1.61):

$$G = \eta\frac{8\pi N_e}{E_0^2}\Delta\varepsilon_{res} = \frac{\eta(\ln 2)^{1/2}}{\pi^{3/2}}\frac{N_e\Gamma_0 L^{5/2}}{\sqrt{d_e}\gamma^{7/2}}\left(\frac{\omega}{\omega_{\max}}\right)^{1/2}K_{2/3}^2\left(\frac{\omega}{\omega_{\max}}\right)\tilde{F}_{res}(\omega) \qquad (2.1.63)$$

where $\alpha = d_e\Omega$, N_e is the electron number density and η is the artificially introduced factor taking into account the difference of dimensions of the beam outside and inside the strophotron. This difference appears due to the electron oscillations which effectively broaden the beam. If we take

$(x_0)_{\max} \approx d_e/2$, the maximum amplitude of oscillations is $a_{\max} = \left((1/4)d_e^2 + \left(\alpha^2/\Omega^2\right)\right)^{1/2}$ and

$$\eta = \frac{d_e/2}{a_{\max}} = \left(1 + \frac{4\alpha^2}{d_e^2\Omega^2}\right)^{-1/2} \tag{2.1.64}$$

If, in particular, $d_e = \alpha/\Omega$, $\eta = 1/\sqrt{5}$.

2.2. The Nonlinear Theory

The relativistic strophotron FEL is a system in which electrons move along the parabolic one dimentional potential trough whose vector potential is given by

$$A_z = gx^2/2 \tag{2.2.1}$$

Where x is one of the transverse coordinates, g is the magnetic field gradient. The wave amplified to propagate along the axis of the trough (z - axis). The classical equations of electron motion can be reduced to the form

$$\dot{w} = -\frac{eE_0}{\varepsilon_0}\cos\varphi, \tag{2.2.2}$$

$$(1+w)\dot{\varphi} = \dot{\varphi}\left(t_0\right) - \frac{1}{2}\Omega^2\omega\left(x^2 - x_0^2\right), \tag{2.2.3}$$

$$\begin{aligned}\ddot{x} + \Omega^2 x &= -w\,\ddot{x} - \frac{eE_0}{\varepsilon_0}\left(\frac{\dot{\varphi}}{\omega} - x^2\right)\cos\varphi \\ &+ \frac{\Omega^2 x}{1+w}\left[\frac{\dot{\varphi}(t_0)}{\omega} - \frac{\Omega^2}{2}\left(x^2 - x_0^2\right)\right],\end{aligned} \tag{2.2.4}$$

Where $\mathbf{E}_0 \| Ox$ and ω are the electric field strength and frequency of the wave c=1, e is the electron charge,

$$\varphi = \omega(t - z), \qquad w = \frac{\varepsilon - \varepsilon_0}{\varepsilon_0} \tag{2.2.5}$$

Is the time - independent electron energy, the index "0" indicates the initial value of the variables at the time $t = t_0$ when the electron enters the system

$$\Omega = \left(ge / \varepsilon_0 \right)^{1/2} \tag{2.2.6}$$

Is a frequency of strophotron oscillations [79].

The terms in of Eq. (2.2.4) determine either small corrections to the frequency Ω(2.2.6) or small anharmonicity of oscillations. Here these small corrections will be ignored, and all the mentioned terms in Eq.(2.2.4) will be dropped out. In this (harmonic) approximation the field-free $E_0 = 0$ solution of Eq.(2.2.4) is given by $x^{(0)} = a_0 \cos\left[\Omega(t - t_0) + \theta_0 \right]$, where $a_0 = \left(x_0^2 + \dot{x}_0^2 / \Omega^2 \right)^{1/2}$ is the field free amplidude of strophotron oscillations, $\theta_0 = \operatorname{arctg} \alpha / x_0 \Omega$, $x_0 = x(t = t_0)$, $\dot{x}_0 \square \alpha$, $\alpha \equiv \alpha_x$ is the angle in the plane (x,z) under which the electron enters the system. The first corrections to $x^{(0)}(t)$ $(\propto E_0)$ have been found in Ref. [79] and in this approximation x(t) can be written in the form

$$x(t) = a(t) \cos\left[\Omega(t - t_0) + \theta(t) \right] \tag{2.2.7}$$

Where $a(t)$ and $\theta(t)$ are some slowly varying functions (amplitude and phase).

$$\left| \dot{a} / a \right|, \quad \left| \dot{\theta} \right| << \Omega. \tag{2.2.8}$$

We will assume that in the general case the expression (2.2.7) for x(t) and the condition (2.2.8) hold for any values of E_0. This assumption about slow variation of $a(t)$ and $\theta(t)$ is justified if

$$|w| << 1, \quad a\,\Omega << 1 \tag{2.2.9}$$

i.e. if the total change of electron energy is small in comparision with ε_0 and if the amplitude of oscillations "a" is small in comparision with their period along the z-axis $\lambda_0 = 2\pi/\Omega$. The letter condition means, in particular $\alpha << 1$ and $d_e\,\Omega << 1$, where d_e is the diameter of the beam in the (x,z) plane ($x_0 \le d_e$). We will assume also that $\gamma = \varepsilon_0 / m >> 1$. Under these conditions Eq. (2.2.2) gives $|\dot{\varphi}/\omega| << 1$. Besides, it is possible to show that the change of amplitude $\delta a \equiv a(t) - a_0$ is small in comparision a_0, $|\delta a| << a_0$. The condition $a\,\Omega << 1$ (2.2.9) justifies also the mentioned above possibility to neglect all the terms in the square brackets of Eq. (2.2.4).

The relative emitted energy w contains both fast and slow varying parts w_{fast} and w_{slow}. The equations of motion (2.2.4) can be averaged over fast period oscillations $2\pi\,\Omega^{-1}$ to give equation for the slowly varying functions w_{sl}, θ and δa only.

A procedure of separation of fast and slow motions does work well enough only near resonances.

The strophotron FEL is characterized by it's resonance frequency

$$\omega_{res} = \frac{\Omega}{\frac{1}{2\gamma^2} + \frac{a_0^2\Omega^2}{4}}. \qquad (2.2.10)$$

Amplification can occur near odd harmonics of ω_{res}, $\omega \approx (2s+1)\omega_{res}$, $s = 0, \pm 1, \pm 2, \ldots$ [79,66]. We will consider the case $s \neq 1$ assuming the detuning from the (2s+1)-st harmonic

$$\Delta_s = \omega\left(\frac{1}{2\gamma^2} + \frac{a_0^2\Omega^2}{4}\right) - (2s+1)\Omega \tag{2.2.11}$$

Is small $\Delta_s << \Omega$.

Under these conditions the equations for w_{sl}, θ and δa can be found from Eq. (2.2.2), (1.3.3) and (2.2.4)

$$\dot{w}_{sl} = -\frac{eE_0\Omega a_0}{2\varepsilon_0}\left[J_s(Z) - J_{s+1}(Z)\right]\sin\psi \tag{2.2.12}$$

$$\dot{\theta} = -\frac{\Omega}{2}w_{sl}, \tag{2.2.13}$$

$$\delta\dot{a} = -\frac{eE_0}{4\gamma^2\varepsilon_0\Omega}\left[J_s(Z) - J_{s+1}(Z)\right]\sin\psi, \tag{2.2.14}$$

Where w_{sl} is the slow varying part of w, $Z = a_0^2\Omega\omega/8$,

$$\psi = \omega t_0 + \Delta_s\left(t - t_0\right) - (2s+1)\theta + Z\sin 2\theta - \frac{\Omega^2\omega a_0}{2}\int_{t_0}^{t}\delta a dt - \omega\left(\frac{1}{2\gamma^2} + \frac{a_0^2\Omega^2}{4}\right)\int_{t_0}^{t} w_{sl}dt \tag{2.2.15}$$

Is the phase of slow motion (resonance) motion of electron. The phase ψ is determined not only by detuning Δ_s and the phase θ of the transverse electron coordinate x(t) (2.2.7), but also by the change of amplitude of x(t) (2.2.7) $\delta a(t)$ and by the change of electron energy w(t).

Combining Eqs. (2.2.12), (2.2.13) and (2.2.14) we find equation for the phase ψ (2.2.15), which can be written as the usual pendulum equation [80]

$$\frac{d^2\psi}{d\mu^2} = \sin\psi \tag{2.2.16}$$

With the initial conditions

$$\psi(\mu=0)=\omega t_0, \quad \frac{d\psi}{d\mu}(\mu=0)=\frac{\Delta_\varepsilon}{\Delta_m}, \tag{2.2.17}$$

Where the dimensionless time (or the saturation parameter) μ is given by

$$\mu = t - t_0 - \left\{ \frac{eE_0\omega\Omega a_0}{4\varepsilon_0}\left(\frac{1}{2\gamma^2}+\frac{a_0^2\Omega^2}{4}\right)\left[J_s(Z)-J_{s+1}(Z)\right]\right\}^{1/2}, \tag{2.2.18}$$

$\Delta_\varepsilon = \varepsilon - \varepsilon_{res}$, ε_{res} is that value of the initial electron energy at which $\Delta_s = 0$

(2.2.10)

$$\Delta_m = \frac{4\varepsilon}{\omega}\tilde{\Delta}_m \Big/ \left(-\frac{3}{\gamma^2}+\frac{\alpha^2+x_0^2\Omega^2}{4}\right), \tag{2.2.19}$$
$$\tilde{\Delta}_m = \mu / t.$$

The emitted energy $\Delta\varepsilon = \varepsilon_0 w_{sl}$ is given by Eq. (2.2.12) or by the following equivalent equation

$$\Delta\varepsilon = \frac{2\varepsilon}{\omega\left(\frac{1}{\gamma^2}+\frac{a_0^2\Omega^2}{4}\right)}\left(\Delta_s - \tilde{\Delta}_m\frac{d\psi}{d\mu}\right). \tag{2.2.20}$$

In the weak field approximation Eq. (2.2.16) solved by the iteration method to give results coinciding with the results of [79,66].

In the strong-field assumptions $\mu >> 1$, $\tilde{\Delta}_m >> |\Delta_s|$ the phase ψ obeying the pendulum equation and averaged over its initial value $\psi_0 = \psi(t=t_0)$ and the energy $\overline{\Delta\varepsilon}$ emitted by a single electron are known analytically [80].

The strong field characteristic detuning $\tilde{\Delta}_m$ determines the order of magnitude of the detuning Δ_s at which the emitted energy $\overline{\Delta\varepsilon}(\Delta_s)$ achieves its maximum. The maximum emitted energy $\overline{\Delta\varepsilon}_{\max}$ in the strong field limit has the order of magnitude

$$\Delta\tilde{\varepsilon}_{\max} \square \Delta\bar{\varepsilon}(\Delta_s \square \tilde{\Delta}_m). \qquad (2.2.21)$$

Hence, as a whole the function $\overline{\Delta\varepsilon}(\Delta_s)$ in the strong field asymptotics $\mu >> 1$ can be written as

$$\Delta\bar{\varepsilon} = \frac{2\varepsilon\tilde{\Delta}_m}{\omega\left(\frac{1}{\gamma^2}+\frac{a_0^2\Omega^2}{4}\right)}\left\{1-\frac{2}{\sqrt{\pi\mu}}\sin\left(\mu+\frac{\pi}{4}\right)\right\}F\left(\frac{\Delta_s}{\tilde{\Delta}_m}\right), \qquad (2.2.22)$$

Where $F(\xi)$ is some dimensionless function , $F(\xi) = -F(-\xi)$, $F(0) = 0$, having its maximum $F(\xi) = .1$ at $\xi = .1$. In the region $\xi << 1$, $F(\xi) = .\xi$. For any $|\xi| > or < 1$, F can not be found and written down analytically and requires a numerical calculation [81].

Sustituting $\omega_s \approx (2s+1)\omega_{res}$ (2.2.10) into Eq. (2.2.21) we obtain an estimate of efficiency of RS FEL:

$$\eta = \frac{\Delta\bar{\varepsilon}_{\max}}{\varepsilon} = .\frac{\mu}{N_0(2s+1)}, \qquad (2.2.23)$$

Where $N_0 = \Omega t / 2\pi = L / \lambda_0$ is the number of strophotron oscillations along the length of the system L. When s=0 the estimate (2.2.23) coincides with the results well known in the usual undulator FEL [3 80]. When s becomes larger, η decreases.

One of the main conclusions of our previous papers [79,66] consisted in the prediction of a very strong inhomogeneous broadening connected with a distribution of electrons over the beam's crossection. The result has been derived earlier [79,66] in the weak-field approximation. But, as a matter of fact, this feature of RS FEL in general enough to hold good for any field strength E_0. The reason of this inhomogeneous broadening is in a

strong dependence of resonance frequency ω_{res} (10) on the initial transverse electron coordinate x_0 (through the amplitude a_0). To take into account this inhomogeneous broadening in the strong field limit we must average the emitted energy $\Delta\bar{\varepsilon}$ (2.2.22) over x_0.

The gain is proportional to the averaged resonance emitted energy $\langle\Delta\bar{\varepsilon}\rangle_{res}$ and has a form

$$G=\frac{8\pi N_e}{E_0^2}\langle\Delta\bar{\varepsilon}\rangle_{res}=\frac{8(\ln 2)^{1/2}\left[\frac{e\alpha^3}{\varepsilon\omega}\left(J_s(Z)-J_{s+1}(Z)\right)\right]^{3/4}}{d_e\Omega E_0^{5/4}\left(\frac{1}{\gamma^2}+\frac{\alpha^2}{4}\right)}\tilde{F}_{res}(\omega)\left\{1-\frac{2}{\sqrt{\pi\mu}}\sin\left(\mu+\frac{\pi}{4}\right)\right\},$$

(2.2.24)

Where N_e is the electron number density, $\tilde{F}_{res}(\omega)$ is the form factor of resonance curve.

As a function of E_0 the nonlinear gain (2.2.24) falls down as $E_0^{-5/4}$ (in contrast with the law $E_0^{-3/2}$ in the usual undulator FEL [80]).

2.3. Quantum Theory of Amplification in RS

The best-known free-electron lasers among the experimentally implemented systems [82-84] are based on the use of undulators in which a static transverse magnetic field varies periodically along the direction of electron motion (Oz axis). A different free-electron laser is discussed in Ref. [85]: in this case a beam of relativistic electrons is traveling in a static magnetic or electric field, the potential of which is homogeneous along the

direction of motion of electrons (OZ axis) and rises parabolically along one of the transverse directions (Ox axis). The name strophotron is sometimes used for these systems [86]. In other cases such systems are not distinguished from undulators and are regarded as class 2 undulators.

The problem of amplification of an external wave is solved in Ref. [85] without full allowance for the longitudinal and transverse electron motion. We shall show that the changes in the longitudinal energy associated with the emission (or absorption) of external wave photons have a considerable influence on the frequency of the oscillations of the electrons in the field and on the nature of the wave functions describing the transverse electron motion. For these reasons there are major changes in the expressions for the lasing frequency and for the gain, and there are also changes in the ability of generation of higher harmonics and of conditions corresponding to optimal amplification.

We shall analyze the dependence of the resonance frequency on the initial transverse coordinate of an electron $\omega_{res}(x_0)$. We shall show that this dependence results in a strong inhomogeneous broadening and overlap of the gain profiles at different harmonics of the fundamental resonance frequency. We shall assume these conditions in determining the gain averaged over x_0, i.e., over the distribution of electrons in a transverse cross section of the beam. We shall show how the average gain retains its resonance structure, but resonance amplification includes contributions of only a small fraction of the beam electrons that enter the system close to the axis (small values of x_0). We shall conclude with numerical

estimates of the maximum attainable lasing frequency and of the corresponding gain.

A geometry of the fields similar to that considered in the present study applies also to the case of emission of radiation as a result of channeling of electrons and positrons in crystals [88,89]. In contrast to the conventional channeling, the interaction of electrons with an external macroscopic field (which can be described as macroscopic channeling) is much simpler because there are no such problems as the absorption of electromagnetic waves in a crystal, possible limits on the channeling length, etc.

The feasibility of practical realization of a potential of this type is considered in Ref. [90], when a system of specially oriented magnetic quadrupole lenses located at equal distances from one another on the beam axis is proposed.

We shall use a method based on the direct solution of the initial secular quantum-mechanical problem, which in this respect differs from the S-matrix approach [85]. We shall consider only the linear approximation although the general equations obtained are valid also in the case of many-photon processes and saturation.

2.4. EQUATIONS FOR THE AMPLITUDES OF TRANSITION PROBABILITIES

Following Ref. [85], we shall consider planar geometry and assume that a static electric or magnetic field is independent of one of the transverse coordinates, for example, *y*. The field gradient is directed along the *OX* axis.

We shall consider an ultrarelativistic electron of energy $\varepsilon = m\gamma >> m\,(\hbar = c = 1)$ movinginthe *XOZ* plane at a small angle α to the *OZ* axis and experiencing at an initial moment t=0 a static electric or magnetic field with the potential or

$$\Phi(x) = \Phi_0(x^2/d^2) \quad \mathbf{A}(x) = \mathbf{A}_0(x^2/d^2), \tag{2.4.1}$$

where $e\Phi_0 = e|\mathbf{A}_0|$ and 2d are, respectively, the maximum height of a transverse potential barrier and the size of the region of its localization (aperture) in the direction of the *OX* axis; the $\mathbf{A}_0$ vector is parallel to the *OZ* axis, i.e., the magnetic field is directed along the *OY* axis.

In the absence of an electromagnetic wave an electron experiences translational motion along the *OZ* axis, characterized by a momentum $\mathbf{p}_\perp$ and an energy $\varepsilon_\perp = \sqrt{p_\perp^2 + m^2}$, oscillating in the transverse direction (along the *OX* axis). The oscillation wave functions $\varphi_1(x, \varepsilon_\perp)$, satisfy the usual Schrodinger equation obtained from the initial Klein-Gordon equation ignoring the square of the potential Φ(x) (we shall now obtain estimates justifying these and other approximations):

$$d^2\varphi_l(x,\varepsilon_\perp)/dx^2 = \left[2\varepsilon_\perp e\Phi(x) - 2\varepsilon_\perp\Omega(\varepsilon_\perp)(l+1/2)\right]\varphi_l(x,\varepsilon_\perp), \tag{2.4.2}$$

where $\Omega(\varepsilon_\perp) = \left(2e\Phi_0/\varepsilon_\perp\right)^{1/2}/d$ is the oscillation frequency in a parabolic well; / = 0, 1,2,... are the oscillation quantum numbers; $\varphi_l(x,\varepsilon_\perp) = \left[\Omega(\varepsilon_\perp)\varepsilon_\perp\right]^{1/4}\chi_l(\varsigma)$, $\chi_l(\varsigma)$ are the usual oscillation functions dependent on the dimensionless variable $\varsigma = (\Omega\varepsilon_\perp)^{1/2}$ and expressed in terms of Hermite polynomials [91].

We shall assume that an electromagnetic wave of frequency ω linearly polarized in the *XOZ* plane and described by the vector potential

$$A_{em} = (E_0/\omega)\cos[\omega(t - z)], \tag{2.4.3}$$

where E_0 is the amplitude of the electric field in the wave, travels along the OZ axis parallel to the direction of longitudinal motion of an electron beam.

We shall represent the wave function Ψ of an electron by an expansion

$$\Psi = \sum_n C_n(t,x) \exp\left\{ i\left[(p_\square + n\omega)z - (\varepsilon_\square + n\omega)t \right] \right\}, \qquad (2.4.4)$$

where *n* = 0, + 1, + *2*,... and the exponential factor allows explicitly for the change in the longitudinal energy and the corresponding momentum as a result of the absorption (n<0) or stimulated emission (n>0) of |n| quanta of the wave (2.4.3).

The coefficients $C_n(t,x)$ can be expanded in terms of any complete system of functions dependent on x. The most convenient basis is a system of functions $\varphi_l^{(n)}(x) \equiv \varphi_l(x, \varepsilon_\parallel + n\omega)$, which satisfy Eq. (2.4.2) with a shifted energy $\varepsilon_\parallel + n\omega$f and correspond to a shifted oscillation frequency $\Omega^{(n)} = \Omega(\varepsilon_\parallel + n\omega)$*:*

$$C_n(t,x) = \sum_l (-1)^l a_{nl}(t) \varphi_l^{(n)}(x). \qquad (2.4.5)$$

The coefficients $a_{nl}(t)$ represent the amplitudes of the probability of finding an electron at the l th oscillation level on absorption (emission) of \n\ quanta of the field (2.4.3). The equations for $a_{nl}(t)$ follow from the Klein-Gordon equation where we can ignore terms proportional to the quantities Φ^2, A_{em}^2, $d^2 a_{nl}/dt^2$, and $\Phi(da_{nl}/dt)$ (for estimates see below):

$$
\begin{aligned}
& i\frac{da_{nl}}{dt}+\left[\frac{n\omega}{2\gamma^2}-(l+1/2)\Omega-\frac{(n\omega)^2}{2\varepsilon_{\square}\gamma^2}+\frac{n\omega(l+1/2)\Omega}{2\varepsilon_{\square}}-\frac{3}{8}\frac{(n\omega)^2(l+1/2\Omega}{2\varepsilon_{\square}^{\ 2}}\right]a_{nl} \\
& =i\frac{eE_0}{2\varepsilon_{\square}\omega}\sum_{l'}(-i)^{l'-l}\left[\left\langle\varphi_l^n\left|\frac{d}{dx}\right|\varphi_{l'}^{(n-1)}\right\rangle a_{n-1,l'}+\left\langle\varphi_l^n\left|\frac{d}{dx}\right|\varphi_{l'}^{(n+1)}\right\rangle a_{n+1,l'}\right], \\
& a_{nl}(0)=\delta_{n0}\delta_{ll_0}.
\end{aligned}
\tag{2.4.6}
$$

On the left-hand side of Eq. (2.4.6) all the terms are expanded in $|n|\omega/\varepsilon_{\square}\square\ 1|$. The relationship between the longitudinal and transverse motion of electrons mentioned in the Introduction governs the dependence of $\Omega^{(n)}$ on *n* and nonorthogonality

of the functions $\varphi_l^{(n)}$ and $\varphi_{l'}^{(n\pm1)}$. The nonorthognality of these functions means that not only the transitions between the neighboring levels are allowed for, but

also those between distant levels / and /'. The difference between the functions is governed by a small parameter $\omega/\varepsilon_{\|}<<1$, but the matrix elements in the system of equations (2.4.6) have to be calculated rigorously bearing in mind that if l >> 1 and $l\omega/\varepsilon_{\|}>>1$, then $l>>k,k'$, where $k=l-l_0$, and $k'=l'-l_0$.

The matrix elements in the system of equations (2.4.6) can be calculated by a method similar to that employed in Ref. [92], which finally gives

$$
\begin{aligned}
& i\dot{a}_{nk}+\left[\frac{n\omega}{2\gamma^2}-k\Omega-\frac{(n\omega)^2}{2\varepsilon\gamma^2}+\frac{n\omega l_0\Omega}{2\varepsilon}+\frac{nk\omega l_0\Omega}{2\varepsilon}-\frac{3}{8}\frac{(n\omega)^2 l_0\Omega}{\varepsilon^2}\right]a_{nk} \\
& =i\mathrm{E}_{\mathrm{int}}\sum_{k'}\left\{\left[J_{\frac{k-k'+1}{2}}(-z)+J_{\frac{k-k'-1}{2}}(-z)\right]a_{n-1,k'}+\left[J_{\frac{k'-k-1}{2}}(-z)+J_{\frac{k'-k'+1}{2}}(-z)\right]a_{n+1,k'}\right\},
\end{aligned}
\tag{2.4.7}
$$

where $z=l_0\omega/4\varepsilon$, $\mathrm{E}_{\mathrm{int}}=(eE_0/2\omega)(l_0\Omega/2\varepsilon)^{1/2}$ and the sum over *k* ′ should include only the terms with the values of *k* ′ which are of parity opposite to *k*.

In the resonance approximation, when

$$\omega \approx \omega_{res}^{(s)} = 2(2s+1)\gamma^2\Omega/(1+l_0\Omega\gamma^2/\varepsilon) \equiv (2s+1)\omega_{res}, \qquad (2.4.8)$$

where s = 0, 1, 2, ... we can substitute $k = (2s + 1)n$, and $k' = (2s + 1)(n \pm 1)$ in the system (2.4.7). Consequently, the equations for $a_n(t) \equiv a_{n,(2s+1)n}$ become identical with the equations known from the theory of a free-electron laser with an undulator [93]:

$$i\dot{a}_n - \mathrm{E}_{anh}(2n\Delta/\omega + n^2)a_n = \tilde{\mathrm{E}}_{\mathrm{int}}\left(a_{n+1} + a_{n-1}\right), \quad a_n(0) = \delta_{n0}, \qquad (2.4.9)$$

where

$$\tilde{\mathrm{E}}_{\mathrm{int}} = (-1)^s \mathrm{E}_{\mathrm{int}} F_s(z); \quad F_s(z) = J_s(z) - J_{s+1}(z), \qquad (2.4.10)$$

and the following usual notation is introduced for the energy detuning Δ_s and the anharmonicity energy E_{anh}:

$$\Delta_s = (\omega/2\mathrm{E}_{anh})\left[(2s+1)\Omega - 1/2\omega\left(1/\gamma^2 + l_0\Omega/\varepsilon\right)\right], \qquad (2.4.11a)$$

$$\mathrm{E}_{anh} = (\omega/2\varepsilon)\left[\omega/\gamma^2 - (2s+1)\Omega + 3l_0\Omega\omega/4\varepsilon\right]. \qquad (2.4.11b)$$

We shall finally obtain estimates of the approximations made on transition from the Klein-Gordon equation to the system (2.4.7) bearing in mind that $\langle x^2 \rangle = .l_0/(\Omega\varepsilon)$, $\langle x^4 \rangle = .l_0^2/(\Omega\varepsilon)^2$, $\partial/\partial t = .1/t$, and using in estimates the approximation $\varepsilon_\perp = .m$. We can easily show that the relative smallness of the ignored terms proportional to d^2a_{nl}/dt^2, $e\Phi(da_{nl}/dt)$ and $e^2A_{em}^2a_{nl}$ is governed by the small parameters $1/\varepsilon t$, $\varepsilon_\perp/\varepsilon \le 1/\gamma$, and $eA_{em}/m\gamma^{1/2}$, respectively. The term proportional to Φ^2 introduces into the system (2.4.9) a contribution $= .(l^2\Omega^2/\varepsilon)a_n = \left[l_0^2\Omega^2/\varepsilon + 2l_0n\Omega^2/\varepsilon + (n\Omega)^2/\varepsilon\right]a_n$. The n-independent part of this contribution is readily removed by a phase transformation. The part linear in n determines the correction to the detuning Δ_s, which is small compared with $l_0\omega n\Omega/\varepsilon$ in respect of the parameter $\Omega/\omega << 1$; the part quadratic in respect of n governs the correction

to E_{anh}, which is small compared with $l_0\Omega\omega^2/\varepsilon^2$ in respect of the parameter $\varepsilon_\perp/\varepsilon \le 1/\gamma << 1$.

2.5. RESONANCE FREQUENCY AND OUTPUT ENERGY

Equation (2.4.8) gives the resonance frequency of the system ω_{res} expressed in terms of the number of an oscillatory level l_0 filled most effectively at the initial moment in time t = 0.

The value of l_0 can be expressed in terms of the initial parameters of the electron beam. A correct determination of l_0 requires the knowledge of the initial transverse wave function of an electron in the form of a packet localized at some

point x_0. Expanding this function in terms of $\varphi_l(x)$ of Eq. (2.4.2), we find that the squares of the moduli of the coefficients in the expansion have a narrow maximum at

$$l \approx l_0 \equiv p_\perp^2/2\varepsilon + x_0^2\Omega\varepsilon/2 = (\varepsilon/2\Omega)\left(\alpha^2 + x_0^2\Omega^2\right) = \varepsilon\Omega a^2/2, \qquad (2.5.12)$$

where $a(x_0) = \left(x_0^2 + \alpha^2/\Omega^2\right)^{1/2}$ is the classical amplitude of transverse oscillations of an electron in a strophotron with an initial coordinate x_0 and the angle of entry α into the field.

Substitution of l_0 from Eq. (2.5.12) into Eq. (2.4.8) gives

$$\omega_{res} = 2\lambda^2\Omega/[1+(\gamma\Omega a)^2/2]. \qquad (2.5.13)$$

This expression for the resonance frequency has been obtained earlier in the theory of spontaneous emission during channeling of particles in a crystal [88,94]. If $\gamma\Omega a << 1$, then the frequency ω_{res} of Eq. (2.5.13) is identical with the result obtained in Ref. [85]: $\omega_{res} = 2\gamma^2\Omega$.

We shall now calculate the energy ΔE emitted by an electron at a frequency ω in the direction of the *OZ* axis and governed by the expression

$$\Delta E = -\omega \sum_n n|a_n|^2. \qquad (2.5.14)$$

According to Ref. [93], the simplest method of finding ΔE *in an* approximation which is linear in E_0^2 involves solution of the system (2.4.9) by perturbation theory in terms of $\tilde{E}_{int}$, which gives

$$\Delta E = \frac{(eE_0)^2 t^3 \omega}{64\varepsilon} (\Omega a)^2 \left[\frac{1}{\gamma^2} + \frac{(\Omega a)^2}{4} \right] F_s^2 \frac{d}{du_s} \left(\frac{\sin^2 u_s}{u_s^2} \right), \qquad (2.5.15)$$

where

$$u_s = \frac{-(\Delta_s E_{anh} t)}{\omega} = \frac{t}{4} \left[\omega \left(\frac{1}{\gamma^2} + \frac{(a\Omega)^2}{2} \right) - 2(2s+1)\Omega \right]. \qquad (2.5.16)$$

The quantity ΔE_s represents the energy emitted by an electron at a frequency $\omega \approx \omega_{res}^s = (2s+1)\omega_{res}$. For fixed values of α and x_0 the widths of the gain profiles associated with the finite interaction time between an electron and the system are $\delta\omega \approx \omega_{res} / N_{osc}$, where $N_{osc} = \Omega t / 2\pi$ is the number of transverse oscillations of an electron in the transit time *t* across the system. The separation between neighboring gain profiles is $\Delta\omega = 2\omega_{res} >> \delta\omega$, i.e., in the case of a single electron the lines do not overlap if $N_{osc} = \Omega t / 2\pi >> 1$. However, in view of the dependence $\omega_{res}(x_0)$ of Eq. (2.5.13), different electrons (corresponding to different values of x_0 have different resonance frequencies ω_{res} and, consequently, different positions of the resonance amplification lines.

The energy emitted by a beam at a frequency ω can be found by summing Δ ΔE_s over *s* and averaging the total emitted energy

$$\Delta E = \sum_s \Delta E_s \qquad (2.5.17)$$

with respect to x_0. This procedure and the corresponding conditions are described in the next section, where the average gain is found. However, we shall first consider the problem of the similarity and difference between free-electron lasers with an undulator and a parabolic trough (strophotron).

It is known that a free-electron laser with a planar linearly polarized undulator can amplify a wave traveling along the axis at a frequency ω close to the odd harmonics of the fundamental resonance frequency [95-101]. The formulas (2.5.13), (2.5.15), and (2.5.16) governing the energy emitted by a single electron can be reduced to the form similar to the corresponding formulas for a free-electron laser with an undulator [95-101] if we introduce a parameter $K_{str} = \gamma\Omega a / c$, which

replaces the usual parameter for an undulator $K_{und} = eB_0\lambda_0 / mc^2$ (B_0 and λ_0 are the undulator intensity and period). The major differences between these two systems are observed when we consider a beam as a whole rather than one electron. If K_{und} is independent of the initial conditions, then in the system under discussion we have $K_{str} = K_{str}(x_0, \alpha)$. For this reason the averaging over x_0 is not as trivial as in the case of an undulator.

The relative efficiency of stimulated emission of the (2s + 1)th harmonic by a single electron is governed by the factor *Fs* of Eq. (2.4.10) in Eq. (2.5.15). If $\gamma\Omega a << 1$, then $\omega_{res} = 2\gamma^2\Omega$ and the factor is $z[\omega \approx (2s+1)\omega_{res}] \approx (1/4)(2s+1)(\gamma\Omega a)^2 \approx s\zeta$. Since the argument of the Bessel functions in Eq. (2.4.10) is small compared with the index, it follows that amplification of high harmonics is then impossible (ΔE_s falls rapidly on increase in s).

Effective amplification at higher harmonics requires that the parameter K_{str} should be large: $K_{str} >> 1$, which we shall henceforth assume to be correct. If $K_{str} >> 1$, then the resonance frequency ω_{res} of Eq. (2.5.13) differes considerably from $2\gamma^2\Omega$ $(\omega_{res} << 2\gamma^2\Omega)$. However, the lasing frequencies $\omega_{res}^s = (2s+1)\omega_{res}$ need not be small compared with $2\gamma^2\Omega$ because the number *s* is fairly large. The possibility of increasing *s* is governed, as usual, by the condition of a moderately strong fall of the average gain on increase in *s*.

2.6. AVERAGING OVER THE DISTRIBUTION OF ELECTRONS IN A BEAM. GAIN

We shall consider a specific distribution of electrons in a beam along the initial transverse coordinate described by the Gaussian function

$$f(x_0) = \frac{1}{\sqrt{\pi}\tilde{d}_e} \exp\left[-\frac{x_0^2}{\tilde{d}_e^2}\right], \qquad (2.6.18)$$

where $\tilde{d}_e = d_e / (2\sqrt{\ln 2})$ (d_e is the diameter of the electron beam satisfying the condition de <2d).

We shall first estimate the scale of inhomogeneous broadening of the lines due to the scatter of x_0 and assume that the condition $d_e\Omega/\alpha \ll 1$ is satisfied.

The change in ω_{res} of Eq. (2.5.13) on variation of x_0 from 0 to $d_e/2 \approx d_e$ is equal to $\Delta\omega_{res} \approx (1/16) d_e^2 \Omega \omega_{res}^2$. The corresponding shift of the emission line representing the (2s+l)th harmonic is $\omega_s = (2s+1)\omega_{res} \approx \frac{1}{16}(2s+1) d_e^2 \Omega \omega_{res}^2$.

This shift exceeds the homogeneous line width $\delta\omega \approx \omega_{res} / N_{osc}$, if the parameter of the distribution (2.6.18) satisfies the inequality

$$d_e^2 > \Delta x_0^2 \equiv 16 / N_{osc}\Omega\omega. \tag{2.6.19}$$

If

$$d_e^2 > \Delta x_1^2 \equiv 32 / \Omega\omega,$$

then $\Delta\omega_{res}$ exceeds also dissipation between the neighboring emission lines $\Delta\omega \approx 2\omega_{res}$ and these lines overlap due to inhomogeneous broadening.

Clearly, if the condition $d_e < \Delta x_0$ is obeyed, an inhomogeneous broadening plays no significant role and averaging over x_0 does not alter ΔE or, consequently, the gain. Therefore, the gain found in Ref. [85] is correct if $K_{str} << 1$ and $d < \Delta x_0$.

For sufficiently large values of Ω and *t,* necessary to ensure acceptable values of the lasing frequency ω and of the gain, the parameter Δx_0 is very small so that the condition (2.6.19) is always satisfied by real beams.

We shall now carry out averaging of the total output energy ΔE of Eq. (2.5.17) integrating term by term this sum with respect to x_0 allowing for the distribution function (2.6.18). In each term of the sum (2.5.17) the main contribution to the integrals with respect to x_0 is made by small ($\sim \Delta x_0$) regions near the points $x_0^{(s)}$ such that $u_s(x_0^{(s)}) = 0$:

$$(x_0^{(s)})^2 = \frac{4}{\Omega\omega}(2s+1) - \frac{\alpha^2}{\Omega^2} - \frac{2}{\gamma^2\Omega^2} \equiv \frac{8}{\Omega\omega}(s - s_{\min}) \geq 0, \tag{2.6.20}$$

where

$$s_{\min} \equiv \frac{\alpha^2\omega}{8\Omega} + \frac{\omega}{4\gamma^2\Omega} - \frac{1}{2}. \tag{2.6.21}$$

The argument of the Bessel functions $z(x_0)$ at the point $x_0 = x_0^{(s)}$

$$z(x_0 = x_0^{(s)}) \equiv z_s = s + \frac{1}{2} - \frac{\omega}{4\gamma^2\Omega}. \qquad (2.6.22)$$

In view of the need to consider the possibility of amplification of higher harmonics [$s = .(\alpha\gamma)^3$], when $z_s \le s$ and $z_s, s >> 1$, we shall express the Bessel functions in terms of the MacDonald functions [102]; then, the relevant factor is

$$F_s \approx \frac{2(s - z_s)}{\pi\sqrt{3}s} K_{2/3}\left[\frac{2(s - z_s)^{3/2}}{3\sqrt{s}}\right] \approx \frac{\omega K_{2/3}\left[\frac{\omega}{\omega_{\max}}\sqrt{\frac{s_{\min}}{s}}\right]}{2\sqrt{3}\pi\gamma^2\Omega s}, \qquad (2.6.23)$$

where

$$\omega_{\max} = 3\gamma^3\alpha\,\Omega. \qquad (2.6.24)$$

The range of values of *s* that make the main contribution to the average total energy ($\langle \Delta E \rangle$), emitted at a given frequency ω is found from the condition *s>smin*. At a fixed frequency ω the term in Eq. (2.5.17) with the number *s = s_min* becomes the dominant one after averaging with respect to x_0. This means that the resonance radiation appears mainly because of electrons which enter a strophotron near the axis ($x_0 \approx 0$) and are characterized by the coordinate scatter Δx_0. Such radiation is emitted at frequencies $\omega \approx \omega_{res}^{(s)}(x_0 = 0) = (2s+1)\omega_{res}(x_0 = 0) \approx (8s\Omega)/\alpha^2$.

Averaging of all the other terms with *s* > s_min gives rise to a nonresonance background, the intensity of which is less than the resonance value because of the factor $N_{osc}^{-3/2} << 1$.

The final result of averaging the sum (2.5.17) with respect to x_0 can be represented in the form

$$\langle \Delta \mathrm{E} \rangle = \frac{(eE_0)^2 t^{5/3} \left[\omega_{res}^{(s)}(x_0 = 0) \right]^{1/2}}{24\sqrt{2}\pi^{5/2} \tilde{d}_e \varepsilon \gamma^4 \Omega} K_{2/3}^2 \left[\frac{\omega}{\omega_{\max}} \right] F_{res}(\omega), \qquad (2.6.25)$$

where

$$F_{res}(\omega) = \int_{-\infty}^{\infty} \frac{d\xi}{\xi} \frac{d}{d\xi} \frac{\sin^2 \left[\xi^2 + \frac{\alpha^2 t}{8} \left(\omega - \omega_{res}^{(s)}(x_0 = 0) \right) \right]}{\left[\xi^2 + \frac{\alpha^2 t}{8} \left(\omega - \omega_{res}^{(s)}(x_0 = 0) \right) \right]^2} \qquad (2.6.26)$$

is the form factor of the resonance curve of width $\Delta\omega = .\frac{8}{\alpha^2 t} = \frac{2\omega_{res}(x_0 = 0)}{\Omega t} << 2\omega_{res}(x_0 = 0)$ and the value of the maximum is $\left[F_{res}(\omega) \right]_{\max} = .0.5$.

Finally, the gain experienced by an external wave of frequency ω is given by the expression

$$G = \eta \frac{8\pi N_e}{E_0^2} \langle \Delta \mathrm{E} \rangle = \eta \frac{(2\ln 2)^{1/2}}{\sqrt{2}\pi^{3/2}} \frac{N_e r_0 L^{5/3} \alpha^{1/2}}{d_e \gamma^{7/2} \Omega^{1/2}} \left(\frac{\omega}{\omega_{\max}} \right)^{1/2} K_{2/3}^2 \left[\frac{\omega}{\omega_{\max}} \right] F_{res}(\omega), \qquad (2.6.27)$$

where N_e is the density of electrons in a beam; $r_0 = e^2 / mc^2$ is the classical radius of an electron; $\eta = d_e / 2a(x_0 = 0) = d_e \Omega / 2\alpha$ is a factor which allows for the overlap of the electron beam and the wave being amplified.

The dependence of the gain *G* of Eq. (2.6.27) on the frequency ω exhibits a steep fall at $\omega > \omega_{\max}$, when the argument of the MacDonald function becomes large. Therefore, $\omega_{\max}$ of Eq. (2.6.24) is the maximum frequency in a free-electron laser of the strophotron type and right up to this frequency the gain can be significant.

2.7. CONCLUSIONS

Relativistic strophotron is a system in which fast electrons move along a potential “trough” produced hy quadrupole magnetic or electric lenses.

Spectral intensity of a spontaneous emission and the gain of an external wave in the strophotron are given by a superposition of contributions from emission or amplification at different (odd) harmonics of the main resonance frequency $\omega_{res}(x_0)$. The main resonance frequency is shown to depend on the initial conditions of the electron, and in particular on its initial transversal coordinate x_0. This dependence $\omega_{res}(x_0)$ is shown to give rise to a very strong inhomogeneous broadening of the spectral lines. The broadening can become large enough for the spectral lines to overlap with each other. The spectral intensity of a spontaneous emission and the gain are averaged over x_0. The averaged spectral intensity is showh to have only a very weakly expressed resonance structure, whereas in the averaged gain, the resonance peaks are shown to be much higher than the nonresonant background. A physical nature of these resonances remaining after averaging is discussed. The maximum achieveable averaged gain and frequency of the strophotron FEL are estimated.

Using (1.5.32) and (2.1.63) and taking $\omega \approx \omega_{\max}$, $d_e \approx \alpha/\Omega$, $K_{2/3}(1) \approx 0.5$, and $\left[\tilde{F}_{res}(\omega)\right]_{\max} \approx 0.5$, we find the follow ing formulas for the gain G and frequency ω :

$$G = 6.8\times10^{-3} \times \frac{N_e T_0 L^{5/2}}{\sqrt{d_e}\gamma^{7/2}} = 1.8\times10^{6} \times \frac{J(\mathrm{A}) T_0 L^{5/2}}{d_e^{5/2}\gamma^{7/2}} \qquad (2.7.1)$$

$$\omega = 5.3\times10^{7} \times \lambda^2 d_e g \qquad (2.7.2)$$

where g is the gradient of the static f ield in the strophotron and *J(A)* is the peak current in the beam (in amperes). When $\omega = \omega_{res}$ the gain *G* (2.7.1) does not depend on the static field of the strophotron. When $\omega \neq \omega_{res}$ the gain G depends on *g* only parametrically through $\omega \approx \omega_{\max}$ (1.5.32*)* (1.2.8) .

For $d_e = 1cm$, *J = 10* A, $\gamma = 10$, $g = 10^4 Oe/cm$, and *L = 3* m (65) (1.6.1) and (1.2.66) gives

$$G = 0.2\%, \quad \omega = 5.2 \times 10^{13} \ (\lambda = 36\mu).$$

These estimates indicate a possibility of using the strophotron to construct such a FEL in the IR region. Probably both the gain G and the frequency $\omega = \omega_{res}$ can be increased with the help of an additional optirnization of the system [e.g., by the use of a "trough" with a varying field gradient g = g *(z)*] .

We would like to indicate here two features of the strophoton FEL differentiating this device from the usual undulator FEL. *1)* The frequency $\omega = \omega_{res}$ linearly depends on the angle α under which the electron enters the system.

Hence, $\omega = \omega_{res}$ can be easily varied by a variation of α. *2)* The value of the "undulator" parameter K in the strophotron can be rather large. For example, the parameters used above for the estimates correspond to $\Omega \approx 2.2 \times 10^{10} s^{-1}$, $\alpha \approx 0.7$, $\alpha\gamma \approx 7$, $K(x_0 = 0) \approx 7$, and

$$s_{\max} \equiv \omega_{\max} / 2\omega_{res}(x_0 = 0) = \frac{3}{8}\left[K^3(x_0 = 0)\right] \approx 130.$$

It seems also to be worthwhile to summarize the conditions under which the results described are applicabie. These conditions are given by inequalities (1.2.26) , (1.2.30) , by the assumptions $\alpha << 1$, and $x_0\Omega \le d_e / \lambda_0 << 1$, $\Omega T \gg 1$, and also by the condition $d_e \approx \alpha / \Omega$ under which the factor η in (1.2.63) is not too small. The strongest restrictions result from the conditions $\alpha \gg 1$ and $\alpha\gamma >> 1$ which give, for $d_e \approx \alpha / \Omega$

$$(\lambda_0 / 2\pi) > d_e > \lambda_0 / 2\pi\gamma .$$

These inequalities are fulfilled for the parameters used above in estimates. We have ignored above both angle ($\Delta\alpha$ and energetic ($\Delta\varepsilon$) widths of the beam. This approximation is justified if

$$\Delta\alpha/\alpha, \quad \Delta\varepsilon/\varepsilon << \Delta\omega/\omega = .1/\Omega T.$$

The corresponding restrictions are not too strong because ΩT is really not too large ($\Omega T \approx 220$ in the example considered above).

nonlinear

Taking $\omega = \omega_{\max} \approx 3\gamma^3\alpha\,\Omega$, $s = s_{\min}(\omega = \omega_{\max}) \approx \frac{3}{8}(\alpha\gamma)^3$ [79] for the saturation parameter μ we obtain

$$\mu = \left(\frac{\sqrt{3}}{8\pi}\frac{eE_0\alpha^2\Omega}{mc}\right)^{1/2} t. \qquad (2.7.3)$$

A saturation occurs when $\mu > 2$, $E_0 \geq E_{0,sat}$ where the saturation field strength is given by

$$E_{0,sat} = \frac{32\pi mc}{\sqrt{3}e\Omega(\alpha t)^3}. \qquad (2.7.4)$$

Substituting here $g = 10^4 Oe/cm,\ L = 3m,\ \alpha = 0.7$ we find $E_0 = .10^3 V/cm$.

This estimate shows that the gain saturates at rather moderate field E_0 and hence the efficiency of the RS FEL is not too high. This result is not surprising because we have considered here an amplification at very high harmonics (s=100) . There is an evident way to increase the efficiency constructing a tapered RS FEL, i.e. a system with g=g(z).

Quant

Quantum-mechanical equations are derived for the amplitudes of the probabilities of transitions in a free-electron laser when transverse electron oscillations are due to a static potential, which is homogeneous in the direction of motion of the beam, but has a transverse gradient. The resonance frequency of the system is found and the linear gain is derived for the odd harmonics of this frequency. Averaging of the gain is carried out over the initial distribution of electrons in a transverse cross section of the beam. Estimates are obtained of the maximum lasing frequency and of the gain at this frequency.

Assuming that $\omega \approx \omega_{\max}$, $\alpha \approx d_e\Omega$, $(\eta \approx 0.5)$, $(K_{2/3}(1) \approx 0.5$, and $[F_{res}(\omega)]_{\max} \approx 0.5$, we can write Eqs. (1.4.24) and (1.4.25) in the form

$$\omega = 5.3\times 10^7 \gamma^2 d_e g, \tag{1.4.28}$$

$$G = 7.6\times 10^{-3} N_e r_0 L^{5/2} / d_e^{1/2}\gamma^{7/2} = 2.1\times 10^6 J_{\max} r_0 L^{5/2} / d_e^{5/2}\gamma^{7/2} \tag{1.4.29}$$

where g is the gradient of the field in a parabolic potential trough on the axis of the system OZ (expressed in gauss per centimeter in the case of magnetic quadrupole lenses); $J_{\max}$ is the total maximum current in the beam (in amperes). It is interesting to note that the gain G of Eq. (1.4.29) at the maximum frequency $\omega = \omega_{\max}$ is independent of g.

Adopting in these estimates the value $d_e = 1cm$, $J_{\max} = 100A$, $\gamma = 10$ A, $L = 2$ m, and $g = 10$ kG/cm, we find that

$$\omega = 5.3\times 10^{13}\,\sec^{-1}(\lambda = 36\mu), \quad G \approx 1\%.. \tag{1.4.30}$$

These estimates show that in the case of the above parameters of the beam and other components of the system, it is in principle possible to construct a strophotron free-electron laser operating in the infrared range.

We shall now note the singularities which distinguish a strophotron free-electron laser from a conventional undulator laser.

1.The undulator parameter K_{str} depends only on the initial conditions and not on the relativistic factor *γ;* it can be numerically large. In the above example, we have

$K_{str}(x_0 = 0) = \alpha\gamma \approx 7.7$. The high value of K_{str} shows that the maximum serial number of the harmonic in which more or less effective amplification is still possible is high: $s_{\max} = \omega_{\max} / 2\omega_{res}(x_0 = 0) \approx 0.3[(1/2)K_{str}(x_0 = 0]^3 \approx 168$.

The gain profile extends from $\omega_{res}(x_0 = 0)$ to $2s_{\max}\omega_{res}(x_0 \approx 0)$ and it consists of a large number of equidistant narrow gain lines.

2.The frequency of a wave amplified in a strophotron depends strongly on the angle at which an electron enters a system. For a fixed value of *s,* we have $\omega \propto 1/\alpha^2$, whereas at $s = s_{\max}$, we find that $\omega \propto \alpha$. Hence, it follows that a strophotron provides an opportunity for continuous tuning of the emission frequency because of a change in the entry angle α.

Clearly, there is a margin for increasing the gain. In particular, preliminary shaping of an electron beam so that the angle of entry of electrons into a strophotron depends on the initial transverse coordinate x_0 is a promising approach. In this sense the optimal distribution is that for which the quantity $\alpha^2 + x_0^2\Omega^2$ remains constant over the whole beam diameter. This can be achieved by, for example, use of a focusing device based on electron-optical lenses.

In a system of this kind there is no strong inhomogeneous broadening because of the distribution of electrons over x_0, so that the gain

of Eq. (29) increases by a factor $(d_e / \Delta x_0)^2$, i.e., by the two orders of magnitude.

A quantum-mechanical description of the motion of an electron in classical fields is not in conflict with the fact that the final results obtained here do not contain the Planck constant $\hbar$. It is natural to expect the main results of the present study apply also in the classical approach [79].

Chapter 3

Channeling on an intense light wave and in Wiggler with Inhomogeneous Magnetic Field

The Chapter based on 5 publications [116,117,161,162,163]

3.1. Overview

The existing free-electron lasers (FELs) are based on the magnetic undulator principle [103]. There have been many suggestions for the construction of FELs based on different schemes[80] and an alternative FEL utilizing channeling in a crystal has been proposed [61,62].

Similar ideas underlie the proposal to construct FELs on the basis of "macroscopic channeling," i.e., by creating potentials of the type represented by a flat parabolic trough ("strophotron") by a system of magnetic or electrostatic quadrupole lenses [104,59,66,79,105].

We shall propose and describe an FEL in which an electron beam interacts with a strong standing wave and the conditions are favorable for the channeling of electrons between constant-phase planes. In this way the channeling concept is extended to the interaction of electrons with an optical electromagnetic field.

The radiation emitted by electrons interacting with a standing wave under the above-barrier transmission conditions was considered recently in Ref. [106]. To the best of our knowledge the possibility of channeling of electrons by a standing wave has not been discussed in the literature.

3.2. CHANNELING OF ELECTRONS BY A STANDING WAVE

We shall consider a relativistic classical electron in the field of a standing wave in the geometry shown in Fig. 1. The potential of a standing wave will be described in the form ($c = 1$)

$$\overrightarrow{A^{(0)}} \parallel Oy \quad , \qquad A^{(0)} = \frac{1}{\omega_0}[E_1 \cos\omega_0(t-x) - E_2 \cos\omega_0(t+x)] \qquad (3.2.1)$$

where $E_{1,2}$ are the amplitudes of the electric-field intensity of two traveling waves propagating in opposite directions along the Ox axis and forming a standing wave and ω_0 is the frequency of this standing wave.

The Hamilton function of an electron in the field described by Eq.(3.2.1) is

$$H = \left[P_z^{\,2} + P_x^{\,2} + \left(P_y - eA^{(0)}\right)^2 + m^2\right]^{1/2} \approx p_z + \frac{1}{p_z}\left[p_x^{\,2} + \left(P_y - eA^{(0)}\right)^2 + m^2\right], \tag{3.2.2}$$

where $P_{x,y,z}$ are the components of the electron momentumalong the $Ox, Oy, and\ Oz$ directions, and $P_{x,z} = p_{x,z}$. It is assumed, that the electron momentum p_z along the Oz axis is much greater than the other components of the momentum p_x and p_y . If, moreover, we assume that the translational velocity of an electron along the Oy axis is zero, then $P_y = 0$ and the electron transverse-motion Hamiltonian governed by the second term on the right-hand side of the second equation in the system (3.2.2) becomes

$$H_x \approx \frac{1}{2\varepsilon_0}\left[p_x^{\,2} + e^2 A^{(0)2} + m^2\right] \tag{3.2.3}$$

where it is assumed that $p_z \approx \varepsilon \approx \varepsilon_0$ and ε_0 is the initial electron energy. We shall assume that the motion of an electron along the

axis is slow compared with oscillations of the field described by Eq. (3.2.1) in each of the two traveling waves, i.e., we shall assume that the characteristic time of such motion is much greater than $2\pi/\omega_0$. In this approximation the Hamiltonian of Eq. (3.2.3) can be averaged over the fast oscillations which are included in the explicit dependence of $A^{(0)}$ on time *t,* so that instead of Eq. (3.2.3) we have

$$\overline{H_x} = \frac{{p_x}^2}{2\varepsilon_0} - \frac{e^2 E_1 E_2 \cos 2\omega_0 x}{2{\omega_0}^2 \varepsilon_0} + const \approx \frac{{p_x}^2}{2\varepsilon_0} + \frac{e^2 E_1 E_2 x^2}{\varepsilon_0} + const \ .$$

(3.2.4)

In the last approximate equality it is assumed that $2\omega_0|x| < \pi,$ i.e., that the amplitude a of the oscillations of an electron along the x axis is low compared with $\lambda_0/4$, where λ_0 is the wavelength of each of the two traveling light waves in Eq. (3.2.1).

Averaging of the Hamiltonian H_x of Eq. (3.2.3), dependent on time *t*, over fast oscillations is a generalization of the corresponding procedure used earlier for nonrelativistic electrons in the theory of the Kapitza-Dirac effect [107].

The Hamiltonian of Eq. (3.2.4) describes the motion of an electron in a potential (Fig. 5a)

$$U(x) = -\frac{e^2 E_1 E_2}{2{\omega_0}^2 \varepsilon_0} \cos 2\omega_0 x \ , \qquad (3.2.5)$$

which in the case of low values of x represents a flat parabolic through. In this approximation the motion along the *Ox* axis is in the form of harmonic oscillations of frequency

$$\Omega = \frac{e(2E_1 E_2)^{1/2}}{\varepsilon_0} \equiv \frac{eE_0 2^{1/2}}{\varepsilon_0} \ , \qquad (3.2.6)$$

where $E_0 \equiv (E_1 E_2)^{1/2}$.

On the basis of this assumption about the relative slowness of the motion along the *Ox* axis the frequency Ω and the field intensities E_1 and E_2 are limited from above by the condition

$$\Omega < \omega_0 \qquad (3.2.7)$$

The height of the potential barrier of Eq. (3.2.5) (relative to U_{min}) is

$$U_{max} - U_{min} = \frac{1}{2}\varepsilon_0(\Omega/\omega_0)^2 \ll \varepsilon_0 \qquad (3.2.8)$$

It follows from this inequality that the barrier height is much less than the longitudinal electron energy, but it can be considerably greater than the energy of transverse motion.

This condition reduces to the requirement of the smallness of the amplitude of oscillations of an electron along the Ox axis:

$$a < \lambda_0/4. \qquad (3.2.9)$$

The oscillation amplitude a is governed by the initial parameters of an electron the angle of entry of the electron *a* (in the xz plane relative to the Oz axis) and the initial transverse coordinate x_0 of the electron (Fig. 5a) :

$$a = (x_0{}^2 + \alpha^2/\Omega^2)^{1/2}. \qquad (3.2.10)$$

The entry angle

α can be selected to be zero, which gives $a = x_0$. The condition (3.2.9) then means that approximately half the electrons characterized by $U(x) < 0$ is confined by the channel, whereas the other half characterized by $U(x) > 0$ undergoes strongly nonharmonic oscillations or it passes above the barrier (Fig. 5b).

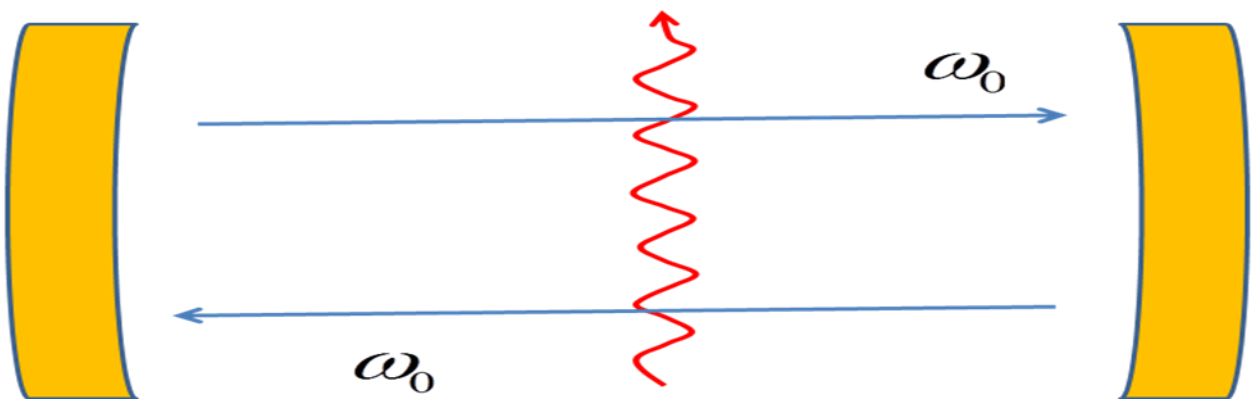

a)

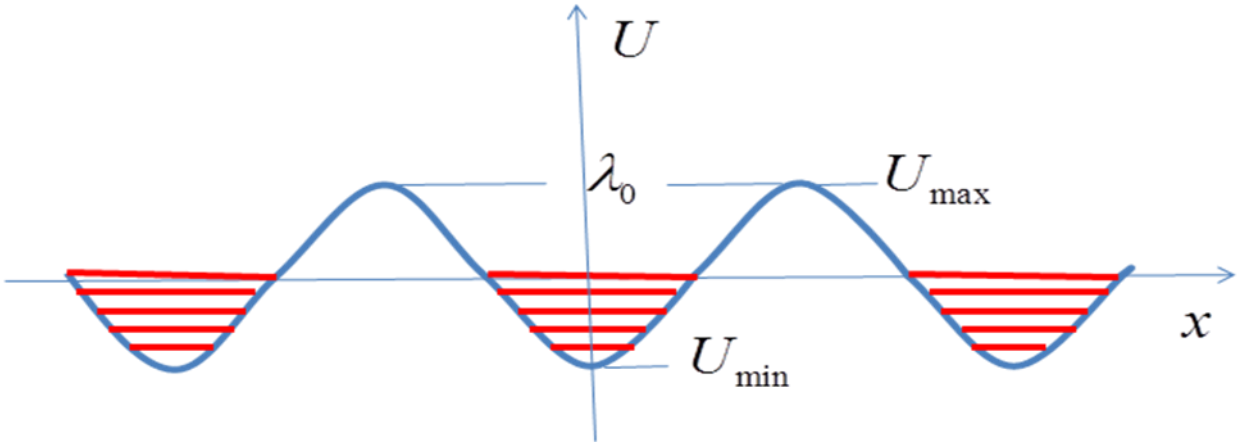

b)

FIG. 5. Schematic representation of the proposed free-electron laser utilizing a standing electromagnetic wave (a) and the effective potential energy of an electron in the field of the standing wave (b).

3.3. Interaction with the Field of a Wave being Amplified and Separation of Fast and Slow Motion

We shall now assume that an electromagnetic wave of frequency ω travels along the Oz axis and the vector potential $\vec{A} \parallel Ox$ of this wave is described by

$$A = \frac{E}{\omega} cos\omega(t - z), \qquad (3.3.11)$$

where E is the amplitude of electric field.

The exact equations of motion of an electron in fields governed by the sum of the vector potentials $\overrightarrow{A^{(0)}}$ of Eq.(3.2.1) and Is $\vec{A}$ of Eq.(3.3.11) are of the form

$$\begin{cases} \frac{dp_x}{dt} = eE(1-v_z)\sin\omega(t-z) - ev_y(E_1\sin\omega_0(t-z) + E_2\sin\omega_0(t+z)), \\ \frac{dp_y}{dt} = e[-E_1(1-v_x)\sin\omega_0(t-z) + E_2(1+v_x)\sin\omega_0(t+z)], \\ \frac{dp_z}{dt} = -ev_xE\sin\omega(t-z), \end{cases}$$

(3.3.12)

where $v_i = p_i/\varepsilon$ are the components of the electron velocity and ε is the electron energy.

The rate of change of the electron energy is equal to the work carried out by the total electric field E_{tot}

$$\frac{d\varepsilon}{dt} = -e\boldsymbol{vE_{tot}} = -ev_xE\sin\omega(t-z) - ev_y[E_1\sin\omega_0(t-z) - E_2\sin\omega_0(t+z).$$

(3.3.13)

The second equation in the system (3.3.12) has the exact solution

$$p_y = \varepsilon v_y = e\left(\frac{E_1}{\omega_0}\cos\omega_0(t-z) - \frac{E_2}{\omega_0}\cos\omega_0(t+z)\right) = eA^{(0)}. \quad (3.3.14)$$

The frequency ω can be less or greater than ω_0. However, in the difference $t-z$ the main terms balance out ($z \approx t$), so that a dependence of the $\sin\omega(t-z)$ type becomes slow

compared with $\sin\omega_0 t$ or $\cos\omega_0 t$.

In Eqs. (3.3.12) and (3.3. 13) we shall separate the motion into fast (of frequency $\geq \omega_0$ ***2*** w,) and slow, compared with with $\sin\omega_0 t$ and $\cos\omega_0 t$, and we shall find equations for the slowly varying components of the velocities and momenta of an electron. We shall assume that the rapidly varying components of ε, x and of the projections of the velocity v_x, v_z and of the momentum p_x , p_z are small compared with the slow components. Substituting the solution given by Eq. (3.3.14) into Eq. (3.3.13) and into the

first equation in the system (3.3.12), we shall average the right-hand sides of these equations over fast oscillations (of frequencies ω_0 and $2\omega_0$). This gives

$$\begin{cases} \frac{dp_x}{dt} = eE(1 - v_z)\sin\omega(t - z) - \frac{e^2 E_1 E_2}{\varepsilon\omega_0}\sin 2\omega_0 x, \\ \frac{dp_z}{dt} = \frac{d\varepsilon}{dt} = -ev_x E\sin\omega(t - z)\,. \end{cases} \tag{3.3.15}$$

If, as usual, the change in the energy E of an electron during one pass through an FEL is small compared with its initial value ε_0 then in the last term on the right-hand side of the first equation in the system (3.3.15) we can replace ε with ε_0. If $p_z \approx \varepsilon_0 \gg p_x,\ eA^{(0)}, m$, then in accordance with the results of Sec. 2 we can distinguish in the electron energy ε a small fraction corresponding to the energy of transverse motion $\varepsilon_\perp$, which in turn can be represented by a sum of the kinetic and potential energies,

$$\varepsilon_\perp = \frac{p_x^{\,2}}{2\varepsilon_0} + U(x), \tag{3.3.16}$$

where $U(x)$ is described by Eq. (3.2.5).

Comparing the resultant equations (3.3.15) and (3.3.16) with the equations for an FEL of the relativistic strophotron type,x we can readily demonstrate that at low values of x [in accordance with the condition (3.2.9)], when $\sin 2\omega_0 x$ can be approximated by a linear function of x in the first equation of the system (3.3.15), there is a complete analogy with a flat electrostatic trough. The role of the effective field gradient along the trough axis is played by the quantity

$$g_{eff} = \frac{2eE_1E_2}{\varepsilon_0}. \tag{3.3.17}$$

3.4. GAIN

Using the above analogy with an electrostatic trough and employing the published results of Refs. [66] and [79], we can write down directly-without any calculations -the change in the energy of an electron in one pass across a standing wave:

$$\Delta\varepsilon = -\frac{e^2 E_0{}^2 t^3 \Omega^2 a^2 \omega}{32\varepsilon_0}\left(1 - v_{z0} + \frac{a^2\Omega^2}{2}\right)\sum_{s=0}^{\infty}\frac{d}{du_s}\left(\frac{\sin u_s}{u_s}\right)^2 [J_s(Z) - J_{s+1}(Z)]^2, \tag{3.4.18}$$

where t is the time for the transit of an electron across a standing wave, v_{z0} is the initial velocity of an electron along the Oz axis, a is the amplitude of the oscillations of an electron described by

Eq. (3.2.10), $Z = 1/(s\omega\Omega a^2)$, and

$$u_s = \frac{t}{2}\left[\omega\left(1 - v_{z0} + \frac{a^2\Omega^2}{4}\right) - \Omega(2s+1)\right]. \tag{3.4.19}$$

At high electron energies such that $\varepsilon \gg m$, we have $1 - v_{z0} = (2\gamma^2)^{-1}$,where $\gamma = \varepsilon/m$ is the usual relativistic factor.

It is known, that if $\gamma\Omega a \gg 1$, the sum in Eq. (3.4.18) includes comparable contributions of many terms with $s \gg 1$, i.e., effective amplification is possible at high odd harmonics of the fundamental resonance frequency. Then, the dependence of u_s on the initial transverse coordinate x_0 [via $a(x_0)$ of Eq. (3.2.10)] and the averaging of $\Delta\varepsilon$ over x_0, i.e., over the distribution of electrons in a transverse cross section of the beam, become important. This complicates greatly the process of calculation of the gain nd reduces its value. The gain decreases also considerably on increase in the harmonic number. We shall therefore consider here only the simpler case when $\gamma\Omega a \ll 1$, $Z \ll 1$, and $s = 0$, so that the dependence of the resonance

frequency on x_0 can be ignored and the averaging over x_0 reduces simply to replacement of a^2 with $\overline{a^2} \sim {a_{max}}^2 = {\lambda_0}^2/16$ of Eq. (3.2.9). In this case the change in the electron energy $\Delta\varepsilon$ of Eq. (3.4.18) is related directly to the gain $G = -8\pi N_e \, \Delta\varepsilon E^{-2}$ (N_e is the electron density in the beam). The gain G and the frequency of the wave being amplified are now given by

$$G = \frac{\pi^3 r_0 N_e l^3 \Omega^3}{16\gamma {\omega_0}^2 {v_{z0}}^3} \frac{d}{du}\left(\frac{\sin u}{u}\right)^2, \quad u = \frac{t}{2}[\omega(1 - v_{z0}) - \Omega], \tag{3.4.20}$$

$$\omega \approx \Omega(1 - v_{z0})^{-1}, \tag{3.4.21}$$

where $r_0 = e^2/mc^2$ is the classical radius of an electron and $l = v_{z0}t$ is its amplification length.

It has been assumed so far that the field of a standing wave is homogeneous. In fact, this is not true: in the focal region where $E_0 = E_0(z)$ and in accordance with the definition of Eq. (6), we have $\Omega = \Omega(z)$. The dependence of the oscillation frequency Ω on the coordinate z along the direction of motion of an electron makes the equations more complex. They can be solved if the dependence $\Omega(z)$ is slow, which is true if $\Omega_0 d \gg 1$, where $\Omega_0 = [\Omega(z)]_{max} = \Omega(0)$ and d is the laser beam diameter. Without considering the details of the solution (see paragraph 3.5), we shall give the results

$$G \approx -2\pi^2 e^2 N_e a^2 (1 - v_0)\Omega_0 \, \omega d^2 {v_0}^{-2} {\varepsilon_0}^{-1} \Phi(x)\Phi'(x), \tag{3.4.22}$$

where $\Phi(x)$ is the Airy function,

$$x = -\Delta(d^2/\Omega_0 {v_0}^2)^{1/2}, \Delta = \Omega_0 - \omega(1 - v_0), v_0 = v_{z0}, v_{x0} = v_{y0} = 0. \tag{3.4.23}$$

The spectral dependence of the gain $G(\omega)$ is shown qualitatively in Fig. 2, where for the sake of comparison we included also the dependence $G(\omega)$ in a homogeneous field [Eq. (3.4.20)]..

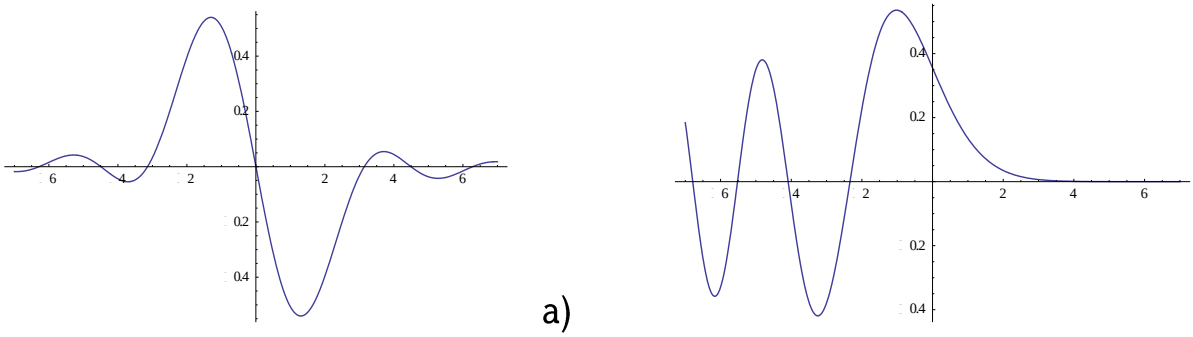

a)

b)

FIG. 6. Spectral dependence of the gain in homogeneous (a) and inhomogeneous (b) fields.

3.5. Inhomogeneity of the field in the focal region

If the standing wave electromagnetic field be homogeneous in the transverse direction and had sharp edges, then the length in the gain formula for amplification will be coincided with the beam diameter. But really it is not so.

The field $E=\sqrt{E_1E_2}$ in nonuniform in fjcal region. It can usually approximated by Gaussian dependence

$$E_0 = E_{0,\max} e^{-z^2/d^2}, \quad d = d_0/\sqrt{2\ln 2}, \tag{3.5.1}$$

where d_0 is a diameter of laser beam defined as the offset from the axis z=0, where the radiation intensity is reduced by half compared with its maximum value.

Since, the electron oscillation frequency Ω (3.2.6) depends on E_0, and therefore on z dependences on z (or on time t) will appear in resonance detuning u (3.4.19). This fact forces us to revise a derivation of formulas for the change of the electron energy $\Delta\varepsilon$ (3.4.18) and gain G (3.4.20). Finally, such revision lead to certain connection between l and d_0 in (3.4.20) and also qualitative changes in the form of dispersion dependence $G(\omega)$.

On the basis of the equation (3.3.13) is easy to see, that in the second-order perturbation theory on E the electron energy change rate is mainly determined by the expression

$$\frac{d\varepsilon^{(2)}}{dt} = ev_x^{(0)}\omega z^{(1)} E\cos\omega(t - z^{(0)}) \tag{3.5.2}$$

where $v_x^{(0)} \equiv \dot{x}^{(0)}$, $z^{(0)}$ and $z^{(1)}$ are solutions of (3.3.15) in the zero and first order on field E.

Equations for z(t) and x(t) following from (3.3.15) in the same approximation as earlier (paragraph 3.4) turn to

$$\begin{aligned} \varepsilon\ddot{z} &= -eE\dot{x}(1-\dot{z})\sin\omega(t-z), \\ \ddot{x} + \Omega^2(z)x &= -eE(1-\dot{z}-\dot{x}^2)\sin\omega(t-z), \end{aligned} \tag{3.5.3}$$

where frequency Ω is determined by the same equation (3.2.6), but now depends on z in accordance with (3.5.1).

In the first order approximation on E from equation (3.5.3) one can find

$$\begin{aligned} z^{(0)} &= z_0 + v_{z0}t, \\ \ddot{x}^{(0)} + \Omega^2(z_0 + v_{z0}t)x &= 0. \end{aligned} \tag{3.5.4}$$

We assume $\Omega(t)$ dependence is slow

$$\left|\frac{d\Omega}{dt}\right| \ll \Omega^2 \tag{3.5.5}$$

In this approximation

$$x^{(0)}(t) \approx x_0 \cos\left(\int_{-\infty}^{t} \Omega(z_0 + v_{z0}t')dt' \right) \qquad (3.5.6)$$

For simplicity is accepted that $\dot{x}(-\infty) = 0$, $(\alpha = 0)$, and hence $v_{z0} = v_0$.

The condition (3.5.5) is certainly not satisfied at very big values of $|t|$, t<0, at the same time, however Ω(3.5.1) is very small, and $x^{(0)} \approx x_0$. Therefore, the solution (3.5.6) can be considered as a result of "sewing" of solution $x^{(0)} \approx x_0$ in the region large negative t and quasiclassic solution (3.5.6) in the region small values of | t | , where the condition (3.5.5) is fulfilled. In this region under $z_0 + v_0 t = .d_0$ the condition (3.5.5) takes form

$$\Omega(d_0 / v_0) >> 1 \qquad (3.5.7)$$

i.e. the number of oscillations on the length d_0 should be larger.

The first order correction to $z^{(0)}$ (3.5.4) is easy to find using Eqs. (3.5.3), (3.5.4), (3.5.6). It contains integral over function

$$\begin{aligned} &\sin \int_{-\infty}^{\infty} \Omega(z_0 + v_0 t')dt' \cdot \sin\left[\omega(1-v_0)t - \omega z_0\right] = \\ &\frac{1}{2}\left\{ \cos\left[\int_{-\infty}^{\infty} \Omega(z_0 + v_0 t')dt' - \omega(1-v_0)t + \omega z_0 \right] - \right. \\ &\left. - \cos\left[\int_{-\infty}^{\infty} \Omega(z_0 + v_0 t')dt' + \omega(1-v_0)t - \omega z_0 \right] \right\} \approx \\ &\frac{1}{2}\cos\left[\int_{-\infty}^{\infty} \Omega(z_0 + v_0 t')dt' - \omega(1-v_0)t + \omega z_0 \right] \end{aligned} \qquad (3.5.8)$$

In the last approximate equality term varying with the total frequency $= .\Omega + \omega(1-v_0)$ is omitted. Neglect of such rapidly oscillating terms is based on the resonance approximation, in which it is assumed that the difference $\Omega - \omega(1-v_0)$ is small compared with $\omega(1-v_0)$. Using approximate equality (3.5.8) $z^{(1)}$ is presented as

$$z^{(1)} = \frac{eEx_0(1-v_0)}{2\varepsilon_0} \int_{-\infty}^{t} dt' \int_{-\infty}^{\infty} dt'' \Omega(z_0 + v_0 t'') \cdot \cos\left[\int_{-\infty}^{t'''} dt''' \Omega(z_0 + v_0 t''') - \omega(1-v_0)t''' - \omega z_0 \right] \qquad (3.5.9)$$

According to (1.5.6), (3.5.1), (3.5.4) frequency $\Omega(z_0 + v_0 t)$ has a maximum value $\Omega_{\max} \equiv \Omega_0$ at $t = t_0 = -z_0 / v_0$. We carry out the change of variables in (3.5.9) $t' \to t' + t_0$, $t'' \to t'' + t_0$, $t''' \to t''' + t_0$. The argument of cosine (3.5.9) can be presented as

$$\varphi + \int_0^{t''} dt''' \Omega(v_0 t''') - \omega(1 - v_0) t'' \approx \varphi + t''\Delta - \frac{t'' v_0^2 \Omega_0}{3d^2} \qquad (3.5.10)$$

where

$$\varphi = \int_{-\infty}^{0} dt \Omega(v_0 t) - \omega z_0 / v_0 \qquad (3.5.11)$$

is constant phase, which depends on the unperturbed value of the coordinate z_0 at the moment t=0,

$$\Delta = \Omega_0 - \omega(1 - v_0) \qquad (3.5.12)$$

is resonance detuning in the region of maximal E .

The condition of application above used resonance approximation has a form

$|\Delta| << \Omega_0$.

In approximate equality (3.5.10) it was accepted $t'' << d_0 / v_0$. It is this region of small t , which gives the main contribution to $z^{(1)}$ (3.5.9). The value of corresponding interval Δt is determined from the condition , that the last term in right side of equation (3.5.10) equals of the order of unity.

$$\Delta t = . \left(\frac{d^2}{\Omega_0 v_0^2} \right)^{1/3} \qquad (3.5.13)$$

Integrand in (3.5.9) oscillates rapidly out of the interval $|t''| < \Delta t$, and contribution of corresponding intervals in $z^{(1)}$ is small. By this reason integrand dependence on t' has almost stepped character: it is small at $t' < \Delta t$, rapidly increases in $-\Delta t < t' < \Delta t$ and remains constant at $t' > \Delta t$. Taking into account this and neglecting changes of $\Omega(t'')$ on the small

interval $-\Delta t < t'' < \Delta t$, i.e. assuming $\Omega(t'') \approx \Omega_0$ one can write from equqtion (3.5.9)

$$z^{(1)} = \frac{eEx_0(1-v_0)\Omega_0}{2\varepsilon_0}(t-t_0)\theta(t-t_0)\int_{-\infty}^{\infty} dt' \cos\left[\varphi + t'\Delta - \frac{t'^3 v_0^2 \Omega_0}{3d^2}\right] \tag{3.5.14}$$

where $\theta(x) = 0$ at x < 0, and $\theta(x) = 1$, at x > 0 .

Product $v_x^{(0)} \cos\omega(t - z^{(0)})$

$$\begin{aligned} v_x^{(0)} \cos\omega(t - z^{(0)}) &= \frac{x_0\Omega(t)}{2}\sin\left[\int_{-\infty}^{t} \Omega(z_0 + v_0 t'')dt' - \omega(1-v_0)t - \omega z_0\right] \\ &\approx -\frac{x_0\Omega(t)}{2}\sin\left[\varphi + (t-t_0)\Delta - \frac{(t-t_0)^3 v_0^2\Omega_0}{3d^2}\right]. \end{aligned} \tag{3.5.15}$$

As a result electron energy change rate, using $z^{(1)}$(t) (3.5.14), can be presented in the form

$$\begin{aligned} \frac{d\varepsilon^{(2)}}{dt} &= -\frac{e^2E^2x_0^2(1-v_0)\Omega_0^2\omega^2}{4\varepsilon_0}(t-t_0)\theta(t-t_0) \\ &\sin\left[\varphi + \Delta(t-t_0) - \frac{v_0^2\Omega_0}{3d^2}(t-t_0)^3\right]\int_{-\infty}^{\infty} dt' \cos\left[\varphi + t'\Delta - \frac{t'^3 v_0^2\Omega_0}{3d^2}t'^3\right]. \end{aligned} \tag{3.5.16}$$

We integrate this equation with respect to time, average over the constant phase φ and find the average change in the electron energy

$$\begin{aligned} \Delta\bar{\varepsilon} &= -\frac{e^2E^2a^2(1-v_0)\Omega_0^2\omega}{8\varepsilon_0}\int_0^{\infty} tdt\int_{-\infty}^{\infty} dt'\sin\left[\Delta(t-t') - \frac{v_0^2\Omega_0}{3d^2}(t^3 - t'^3)\right] \\ &= -\frac{\pi e^2E^2a^2(1-v_0)\Omega_0\omega}{4v_0^2\varepsilon_0}\Phi(x)\Phi'(x) \end{aligned} \tag{3.5.17}$$

where $\Phi(x)$ Ayry function and her argument is

$$x = -\Delta 1/3\left(\frac{d^2}{v_0^2\Omega_0^2}\right) \tag{3.5.18}$$

Now taking into account known asymptotic expansions of Ayry function at |x|<<1, x > 0, x < 0 one can find

$$\Delta\bar{\varepsilon} = -\frac{\pi e^2 E^2 a^2 (1-v_0)\Omega_0 \omega d^2}{4v_0^2 \varepsilon_0} \exp\left\{-\frac{4}{3}|\Delta|^{3/2} \frac{d}{v_0 \Omega_0^{1/2}}\right\}, \ \Delta < 0 \qquad (3.5.19)$$

$$\Delta\bar{\varepsilon} = -\frac{\pi e^2 E^2 a^2 (1-v_0)\Omega_0 \omega d^2}{8v_0^2 \varepsilon_0} \cos\left\{\frac{4}{3}\Delta^{3/2} \frac{d}{v_0 \Omega_0^{1/2}}\right\}, \ \Delta > 0. \qquad (3.5.20)$$

Under condition $\Delta >> \left(\frac{v_0}{d}\right)^{2/3} \Omega_0^{1/3}$, but $|\Delta| << \Omega_0$.

Under condition $\Delta < 0 \quad (\omega > \Omega_0/(1-v_0))$, $\Delta\bar{\varepsilon} > 0$ (3.5.19) , i.e. the energy of ekectron increases, amplification effect of wave with frequency ω is absent.

Under condition $\Delta > 0 \quad (\omega < \Omega_0/(1-v_0))$, $\Delta\bar{\varepsilon}$ oscillates, changing the sign. Several maxima occur in this frequency range in amplification, gathering with decreasing frequency and their locations are determined from condition

$$\frac{4}{3}\Delta_n^{3/2} \frac{d}{v_0 \Omega_0^{1/2}} = (2\mathrm{n}+1)\pi, \quad \mathrm{n} = 0,1,2,.... \qquad (3.5.21)$$

The gain qualitative spectral dependence $G(\omega)$ is shown in Fig. 6., where the gain spectrum of the homogeneous fild is presented too for comparison. Amplification line maximum numbers $n_{\max}$ having approximately the same height is determined from the condition of application of resonance approximation $\Delta_n < \Omega_0$, which gives

$$n_{\max} = .\left(\frac{\Omega_0 d}{v_0}\right)^{3/2} >> 1. \qquad (3.5.22)$$

The width of each maximum has a same order as distance between them

$$\frac{\Delta\omega}{\omega} = .\frac{1}{n}, \quad n > 1. \qquad (3.5.22)$$

3.6. On the Influence of Magnetic Field Inhomogeneity of the Plane Wiggler on the Spectral Distribution of Spontaneous Radiation and on the Gain

The free electron lasers (FEL) are high power tunable sources of coherent radiation that are used in science research, for heating of plasma, in the physics of condensed media, in atomic, molecular and optical physics, in biophysics, biochemistry, biomedical engineering etc. The radiation produced by present-day FELs has a range from the millimeter to the X-rays waves, which no other similar high intensity tunable sources cover [110,111]. In contemporary science this range is of interest both from the viewpoint of fundamental research and application.

In FELs [112,43] the kinetic energy of relativistic electrons moving through the spatially modulated magnetic field of a wiggler is used for production of coherent radiation. The frequency of radiation is determined by the energy of electrons, the space period and the magnetic field strength of a wiggler. This permits a retuning of FEL to be made in a wide range as opposed to the atomic and molecular lasers. In a conventional FEL the magnetic field of wiggler is constant, but it is inhomogeneous in the transverse direction [113]. It is important to take into account this inhomogeneity that causes a composite motion of electrons: fast undulator oscillations along the wiggler axis and slow strophotronic ones [79,66,105,114-119] in the transverse direction.

In the present work we describe the equations of motion of electrons moving along the wiggler axis, the magnetic field in which is spacially inhomogeneous. The aim of the work is to calculate the spectral distribution of spontaneous radiation as well as the gain.

3.7. EQUATIONS OF MOTION

The vector potential of the magnetic field of undulator has the form [120]

$$\mathbf{A}_w = -\frac{H_0}{q_0}\cosh q_0 x \sin q_0 z \mathbf{j}, \tag{3.7.1}$$

where H_0 is the magnetic field strength, $q_0 = 2\pi/\lambda_0$, λ_0 the wiggler period, $\mathbf{j}$ the unit vector in *y* direction. Bellow we consider the problem in the paraxial approximation

$$q_0 x << 1. \tag{3.7.2}$$

Taking into account (3.7.2) the expression for magnetic field (3.7.1) acquires the form:

$$H_x = H_0\left(1+\frac{q_0^2 x^2}{2}\right)\cos q_0 z; \quad H_y = 0; \quad H_z = H_0 q_0 x \sin q_0 z. \tag{3.7.3}$$

The equations of motion ($c=1$)

$$d\mathbf{p}/dt = e[\mathbf{vH}] \tag{3.7.4}$$

in magnetic field (3.7.3) have the form:

$$\ddot{x} = -\frac{eH_0 q_0}{\varepsilon} x\dot{y}\sin q_0 z,$$

$$\ddot{y} = \frac{eH_0}{\varepsilon}\left[\dot{z}\left(1+\frac{q_0^2 x^2}{2}\right)\cos q_0 z + q_0 x\dot{x}\sin q_0 z\right], \tag{3.7.5}$$

$$\ddot{z} = \frac{eH_0}{\varepsilon}\left(1+\frac{q_0^2 x^2}{2}\right)\dot{y}\cos q_0 z,$$

and the energy change is

$$d\varepsilon/dt = 0, \quad \varepsilon = \text{const}.$$

Expression (3.7.5) was obtained taking into account that $p_{x,y,z} = v_{x,y,z}\varepsilon$.

It is seen that

$$\left(\frac{q_0 x^2}{2}\sin q_0 z\right)' = q_0 x\dot{x}\sin q_0 z + \frac{{q_0}^2 x^2}{2}\dot{z}\cos q_0 z\,, \tag{3.7.6}$$

$$\int \dot{z}\cos q_0 z dt = \int \cos q_0 z dz = \frac{\sin q_0 z}{q_0}\,. \tag{3.7.7}$$

Using relations (3.7.6) and (3.7.7) we obtain after integration of the second equation of (3.7.5)

$$\dot{y} = \frac{eH_0}{\varepsilon q_0}\left(1 + \frac{{q_0}^2 x^2}{2}\right)\sin q_0 z\,. \tag{3.7.8}$$

By substitution of (3.7.8) in the first and third equations of (3.7.5) we obtain with due regard for (3.7.2)

$$\begin{cases} \ddot{x} = -\left(\dfrac{eH}{\varepsilon}\right)^2 x\sin^2 q_0 z, \\ \ddot{z} = -\dfrac{1}{2q_0}\left(\dfrac{eH}{\varepsilon}\right)^2 \sin 2q_0 z\left(1 + {q_0}^2 x^2\right). \end{cases} \tag{3.7.9}$$

Averaging the first equation of (3.7.9) with respect to the wiggler period $2\pi / q_0$ and taking into account that $\overline{(\sin^2 q_0 z)} = 1/2$, we have

$$\ddot{x} + \Omega^2 x = 0\,. \tag{3.7.10}$$

The latter has a solution

$$x = a_0\cos(\Omega t + \theta_0), \tag{3.7.11}$$

where

$$\Omega = \frac{eH_0}{\sqrt{2}\varepsilon}, \quad a_0 = \sqrt{{x_0}^2 + \frac{\alpha^2}{\Omega^2}}, \quad \cos\theta_0 = \frac{x_0}{a_0}, \quad \sin\theta_0 = -\frac{\alpha/\Omega}{a_0}. \tag{3.7.12}$$

The averaging of the second equation of (3.7.9) gives

$$(\ddot{z})^{(0)} = 0, \quad (\dot{z})^{(0)} = v, \quad (z)^{(0)} = vt. \tag{3.7.13}$$

Taking into account (3.7.11) and (3.7.13) the second equation of (3.7.9) admits a solution

$$\delta z = -\frac{\Omega^2}{2q_0{}^2}t + \frac{\Omega^2}{2q_0{}^3}\sin 2q_0 t + \frac{a_0{}^2\Omega^2}{16q_0}\sin\{2(q_0+\Omega)t + 2\theta_0\} + \frac{a_0{}^2\Omega^2}{16q_0}\sin\{2(q_0-\Omega)t - 2\theta_0\}.$$

(3.7.14)

Thus, for $z = z^{(0)} + \delta z$ we have

$$z = t\left(1 - \frac{1}{2\gamma^2} - \frac{\Omega^2}{2q_0{}^2}\right) + \frac{\Omega^2}{4q_0{}^3}\sin 2q_0 t + \frac{a_0{}^2\Omega^2}{16q_0}\sin\{2(q_0+\Omega)t + 2\theta_0\} + \\ + \frac{a_0{}^2\Omega^2}{16q_0}\sin\{2(q_0-\Omega)t - 2\theta_0\}. \tag{3.7.15}$$

Here the allowance was made for the fact that $1 - v = 1/(2\gamma^2)$, where $\gamma = \varepsilon/(mc^2)$ is the relativistic factor, *m* the electron mass, c the velocity of light and ε the electron energy.

The obtained results are valid in case of the following approximations:

$$a_0 q_0 < 1, \quad \frac{\Omega}{q_0} < 1, \quad a_0\Omega < 1. \tag{3.7.16}$$

The electrons perform fast (undulator) oscillations in the longitudinal direction (along the wiggler axis), whereas in the transverse one they perform slow (strophotronic) oscillations in the direction of *x*. axis and fast (undulator) oscillations in the direction of y axis.

3.8. SPONTANEOUS RADIATION

Using the solutions for x(3.7.11), $\dot{y}$(3.7.8) and z(3.7.15) one can find the spectral intensity of spontaneous radiation, that in the direction of z axis (wiggler axis) is determined by formula [67]

$$\frac{d\varepsilon}{d\omega do} = \frac{e^2\omega^2}{4\pi^2}\left|\int_0^T dt\left[\mathbf{n}\times\mathbf{v}\right]e^{i\omega(t-z)}\right|^2, \tag{3.8.17}$$

where do is an infinitesimal solid angle in the direction of z axis and T is the time of electron flight through the undulator.

Using formula [102]

$$e^{-iA\sin x} = \sum_{n=-\infty}^{\infty} J_n(\mathrm{A})e^{-inx} \tag{3.8.18}$$

with Bessel functions $J_n(\mathrm{A})$, and omitting cumbersome calculations we obtain

$$\frac{d\varepsilon}{d\omega do} = \frac{e^2\omega^2\Omega^2T^2}{8\pi^2{q_0}^2}\sum_{n,m,k=-\infty}^{\infty}\left(I_{n+1,k,m}-I_{n,k,m}\right)^2\left(\frac{\sin u}{u}\right)^2, \tag{3.8.19}$$

where

$$\begin{cases} u = \dfrac{T}{2}\left[\omega\left(\dfrac{1}{2\gamma^2}+\dfrac{\Omega^2}{2{q_0}^2}\right)-(2\mathrm{n}+1)q_0-2m\Omega\right], \\ I_{n,k,m} = J_{n-k}\left(Z_1\right)J_{\frac{k+m}{2}}\left(Z_2\right)J_{\frac{k-m}{2}}\left(Z_2\right), \\ Z_1 = \dfrac{\omega\Omega^2}{4{q_0}^3}, Z_2 = \dfrac{\omega{a_0}^2\Omega^2}{4q_0}. \end{cases} \tag{3.8.20}$$

Equation (3.8.19) describes the radiation spectrum consisting of a superposition of spectral lines localized at combinated frequencies of odd harmonics $(2\mathrm{n}+1)\omega_{\mathrm{res,und}}$ of undulator resonant frequency and even harmonics $2m\omega_{\mathrm{res,str}}$ of strophotronic resonant frequency, where $m,n=0,1,2,3,\ldots$. Here

$$\omega_{\mathrm{res,und}} = \frac{2\gamma^2q_0}{1+\gamma^2\Omega^2/{q_0}^2}, \qquad \omega_{\mathrm{res,str}} = \frac{2\gamma^2\Omega}{1+\gamma^2\Omega^2/{q_0}^2}. \tag{3.8.21}$$

3.9. GAIN

The gain may be found from the expression for spontaneous radiation (3.8.19) with the help of the Madey theorem [70]. To avoid the use of some assumptions made at obtaining of these general relations for the spontaneous and stimulated radiations, we preferred to obtain the gain immediately from the equations of motion.

Let an electromagnetic wave with vector potential propagates along *z* axis (wiggler axis)

$$\mathbf{A}_w = -\frac{E_0}{\omega}\sin\omega(t-z)\mathbf{i}\,, \tag{3.9.22}$$

where ω is the frequency of electromagnetic wave, E_0 the strength of electric field, $\mathbf{i}$ an unit vector in the *x* direction.

The equations of electron motion in the wiggler (3.7.3) and electromagnetic wave (3.9.22) fields are

$$\begin{cases} \dfrac{dp_x}{dt} = -eH_0 q_0 x v_y \sin q_0 z + eE_0\left(1-v_z\right)\cos\omega(t-z), \\ \dfrac{dp_y}{dt} = eH_0\left[v_z\left(1+\dfrac{q_0^2x^2}{2}\right)\cos q_0 z + q_0 v_x x \sin q_0 z\right], \\ \dfrac{dp_z}{dt} = -eH_0 v_y\left(1+\dfrac{q_0^2x^2}{2}\right)\cos q_0 z + eE_0 v_x\cos\omega(t-z), \end{cases} \tag{3.9.23}$$

and the energy change is

$$\frac{d\varepsilon}{dt} = e\boldsymbol{v}\boldsymbol{E} = eE_0 v_x \cos\omega(\mathrm{t}-\mathrm{z}). \tag{3.9.24}$$

The linear gain (field independent) is determined by the second order electric field strength $(\propto E_0^2)$ and is obtained from equation (3.9.24):

$$\frac{d\varepsilon}{dt} = eE_0 v_x^{(1)}\cos\omega\left(t-z^{(0)}\right) + eE_0\omega v_x^{(0)} z^{(1)}\sin\omega\left(t-z^{(0)}\right). \tag{3.9.25}$$

To obtain the gain one needs to find the first-order corrections in the field $(\propto E_0)$ $x^{(1)}(t),\ z^{(1)}(t)$ to $x^{(0)}(t)$ (3.7.11) and $z^{(0)}(t)$ (3.7.15).

The first-order corrections obtained from (3.9.23) satisfy the following equations:

$$\begin{cases} \dfrac{dp_x^{(1)}}{dt} = -\varepsilon_0\Omega^2 x^{(1)} + eE_0\left(1 - v_z^{(0)}\right)\cos\omega\left(t - z^{(0)}\right), \\ \dfrac{dp_z^{(1)}}{dt} = eE_0 v_x^{(0)}\cos\omega\left(t - z^{(0)}\right). \end{cases} \tag{3.9.26}$$

Then we find $x^{(1)}(t),\ z^{(1)}(t)$ from equations (3.9.26) and using the expressions for $x^{(0)}(t)$ (3.7.11) and $z^{(0)}(t)$ (3.7.15) obtain an expression for the energy radiated by the electron $\Delta\varepsilon = \int_0^T \dfrac{d\varepsilon}{dt}dt$ during T time of flight through the undulator, as well as for the gain

$$G = \frac{4\pi N_e}{E_0^{\,2}}\Delta\varepsilon, \tag{3.9.27}$$

where N_e is the concentration of electrons in the beam.

Since all these calculations are simple, but laborious and cumbersome, here we give only the resultant expression:

$$G = \frac{e^2\omega^2\Omega^2 N_e T^3}{4\pi q_0^{\,2}\gamma^2}\left(1 + \gamma^2\frac{\Omega^2}{q_0^{\,2}}\right)\sum_{n,m,k}^{\infty}\left(I_{n+1,m,k} - I_{n,m,k}\right)^2 \frac{d}{du}\left(\frac{\sin u}{u}\right)^2, \tag{3.9.28}$$

where the notations (3.8.20) were used. Equation (3.9.28) describes the gain comprising the superposition of spectral lines, localized at combinated frequencies of odd harmonics of $(2\mathrm{n}+1)\omega_{\mathrm{res,und}}$ undulator resonant frequency and even harmonics of $2m\omega_{\mathrm{res,str}}$ strophotronic resonant frequency, where $m, n = 0,1,2,3,\ldots$, and $\omega_{\mathrm{res,str}}$ and $\omega_{\mathrm{res,und}}$ are determined by formula (3.8.21).

3.10. CONCLUSION

ESTIMATES AND DISCUSSION

It should be pointed out straight away that within the existing capabilities of laser energetics we can hardly expect amplification and emission on the basis of the proposed scheme at very high frequencies. The most realistic possibility is the use of such a scheme in the infrared frequency range.

We shall express the maximum gain G of Eq. (2.1.22) and the frequencies of the oscillations [Eq. (2.1.6)] and of the wave being amplified [Eq. (2.1.21)] in terms of the energy in a laser pulse W and the pulse duration τ:

$$\Omega_0 = 3.27\times 10^{11}\frac{W^{1/2}}{\gamma d(c\tau)^{1/2}}, \quad \omega = \frac{\Omega_0}{1-v_0}, \quad G = 4.5\times 10^{-12}\frac{N_e {d_0}^2\gamma}{\gamma^2-1}\left(\frac{\Omega_0}{\omega_0}\right)^2, \quad (24)$$

where W is in joules, whereas W and $c\tau$ are in centimeters. We shall assume that a standing wave is created by CO_2 laser radiation characterized by $\lambda_0 = 9.6\times 10^{-4} cm$ and $\omega_0 = 1.96\times 10^{14} sec^{-1}$. We shall assume that, in accordance with the condition of Eq. **(7),** we have $\Omega_0/\omega_0 = 1/3$. In this case the following relationship lies between $W, \gamma, d,$ and τ:

$$\frac{1}{\gamma d}\left(\frac{W}{c\tau}\right)^{1/2} = 2\cdot 10^2. \quad (25)$$

We shall consider the specific wavelength of the radiation to be amplified; $\lambda = 16\mu m$ ($\omega = 1.18\times 10^{14} s^{-1}$). It then follows from Eqs. (2.1.7) and (2.1.21) that if $\Omega_0 = \omega_0/3$, we must ensure that the electron velocity is

$v_0 = 0.44c$, which corresponds to $\gamma = 1.116$ and to a kinetic energy $\varepsilon_{kin} = (\gamma - 1)mc^2 = 65KeV$. We shall assume that the pulse duration τ is such that $d = v_0\tau$ (this is the minimum time τ in which an electron can cross the whole interaction region). In this case Eq. (2.1.25) gives the following relationship between W and d:

$$W = 1.12\times10^5 d^3. \tag{26}$$

The gain is then given by

$$G = 9.8\times10^{-16} N_e W^{2/3}. \tag{27}$$

If $= 1\text{J}$, ($d = 2.1 \times 10^{-2}\text{cm}, \tau = 1.6\,\text{ps}$), we find that $G \approx 1\%$ for $N = 10^{13} cm^{-3}$, which corresponds to a peak current density $j = 50kA/cm^2$. The very high current density has to be maintained over a short distance equal to the diameter d of the laser beam.

If W=30J, ($d = 6.41 \times 10^{-2}\text{cm}, \tau = 4.9\,\text{ps}$), we find that $G \approx 1\%$ for $N = 10^{12} cm^{-3}$, i.e., the peak current density should be $j = 5kA/cm^2$.

It follows from these estimates that, in principle, the above scheme can ensure the necessary amplification in the infrared frequency range. The value of the wavelength to be amplified, $\lambda = 16\mu m$, selected in our estimates is in no way unique: similar estimates are obtained also for the amplification at other frequencies in the infrared range.

In a future communication we shall give a more detailed analysis of the scheme described above, including its possible modifications aimed at increasing the gain.

It is shown that as a result of the allowance for magnetic field inhomogeneity, some additional peaks appear in the spectral distribution of spontaneous radiation and in the gain. Out of the multitude of these peaks one can obtain ultrashort pulses using the well-known mode-locking method. The peaks in the spectral distribution of spontaneous radiation and of the gain are localized at combinated frequencies of the odd harmonics of $(2n+1)\omega_{res,und}$ undulator resonant frequency and even harmonics of $2m\omega_{res,str}$ strophotronic resonance frequency. In case of an undulator with constant magnetic field the peaks are localized at odd harmonics of undulator resonant frequency $\omega_{res,und} = \frac{2\gamma^2 q_0}{1+\gamma^2 \Omega^2/q_0^2}$, and in case of a strophotron they are localized at odd harmonics of strophotronic resonant frequency $\omega_{res,str} = \frac{2\gamma^2 \Omega}{1+\gamma^2 \Omega^2/q_0^2}$. One may conclude thus, that due to the presence of inhomogeneity in the magnetic field in the plane wiggler these two systems (wiggler with the constant magnetic field and the strophotron) are integrated in one unit and there appear peaks in the spectral distribution of spontaneous radiation and in the gain at combined (odd undulator and even strophotronic) resonant frequencies.

Chapter 4.

Free Electron Laser Without Inversion

The Chapter based on 4 publications [54,55,165,173]

4.1. Overview

A threshold condition for amplification without inversion in a free-electron laser without inversion (FELWI) is determined. This condition is found to be too severe for the effect to be observed in an earlier suggested scheme because a threshold intensity of the field to be amplified appears to be too high. This indicates that alternative schemes have to be found for making the creation of an FELWI realistic.

4.2. The threshold conditions for an FELWI (Single Particle Approximation)

According to the realization [47], of FELWI is strongly related to a deviation of electrons from their original direction of motion owing to interaction with the fields of an undulator and co-propagating light wave. The deviation angle appears to be proportional to energy gained or lost by an electron during its passage through the undulator. Owing to this, a subsequent regrouping of electrons over angles provides regrouping over energies. In principle, a proper installation of magnetic lenses and turning magnets after the first undulator in an FELWI can be used in this case for making faster electrons running over a longer trajectory than the slower ones [50]. This is the *negative-dispersion* condition that is necessary for getting *amplification without inversion* [44].

It is clear that the described mechanism can work only if the interaction-induced deviation of electrons (with a characteristic angle α) is larger than the natural angular width beam of the electron

$$\alpha > \alpha_{beam} \tag{4.2.1}$$

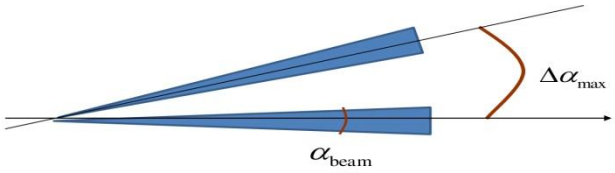

Fig. 7. The scheme of electronbeamafter first wiggler.

As the energy gained/lost by electrons in the undulator and the deviation angle are proportional to the field strength amplitude of the light wave to be amplified, condition (3.2.1) determines the threshold light intensity, only above which amplification without inversion can become possible. This threshold intensity is estimated below.

In the noncollinear FEL the electron slow-motion phase is defined as

$$\varphi = qz + \mathbf{kr} - \omega t \tag{4.2.2}$$

where $q = 2\pi / \lambda_0$ and λ_0 is the undulator period, $\mathbf{k}$ and ω are the wave vector and frequency of the wave to be amplified, $|\mathbf{k}| = \omega / c$, $\mathbf{r} = \mathbf{r}(t)$ is the

electron position vector and $z = z(t)$ is its projection on the undulator axis. Let the initial electron velocity $\mathbf{v}_0$ be directed along the undulator axis Oz. Let the undulator magnetic field $\mathbf{H}$ be directed along the x-axis. Let the light wave vector $\mathbf{k}$ be lying on the (xz) plane under an angle θ to the *z*-axis. Let the electric field strength $\boldsymbol{\varepsilon}$ of the wave to be amplified be directed along the *y*-axis, as well as its vector potential $\mathbf{A}_{wave}$ wave and the undulator vector potential $\mathbf{A}_{und}$, where

$$A_{wave} = \frac{c\varepsilon_0}{\omega}\cos(\mathrm{kr} - \omega t) \quad , \qquad A_{und} = \frac{H_0}{q}\cos qz \, , \tag{4.2.3}$$

and ε_0 and H_0 are the amplitudes of the electric component of the light field and of the undulator magnetic field. The geometry corresponds to that in [47].

The slow motion phase (4.2.2) obeys the usual pendulum equation

$$\ddot{\varphi} = -a^2 \sin\varphi \ , \tag{4.2.4}$$

Where

$$a = \frac{ce\sqrt{\varepsilon_0 H_0}}{E_0} , \tag{4.2.5}$$

$E_0 = \gamma mc^2$ is the initial electron energy and γ is the relativistic factor. If *L* is the undulator length, the ratio *L*/*c* is the time it takes for an electron to pass through the undulator.

The product of this time and the parameter *a* of equation (4.2.5) is known [43] as the saturation parameter μ,

$$\mu = \frac{aL}{c} = \frac{eL\sqrt{\varepsilon_0 H_0}}{E_0} \quad . \tag{4.2.6}$$

Amplification in an FEL (with $H_0 = const$) is an efficient one as long as $\mu \le 1$. At $\mu > 1$ the FEL gain *G* falls. The condition $\mu = .1$ determines the saturation field $\varepsilon_{0,sat}$ and intensity I_{sat}. For example, at $L = 3m$, $H_0 = 10^4 Oe$, $\gamma = 10^2$, we have $\varepsilon_{0,sat} = .1.2 \times 10^2 V/cm$ and $I_{sat} = .2 \times 10^5 W/cm^2$. In our further estimates of the FELWI threshold field and intensity we will have to keep in mind that it is hardly reasonable to consider fields stronger than the saturation field $\varepsilon_{0,sat}$.

The pendulum equation (4.2.4) has the first integral of motion (kinetic + potential energy of a pendulum = const).

$$\frac{\dot{\varphi}^2}{2} - a^2 \cos[\varphi(t)] = \text{const} \tag{4.2.7}$$

Initial conditions of equations (4.2.4) and/or (4.2.7) are given by

$$\varphi(0)=\varphi_0 \qquad \dot{\varphi}(0)=\delta\equiv\frac{\omega-\omega_{res}}{2\gamma^2}$$

(4.2.8)

where φ_0 is an arbitrary initial phase, δ is the resonance detuning and ω_{res} is the resonance frequency for noncollinear FEL given by

$$\omega_{res}=\frac{cq}{1-(v_0/c)\cos\theta}\approx\frac{2\gamma^2 cq}{1+\gamma^2\theta^2} \tag{4.2.9}$$

with $\theta=\square(\mathrm{k},\mathrm{Oz})$.

In the case of a not too long undulator and sufficiently small energy width of the electron beam, a characteristic value of the detuning is evaluated as $|\delta|=.1/t=.c/L$.

The rate of change of the electron energy is defined as the work produced by the light field per unit time, and as it is well known [43], this rate is connected directly with the second derivative of the slow-motion phase

$$\frac{dE}{dt}=\frac{E}{2cq}\ddot{\varphi}\approx\frac{E_0}{2cq}\varphi. \tag{4.2.10}$$

The last approximate expression is written down in the approximation of a small change of the electron energy, $|E-E_0|\ll E_0$. In this approximation, equation (10) gives the following expression for the total gained or lost energy of a single electron after a passage through the undulator:

$$\Delta E = E\left(\frac{L}{c}\right) - E_0 \approx \frac{E_0}{2cq}\left[\dot{\varphi}\left(\frac{L}{c}\right) - \delta\right]. \qquad (4.2.11)$$

In the weak-field approximation ($\mu << 1$) one can use the iteration method with respect to a of equation (4.2.5) for solving equation (4.2.7). The zero-order solution is evident and very simple: $\dot{\varphi}^{(0)} \equiv \delta$. In the first order in a^2 one obtains

$$\dot{\varphi}^{(1)} = \frac{a^2}{\delta}\left(\cos(\varphi_0 + \delta \cdot t) - \cos(\varphi_0)\right) \approx \frac{a^2 L}{c} = \frac{\mu^2 c}{L} \quad . \qquad (4.2.12)$$

By substituting this expression into equation (3.2.11) we find the first-order change of the electron energy

$$\Delta E^{(1)} = \frac{E_0}{2cq}\dot{\varphi}^{(1)} \approx \frac{E_0}{2cq}\frac{\mu^2 c}{L} = \mu^2 E_0 \frac{\lambda_0}{4\pi L}. \qquad (4.2.13)$$

Of course, both $\dot{\varphi}^{(1)}$ and $\Delta E^{(1)}$ turn zero being averaged over an arbitrary initial phase φ_0. But here we are interested in maximal achievable rather than mean values of these quantities, and these maximal values are given just by estimates of equations (4.2.12) and (4.2.13).

In accordance with the results of [47], equation (14), and [50], equation (4.2.13), a transverse velocity v_x and energy ΔE acquired by an electron after a passage through the undulatorare directly proportional to each other

$$v_x = c\theta \frac{\Delta E}{E_0} \quad , \tag{4.2.14}$$

which gives in the first order the following estimate of the electron deviation angle α:

$$\alpha \approx \frac{v_x^{(1)}}{v_0} \approx \frac{v_x^{(1)}}{c} = \theta \frac{\Delta E^{(1)}}{E_0} \sim \theta\mu^2 \frac{\lambda_0}{4\pi L} \sim \mu^2 \frac{d\lambda_0}{4\pi L^2} \quad , \tag{4.2.15}$$

where *d* is the electron beam diameter and we took $\theta = d / L$.

As said above, in the framework of a linear theory we can consider only such fields at which $\mu \le 1$. Moreover, consideration of the case $\mu >> 1$ has no sense at all, because the corresponding fields are too strong and because saturation makes the gain too small. For these reasons let us take for estimates the maximal value of the saturation parameter μ compatible with the weak-field approximation, $\mu = .1$. Let us take also $\lambda_0 = 3cm$, *d* = 0.3 cm and $L = 3 \times 10^2 cm$. Then, we get from equation (4.2.15) the following estimate of the electron deviation angle:

$$\alpha \sim 10^{-6}. \tag{4.2.16}$$

At weaker fields and smaller values of the saturation parameter μ the deviation angle α is even smaller than that given by equation (4.2.16). But even at μ = 1 the angle α is very small. To make the estimate (4.2.16) compatible with the condition of equation (4.2.1) one has to provide a

natural electron beam angular divergence smaller than 10^{-6}. Unfortunately, such weakly diverging electron beams hardly exist. For example, the microtron accelerator in Yerevan produces a with about 3 or 4 orders of magnitude larger angular divergence, and this can be a rather serious obstacle for attempts of creating an FELWI. Hence, the creation of an FELWI requires invention of alternative schemes in which threshold restrictions would be much weaker than in the considered one. The interaction between noncolinear laser and relativistic electron beams in static magnetic undulator has been studied within the framework of dispersion equations. For a free-electron laser without inversion (FELWI), the threshold parameters are found. The large-amplification regime should be used to bring an FELWI above the threshold laser power.

4.3. Collective Regime

Usually FEL [112,43] use the kinetic energy of relativistic electrons moving through a spatially modulated magnetic field(wiggler) to produce coherent radiation. The frequency of radiation is determined by the energy of electrons, the spatial period of magnetic field and the magnetic field strength of the wiggler. This permits tuning a FEL in a wide range unlike atomic or molecular lasers. However for purposes of achievement of short-wavelength region of generation there are important possible limitations of the FEL gain.

The idea of inversionless FEL or FELWI (FEL without inversion) was formulated and discussed by M.O. Scully and coworkers [44-48]. In the

usual FEL the gain G is an anti-symmetric function of the detuning $\Delta = E - E_{res}$, where E and E_{res} are the electron energy and its resonance value in the undulator. The integral of such a gain over Δ (or E) is equal to zero. By definition, in the FELWI $\int G(E)dE \neq 0$ and mainly, $G > 0$. Moreover, if in the usual FEL in the "hot-beam" regime (i.e., in the case of a broad electron energy distribution) the averaged gain is proportional to the squared inverse width of the distribution function, $(\delta E)^{-2}$, in FELWI $G(E) \propto (\delta E)^{-1}$. Hence, in the case of energetically wide beams the FELWI gain can exceed significantly the gain of the usual FEL. This advantage of FELWI (compared to usual FELs) makes such devices particularly interesting and potentially perspective in short-wave-length regions.

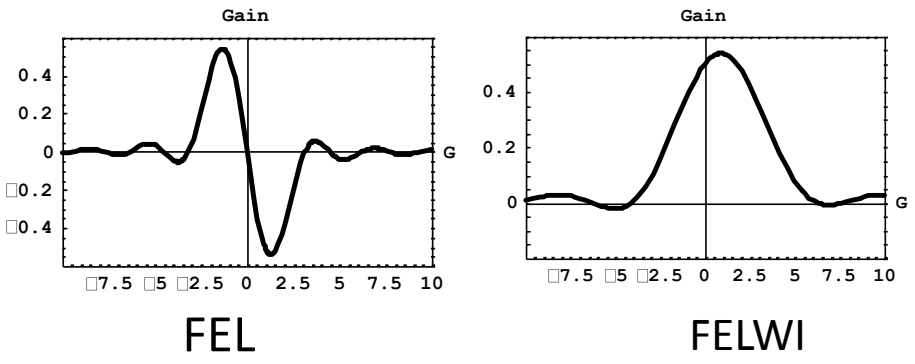

$$\int G(\Omega)d\Omega = 0 \qquad \int G(\Omega)d\Omega > 0$$

Fig.8. The Gain vs detuning, Ω ≡ ω(v0 – vres)/c, which characterizes deviation of the electron velocity or the laser frequency from the resonance condition for usual FEL(left) and for FELWI(right).

The conditions $\int G(E)dE \neq 0$ and $\$G > 0$ imply that amplification of light can take place almost at any position of the resonance energy E_{res} with respect the energy $E = E_0$, at which the electron distribution function $f(E)$ is maximal. In FELWI amplification can take place both at positive and negative slopes of the function $f(E_{res})$, as well as its peak. This feature of FEWI is in a great contrast with that of FEL, where amplification can take place only at the positive slope $f(E_{res}) > 0$. This last condition is easily interpreted as the condition of inversion: in FEL the number of electrons with $E > E_{res}$ must be larger than with $E < E_{res}$. In FELWI amplification can occur independently of the relation between E_{res} and $E(0)$. This means that for amplification in FELWI it does not matter whether the number of particles with energy $E > E_{res}$ is larger than with energy $E < E_{res}$ or not. This explains an origin of the concept "without inversion" for the kind of FEL to be considered.

More specifically, the idea of FELWI is based on a two-wiggler scheme with a specially organized dispersion region between the wigglers. In principle, the two-wiggler scheme is widely used in normal FELs. This scheme (often referred to as an optical clystron) is known to provide a somewhat higher gain with narrower amplification band than in a single-wiggler FEL but it does not provide conditions for amplification without inversions. The reason is in features of devices between two wigglers of a FEL. In all the existing two-wiggler FEL these devices (or no special devices at all) are the so-called positive-dispersion devices. This means that the higher-energy electrons of a beam cross a space between the first and second wigglers in a shorter time than the lower-energy ones. For creation

of FELWI, a device between the wigglers must be rather unusual: it must provide the negative-dispersion regime in which the faster electrons spend longer time in the dispersion region than the slower ones. This goal does not look unachievable but this is not easy to reach it.

A concept of FELWI is related to that of Lasing Without Inversion (LWI) [49] in atomic systems: three-level systems or systems with autoionizing atomic levels. In both cases effects of amplification without inversion are explained by interference. But specific kinds of interference in FELWI and atomic systems are significantly different. In atomic systems amplification without inversion is attributed to interference of different channels of transitions between the same initial and final atomic states. In contrast, interference in FELWI has a purely classical character. A typical scheme of FELWI involves two wigglers and a dispersion zone between them. Field-induce corrections to classical electron trajectories acquired in the first and second wigglers interfere with each other. A proper construction of the dispersion zone can give rise to such a form of interference which provides the described above spectral features of the FELWI gain.

4.4. The Threshold and Deviated Angle

The basic idea of FELWI [44-48,50,51] is that the electrons, that have passed the first undulator have a dispersion of the transverse velocity, and as a consequence of the angle between the vector of velocity and the wiggler axis, and this dispersion is directly connected to final gain of energy.

Therefore the selection of a direction of electron motion is equivalent to the selection of energy, that basically allows to change in a controllable way the length of the drift region of electrons with different energies. This mechanism can work only if the spread of the angle α, arising as a result of interaction of electrons with the field in the first wiggler of FELWI, is larger than the natural dispersion of the directions in the electron beam, $\Delta\alpha_{beam}$. This circumstance leads to the occurrence of the threshold for laser radiation power at the point of entry of the FELWI's first wiggler.

The interaction of electron beam with laser field can be described by laws of conservation for momentum $\mathbf{p}_e + \mathbf{p}_L = \mathbf{p}_e' + \mathbf{p}_L'$ and energy $\varepsilon_e + \varepsilon_L = \varepsilon_e' + \varepsilon_L'$. Here $\mathbf{p}_e$ and $\mathbf{p}_e'$ are initial and final momentums of electrons, $\mathbf{p}_L$ and $\mathbf{p}_L'$ are initial and final momentums of laser field; ε_L and $\varepsilon_{L'}$ are initial and final energies of light beam and ε_e and $\varepsilon_{e'}$ are initial and final energies of electrons. The density of electromagnetic wave momentum is $P_L = (1/4\pi c)[\mathbf{EB}] = \mathbf{k}\omega/(4\pi c)\mathbf{A}_L^2$, where $\mathbf{A}_L$ is an amplitude of a vector-potential of laser field.

We can write for $\mathbf{A}_{L'} = \mathbf{A}_L \exp(k''L)$, where k'' is a spatial growth rate of laser field in a medium of an electron beam; L is a length of interaction. From law of conservation we can expect that $|\Delta p| = |p_e' - p_e| = |p_L' - p_L| = \mathbf{A}_L^2 \exp[(2k''L) - 1]$. We can see that the change of electron momentum $|\Delta p|$ depends on the spatial growth rate k'': with the growth rate k'' rising, the change of electron momentum rises too. This means that for noncolinear interaction the deviation of electron from its original direction depends on both the spatial growth rate k'' and the initial amplitude A_L of laser field. The growth rate k'' is a function on electron

beam current; and the amplitude depends on laser power at the entrance of undulator. Therefore, the condition $\alpha > \alpha_{beam}$ leads to the threshold of either the laser power at the entrance of undulator or the electron beam density.

We consider the induced radiation by a mono-energetic beam of electrons propagating in a wiggler. We assume that the static magnetic field of a plane undulator $\mathbf{A}_w$ is independent on the transverse coordinates x and y. Also we approximate the static magnetic field by a harmonic function $\mathbf{A}_w = A_w \mathbf{e}_y = \left(A_0 e^{-i\mathbf{k}_w \mathbf{r}} c.c.\right)\mathbf{e}_y$, where $\mathbf{k}_w = (0,0,k_w)$ is the wiggler wave vector; "c.c." denotes the complex conjugation, $\mathbf{e}_y$ is the unit vector along y axis. The wiggler field causes an electron to oscillate along the y-axis. For this reason, the electron interacts most efficiently with a light wave if the latter is linearly polarized. We assume that the vector potential of the laser wave has a linear polarization $\mathbf{A}_L = A_L(t,x,z) = a^+ e^{i(\mathbf{k}-\mathbf{k}_w)\mathbf{r}-i\omega t}$.

The dispersion equation of EM oscillations in the plasma like electron beam medium is an algebraic equation of power four for wave vector $\mathbf{k}$ (see equation (2) in [52]). Therefore, there are four solutions k_j describing two beam waves, slow and fast, having the forms $k = \omega/u \pm \sigma\omega_b$ (σ is a shape factor), and two electromagnetic waves, one of which extends to the direction of the beam moving while another propagates to the opposite direction.The solution of the linearized equations for slow motion of the electron in the xz-plane is [52,53]:

$$\delta \mathbf{v}_{\perp} = K^2 \frac{c^2}{\gamma_0^3} \sum_{j=1}^{4} \frac{\beta_{1j} \mathbf{k}_j - \frac{\omega}{c^2} \beta_{2j} u}{D_{b(j)}} a_j e^{i\mathbf{k}_j \mathbf{r}_{\perp} - i\omega t} + c.c$$

(4.4.1)

Here $a_j = a_{+j} / A_0$ is the dimensionless initial amplitude of wave j with wave vector k_j, j numbers four branches of oscillations in the electron beam medium: two laser waves and two beam waves, $\vec{\mathbf{u}} = (-u \sin\alpha; 0; u \cos\alpha)$ is the electron velocity; "c.c." denotes the complex conjugation. $D_b = (\omega - \mathbf{ku})^2 - \Omega_b^2$ is the dispersion function of electron beam wave associated with the beam frequency Ω_b, where $\Omega_b^2 = \omega_b^2 \left[1 - (\mathrm{ku})^2 / (kc)^2\right] / \gamma_0$. Here $\omega_b^2 = 4\pi e^2 n_b / m$ is square of the Langmuir frequency of the electron beam corresponding density n_b. K is the undulator strength parameter, defined as normalized dimensionless vector-potential of the undulator magnetic field $K = \frac{e}{mc^2} |A_0|$. The total relativistic factor of electrons γ_0 is defined as $\gamma_0 = \sqrt{1+2K^2} \left(1 - u^2 / c^2\right)^{-1/2}$. The coefficients β_1 and β_2 are $\beta_1 = \gamma_0 \left(\omega - (k_0 u)\right) - \omega_b^2 (k_0 u) / (k_0 c)^2$ and $\beta_2 = \gamma_0 \left(\omega - (k_0 u)\right) - \omega_b^2 / \omega$.

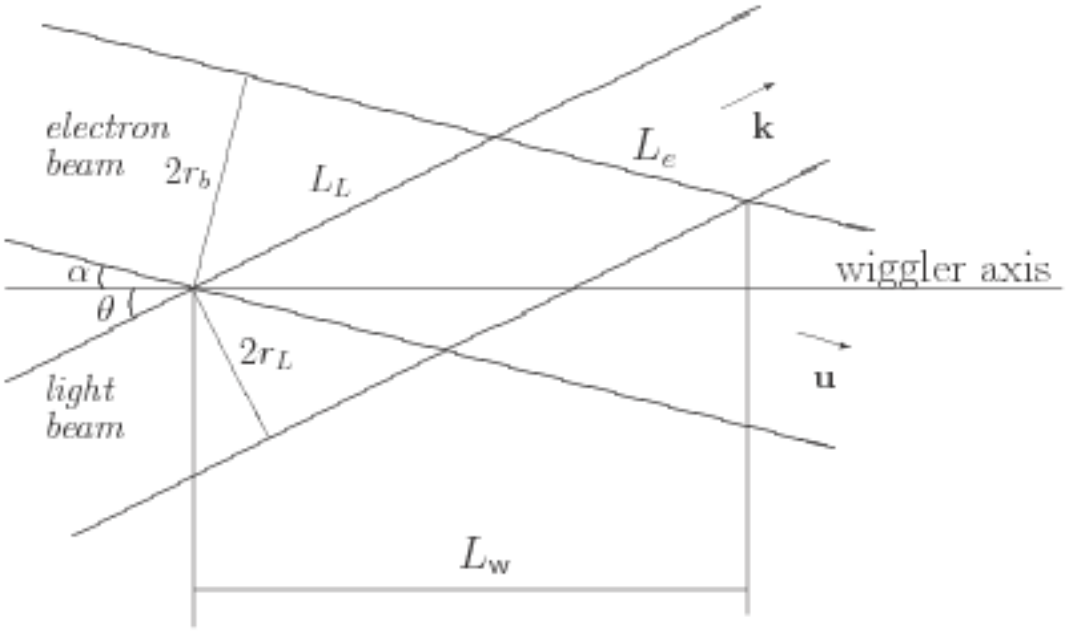

Fig.9. The scheme in xz-plane of undulator with non-collinear arrangement.

The equation of a trajectory (4.4.1) is obtained for mono-energetic electron beam having the unlimited size and, therefore, indefinitely long interacting with a electromagnetic field. Below we take into account the finite size of electron and laser beams . At first, the non-collinear arrangement of electron and laser beams leads to the finite area of them interaction. The length of laser amplification in the medium of electron beam is $L_L = 2r_b / \sin(\alpha+\theta)$. Here $2r_b$ is a width of the electron beam in the xz-plane. The length, at which the electrons move acting by force of laser field, is equal to $L_e = 2r_L / \sin(\alpha+\theta)$. Here $2r_L$ is a width of the laser beam in the xz-plane. The working length of the wiggler is $L_w = L_e \cos\alpha + L_L \cos\theta \approx 2(r_L + r_b)/\sin(\alpha+\theta)$.

Second, at the entrance of undulator the perturbation of the velocity is absent: $\delta v = 0$, that leads to

$$\sum_{j=1}^{4} \frac{\beta_{1j}\mathbf{k}_j - \frac{\omega}{c^2}\beta_{2j}\mathbf{u}}{D_{b(j)}} a_j e^{i\mathbf{k}_j\mathbf{r}_0 - i\omega t} = 0 \qquad (4.4.2)$$

Using Eq.(4.4.2) we can rewrite the Eq.(4.4.1) in form

$$\delta\mathbf{v}_0 = K^2 \frac{c^2}{\gamma_0^3} \sum_{j=1}^{4} \frac{\beta_{1j}\mathbf{k}_j - \frac{\omega}{c^2}\beta_{2j}\mathbf{u}}{D_{b(j)}} a_j e^{i\xi_0} \left(e^{-i\Delta_{\omega(j)}t} - 1\right) + c.c \qquad (4.4.3)$$

Where $\Delta_{\omega(j)} = \omega - \left(\mathbf{k}_j\mathbf{u}\right)$ is the detuning, $\xi_0 = \mathbf{k}_0\mathbf{r}_0$, and $\mathbf{r}_0$ is the initial coordinate in the XZ plane. a_j are the amplitudes of waves at the point of entry of the FELWI's first wiggler. For the problem of spatial amplification, when the spatial growth rate is considered, the initial amplitudes a_j are free parameters. Other words say, we consider the problem of a laser amplifier for the first section of such a FEL.

Assuming that the electron, incoming in the laser field at $t = 0$ and interacting during the time $t = L_e / u$, deviates from the initial direction by the angle $\Delta\alpha$, we obtain

$$\delta\alpha = \frac{\delta v_\perp}{u} = 2K^2 \frac{c^2}{\gamma_0^3} \mathrm{Re}\left\{ \sum_{j=1}^{4} \frac{\beta_{1j}}{D_{b(j)}} \frac{k_j}{u} \sin(\alpha + \theta) a_j e^{i\xi_0} \left(e^{-i\Delta_{\omega(j)}t} - 1\right) \right\}. \qquad (4.4.4)$$

In the electron beam medium there are 4 branches $k_j = k_j(\omega)$ of oscillations, namely, two beams and two laser waves. Under resonant condition $\omega = \omega_+(k_0) = (\mathbf{k}_0\mathbf{u}) - \Omega_b$ only laser wave propagating to the beam direction has maximal positive growth rate k'' [54]. Under the condition of appreciable

amplification $k''L \geq 1$ we can omit all waves in Eq.(4.4.1) except the amplified one. The maximal value of this angle deviation is

$$\Delta\alpha_{\max} \square K^2 c^2 \frac{\beta_1}{D_b \gamma_0^3} \frac{k_0}{u} \sin(\alpha+\theta)\left(e^{ik''L_e} - 1\right) \tag{4.4.5}$$

For single-electron approximation (Thompson regime), Eq.(5) reduces to

$$\Delta\alpha_{\max} = K^2 \left(\frac{c}{u}\right)^2 c^2 \frac{\Omega_b}{k''u} \frac{k_0}{\gamma_0^2} Xa \sin(\alpha+\theta) \frac{e^{ik''L} - 1}{k''} \tag{4.4.6}$$

Here k'' is given by Eq.(12) in Ref. [54]. Note that for the Thompson regime, $\Omega_b / (k''u) << 1$, and

$$\frac{\Omega_b}{k''u} = \frac{2^{4/3}}{\sqrt{3}} K^{-2/3} \gamma_0^{2/3} \left(\frac{k_0 u \Omega_b}{\omega^2}\right)^{1/3} = . \omega_b^{1/3} = .\sqrt{k''} \tag{4.4.7}$$

Hence, the angle deviation of electrons depends on the growth rate as

$$\Delta\alpha_{\max} = .\sqrt{k''} \frac{e^{ik''L} - 1}{k''} \tag{4.4.8}$$

As the growth rate diminishes $k'' \to 0$, the angle of deviation $\Delta\alpha$ goes to zero as

$\Delta\alpha_{\max} = .\sqrt{k''} \to 0$.

The excess of $\Delta\alpha_{\max}$ over the natural dispersion of the beam $\Delta\alpha_{beam}$ gives the threshold value of laser amplitude a at the entry of the first wiggler. We rewrite formula (4.4.5) using the overall laser power $P = \frac{c}{4}(k_0 r_L)^2 |a_+|^2$ at the point of entry of the FELWI's first wiggler, namely

$$P > \frac{c}{8}\left(\frac{mc^2}{e}\right)^2 \frac{(\Delta\alpha_{beam})^2\gamma_0^4}{2K^2 f(k''L_e)}\left(\frac{k''u}{\Omega_b}\right)^2 \qquad (4.4.9)$$

The numerical value is

$$P > P_{th} \approx 10^9 \frac{(\Delta\alpha_{beam})^2\gamma_0^4}{2K^2 f(k''L_e)}\left(\frac{k''u}{\Omega_b}\right)^2 \text{ (W)} \qquad (4.4.10)$$

Here $f(x) = \left(e^x - 1\right)^2 / x^2$.

For calculation we consider the case of small amplification $k''L_e = .1$, when $f(k''L_e) = .1$. We assume also that $\Omega_b / (k''u) = 0.3$. Using the following values of parameters [51]: $\gamma_0 = 15$, $K = 0.635$ and $\Delta\alpha_{beam} = 5\times10^{-4}$ rad, we obtain value of threshold $P > P_{th} \approx 10^8 W$ for laser power P incoming in the first undulator of FELWI. This power exceed the saturation power of the laser field for which the nonlinear regime (saturation of laser field) occurs. Therefore, the amplification regime in the first wiggler cannot be. One should decrease $\Delta\alpha_{beam}$ and/or increase K (the reduction of γ_0 leads to a drop of the frequency of radiation from the optical to the radio-wave range) for lasers in the linear regime of amplification. Using the limit of laser power $= .10^5 \div 10^6 W/cm^2$ we obtain from formula (4.4.9) following estimation $\Delta\alpha = .10^{-6} rad$. This estimate coincides with the results of [54] and [55]. Note that the stable operation of FELWI demands that the value $\Delta\alpha_{\max}$ should exceed the value of natural dispersion $\Delta\alpha_{beam}$ in a few times. It is doubtful that in an accelerator the natural angular dispersion of the electron beam can reach such a small value, which is significantly smaller than $10^{-6} rad$.

This means, that the regime with $k''L_e >> 1$ or $f(k''L_e) >> 1$ should be used of to realize the FELWI application. It can be anomalous Thompson or Raman regime amplification. For collective (Raman) regime the maximal angle of deviation is

$$\Delta\alpha_{\max} = \frac{1}{2}K^2\left(\frac{c}{u}\right)^2 \frac{k_0}{\gamma_0^2} Xa\sin(\alpha+\theta)\frac{e^{ik''L}-1}{k''} \qquad (4.4.11)$$

where $X = 1+\omega_b^2(\mathrm{k_0u})/(k_0c\Omega_b\gamma_0)$. Here k'' is given by Eq.(10) in Ref.[131] and, therefore, k'' takes the large value. The threshold power of laser is

$$P_{th} = \frac{c}{4}\left(\frac{mc^2}{e}\right)^2 \frac{(\Delta\alpha_{beam})^2\gamma_0^4}{K^2 f(k''L_e)} \qquad (4.4.12)$$

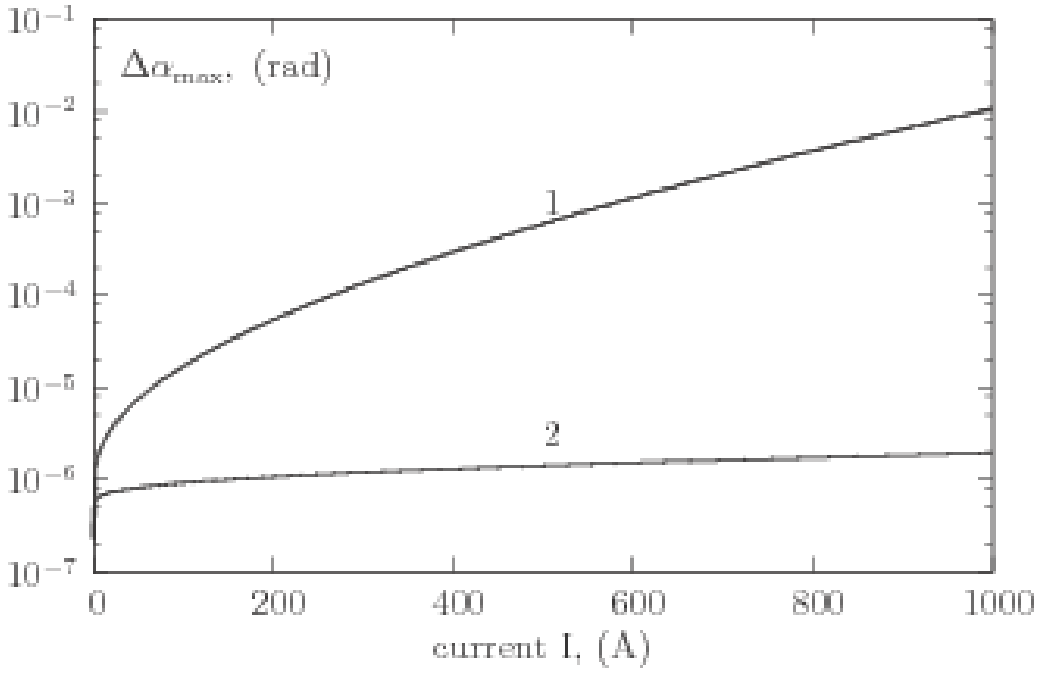

Fig.10. The deviated angle $\Delta\alpha_{\max}$ as a function of a beam current I for two values of the laser beam width: line 1 corresponds r_L=1.0cm and line 2 corresponds r_L=0.1cm. Other parameters are: electron energy $\gamma = 15$, rms electron beam radius r_b=70 μm, laser wavelength $\lambda_L = 359\mu m$, period of the wiggler magnets $\lambda_W = 2.73cm$, normalized wiggler field K=0.635, angle between laser and electron beam $\alpha + \beta = 0.13$.

In paper [51] the tolerance of the FELWI gain to the electron beam energy spread has been demonstrated. For this spread $\delta\gamma$ has been taken to be extremely large, namely, $\delta\gamma = 2.0$ while the emittance was $\varepsilon = 2\pi \times 10^{-6} m \cdot rad$. Simulations have been performed to obtain the dependence of the FELWI gain on the electron beam current. The results show that the gain is about 2 orders of magnitude larger than that for ordinary FEL. The simulation have been carried out with the following set of realistic electron beam and wiggler parameters that are sufficiently close to experimental situations [56]: electron energy $E = 29.35MeV$ ($\gamma = 15$), emittance up to $\varepsilon = 2\pi \times 10^{-6} m \cdot rad$, rms beam radius $r_b = 70\mu m$, laser wavelength $\lambda_L = 359\mu m$, period of the wiggler magnets $\lambda_W = 2.73cm$, number of magnets per section $N = 32$, normalized wiggler field $K = 0.635$, angle between laser and electron beam $\alpha + \theta = 0.13rad$.

For our calculations we choose the same parameters and assume that the power of laser wave incoming in the first wiggler of FELWI is $P = 100W$. The results are presented in Fig. 5, which shows the angle deviation $\Delta\alpha_{\max}$ as a function of a beam current I for two values of the laser beam width: line 1 corresponds $r_L = 1.0cm$ and line 2 corresponds $r_L = 0.1cm$.

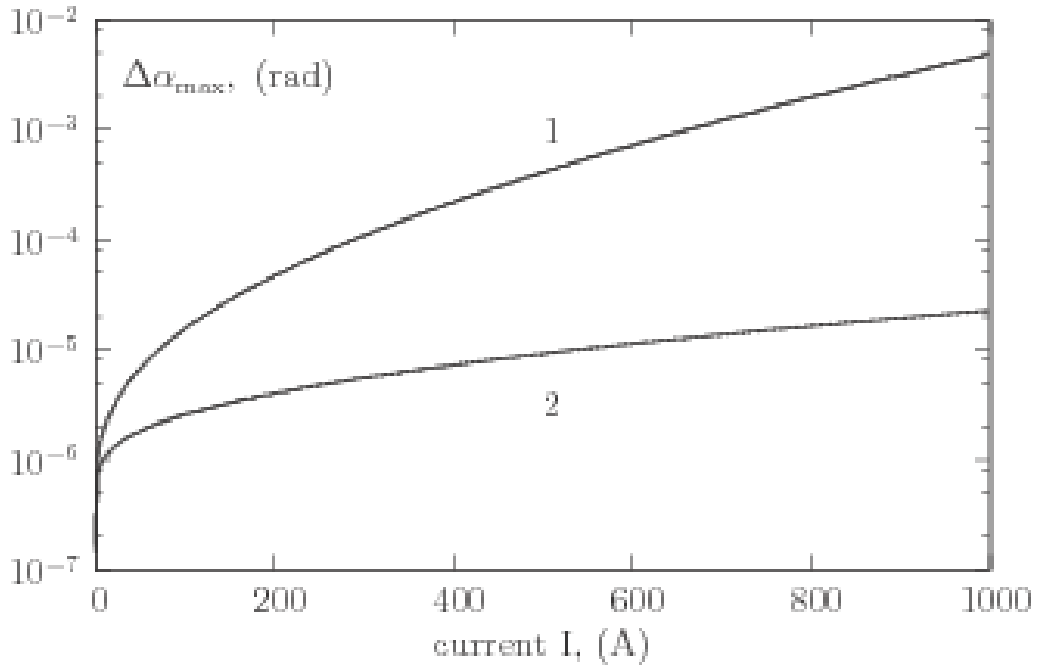

Fig.11. The deviated angle $\Delta\alpha_{\max}$ as a function of a beam current I for two values of the angle between laser and electron beams: line 1 corresponds $\alpha+\beta=0.5$ rad and line 2 corresponds $\alpha+\beta=0.13$rad. Other parameters are: electron energy $\gamma=15$, rms electron beam radius r_b=0.02cm, laser wavelength $\lambda_L=359\mu m$, period of the wiggler magnets $\lambda_W=2.73cm$, normalized wiggler field K=0.635, r_L=1.0cm

Note that, under the condition $I>10A$, Raman amplification [54] takes place. The dependence of the angle deviation $\Delta\alpha_{\max}$ on the laser beam width has simple explanation. On the one hand, with increasing width r_L the laser amplitude drops, under the condition $P=const$. But on the other hand, the length of interaction L_e increases proportional to the width r_L. Hence the exponential term $e^{k''L_e}$ grows.

The length of interaction can be changed with angle $\alpha+\theta$ between the electron and the laser beams. Fig.4 presents results for different values of angle $\alpha+\theta$\$: line 1 corresponds $\alpha+\theta=0.05rad$ and line 1 corresponds

$\alpha+\theta=0.13rad$. The widths of the electron and the laser beams are $r_b=0.02cm$ and $r_L=1.0cm$, respectively. One can see that geometrical parameters, such as the widths of the electron r_b and the laser r_L beams, the angle between the directions of propagation of the electron and the laser beams, allow us to choose an optimal scheme for FELWI operation.

4.5. Conclusion

Taking into account the finite sizes of the beams, the value of the threshold laser power at the entry of the first undulator of FELWI, above which the selection of electrons via the transverse velocity in the drift region is possible, have been obtained for an FEL without inversion (FELWI). We find that an FELWI cannot operate under a weak-amplification Thompson regime, for which the spatial amplification is small: k''L_e << 1. Only a large-amplification regime, $k''L_e>>1$, should be used to build an FELWI. It can be either the anomalous Thompson or the Raman regime of amplification, using an electron beam with overdense current density. For an FELWI operation, the optimal angle $\alpha+\theta$ between the electron and light beams is shown to

depend on the the widths of the electron r_b and the laser r_L beams. The mechanism of an FELWI can be realized in scheme of a ring laser.

Chapter 5.

Smith-Purcell FEL

The Chapter based on 4 publications [126,166,167,168,174]

5.1. Overview

The spontaneous Smith-Purcell (SP) radiation is generated when an electron or another charged particle passes close to the surface of a periodic structure of some conducting material, i.e., a diffraction grating. The radiation mechanism was predicted by Frank in 1942 [121] and observed in the visible spectral range for the first time by Smith and Purcell [31] in 1953 and was called SP radiation. Although the SP radiation has been studied by both experimental and theoretical methods for over 50 years since its discovery, the experimental study of it using relativistic beams was carried out only after 1992 [122-124].

Currently there is substantial interest in the development of THz laser sources for applications to biophysics, medical imaging, nanostructures, and materials science [20]. At the present time, the available THz laser sources fall into three categories: optically or electrically pumped gas lasers, solid state devices, and electron-beam driven devices. An interesting opportunity for a convenient, tunable, narrow-band source is presented by the recent development of a tabletop Smith-Purcell free-electron laser (FEL) at Dartmouth [35]. This device has demonstrated super-radiant emission in the spectral region from 300-900 μ m, but barely exceeded threshold. To improve this performance, it will be necessary to develop electron beams

with improved brightness and a better understanding of how these devices operate. Therefore, the experiment at Dartmouth College [35], where coherent radiation in the SP system was observed, has stimulated new investigations concerning the SP FEL as an open slow-wave structure [127-136].

In [125] a single-particle classical theory of the Smith-Purcell free electron laser is described. The gain is optimized with respect to the grating period and the light incident angle.The optimal parameters of the device and the optimal gain are found. The latter is estimated to be of the order of several percent in thr IR frequency region. Here, only interactions of electrons with a light field reflected from a rippled surface is considered. Finite sizes of grating and of a light waist are taken into account.

In [126] it was found that the dispersion equation describing the induced SP instability is a quadratic equation for frequency; and the zero-order approximation for solution of the equation, which gives the SP spectrum of frequency, corresponds to the mirror boundary case, when the electron beam propagates above plane metal surface (mirror)

Several theories have been proposed to describe the operation of a Smith-Purcell FEL. In particular, Schaechter and Ron [137] proposed a theory based on the interaction of an electron-beam with a wave traveling along the grating. The interaction is found to amplify the waves that are incident on the grating and reflected by it, with a gain that depends on the reflection matrix of the grating. They have found that the gain is proportional to the cube root of the electron-beam current, which with the behavior of

Cherenkov free-electron lasers and other slow-wave devices. More recently, Kim and Song [127] have proposed a theory in which they assume that the electrons interact with a wave that travels along the surface of the grating. Assuming that at least one Fourier component of the traveling wave is radiative, they have found that the gain is proportional to the square root of the electron-beam current $I_b^{1/2}$.

Previous theories of the SP-FEL have assumed that the electron beam interacts with a wave the frequency of which is the same as that of the SP radiation. It has recently been proposed that the beam interacts with an evanescent mode of the grating that lies at a wavelength longer than the SP radiation and radiates only when it reaches the end of the grating [128,129,131]. When the group velocity v_g of this mode is positive, the interaction corresponds to a convective instability and feedback must be provided by an external resonator (or reflections from the ends of the grating). When the group velocity of the evanescent mode is negative, the interaction corresponds to an absolute instability and the SP-FEL oscillates without external feedback if the current is above a threshold value called the start current.

A rectangular grating is considered in the papers [128,129,131], assuming that the entire space above the grating is filled by a uniform electron beam. The authors of [128,129,131] have established the dispersion relation and found the dispersion law **k.** It turns out that the dispersion equation allows only evanescent solutions and the operating point of a Smith-Purcell free electron laser is fixed by the intersection of the dispersion curve with the beam line. The corresponding small signal gain follows the $I_b^{1/3}$ law.

In the present paper we restrict ourselves to the study of only induced Smith-Purcell instability, when the initially unbunched electron beam interacts with a wave the frequency of which is that of the SP radiation. One can select two theoretical target settings for SP radiation: the first is the problem of generation of SP-radiation. In this case no waves are incoming from the infinity. The SP system generates outgoing waves. The second target setting is that the SP-system is amplifying or attenuating the waves incoming from the infinity. One can expect that these different problems have different solutions. In the present work we consider only the problem of generation of waves by the SP-system with no incoming waves. In order that mathematical problems do not cover physical picture, we consider the simplest model of the beam, in which the infinitely thin sheet of beam stabilized by external strong magnetic field is described by hydrodynamical equations.

In the 5.2. paragraph, we present the basic equations that describe the periodic solutions for a self-consistent system of a couple of Maxwell equations and equations for the medium. In paragraph 5.3 we consider a simple model of grating and obtain the dispersion equation for the SP-system. Assuming that the depth of the grating groove h is a small parameter permits us to solve analytically the dispersion equation. In paragraphs 5.3, 5.4 we consider a general model for a metal grating and obtain the dispersion equation and its solutions for the an arbitrary grating profile. Then in paragraph 5.5, as an important example for the application of the obtained results, we present a small signal gain of the SP FEL signal in the case with a rectangular grating.

5.2. Basic equations

In this section, we consider the solutions of a self-consistent system of Maxwell's and beam's equations, which are linear in the field amplitudes. We take a Cartesian coordinate system in such a way that the electron beam propagates to the positive direction of the x axis in the vacuum over the grating (parallel to the surface of the grating) as shown in Fig.13. For the sake of simplicity, we consider a sheet of the beam which is infinite in the z-direction and is stabilized by external strong magnetic field. We assume that the system has the symmetry of translational invariance in the z direction. This means that all physical values depend only on coordinates x and y, and E_z=0.

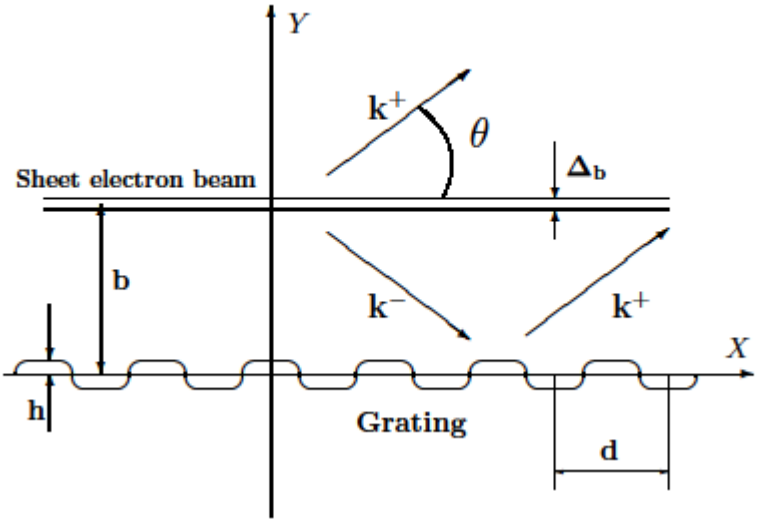

Figure 13. Schematic of a SP-FEL using a sheet electron beam. The sheet electron beam is in the plane $y=b$. θ is the angle of observation, Δ_b is the thickness of the beam, d and h are the period and the amplitude of the grating, respectively.

We start from Maxwell's equations:

$$\nabla\times\mathbf{E}=-\frac{1}{c}\frac{\partial\mathbf{B}}{\partial t},\qquad \nabla\mathbf{B}=0,$$

$$\nabla\times\mathbf{B}=\frac{1}{c}\frac{\partial\mathbf{E}}{\partial t}+\frac{4\pi}{c}\mathbf{j},\quad \nabla\mathbf{E}=4\pi\rho \tag{5.2.1}$$

where $\mathbf{j}$ and ρ are the current and charge density of the beam, respectively. We assume the simplest model of the beam, so that the initial distribution function of the electrons is expressed as

$$f_0(t,\mathrm{r}_0,\mathrm{p}_0)=\Delta_b n_{b0}\delta(y-b)\delta(\mathrm{p}_0-m\gamma_0\,\mathrm{u}) \tag{5.2.2}$$

where $\mathbf{u}=(\mathrm{u},0,0)$ is the initial velocity of electrons, $\gamma_0=(1-\mathrm{u}^2/\mathrm{c}^2)^{1/2}$ is a relativistic factor, Δ_b is the thickness of the beam and n_{b0} is its undisturbed density. For a monoenergetic electron beam we can use the hydrodynamical approach, namely, the equation of motion:

$$\frac{d\mathbf{p}}{dt}=\left(\frac{\partial}{\partial t}+\mathbf{v}\nabla\right)\mathbf{p}=e\mathbf{E}+e\frac{\mathbf{v}}{c}\times\mathbf{B} \tag{5.2.3}$$

and the continuity equation:

$$\frac{\partial\rho}{\partial t}+\mathrm{div}\mathbf{j}=0 \tag{5.2.4}$$

where $\mathbf{j}=\mathbf{v}\rho=en_b\mathbf{v}$, n_b is the beam density.

To describe the electromagnetic field in the vacuum space ($\rho = 0$ and $\mathbf{j} = 0$ in Eqs. (5.2.1), we take advantage of Floquet's theorem and expand the $\mathbf{E}$ and $\mathbf{B}$ fields as:

$$\begin{aligned} \mathbf{E}(y > b) &= \sum_n \mathbf{E}_n e^{-i\omega t + i\mathbf{q}_n^+ \mathbf{r}}, \\ \mathbf{B}(y > b) &= \sum_n \mathbf{B}_n e^{-i\omega t + i\mathbf{q}_n^+ \mathbf{r}} \end{aligned} \tag{5.2.5}$$

above the beam level, and

$$\begin{aligned} \mathbf{E}(y < b) &= e^{-i\omega t} \sum_n \left(\mathbf{E}_n^+ e^{i\mathbf{q}_n^+ \mathbf{r}} + \mathbf{E}_n^- e^{i\mathbf{q}_n^- \mathbf{r}} \right), \\ \mathbf{B}(y < b) &= e^{-i\omega t} \sum_n \left(\mathbf{B}_n^+ e^{i\mathbf{q}_n^+ \mathbf{r}} + \mathbf{B}_n^- e^{i\mathbf{q}_n^- \mathbf{r}} \right) \end{aligned} \tag{5.2.6}$$

below the beam level. Here the wave vectors are

$$\mathbf{q}_n^{\pm} = (\mathrm{q}_{nx}, \pm \mathrm{q}_{ny}) = (\mathrm{k}_x + \mathrm{n}\,\chi, \pm \mathrm{q}_{ny}) \tag{5.2.7}$$

Where $\chi = 2\pi / d$ is the wave number of the grating, and d is its period. The sums in Eq. (5.2.5) contain only the waves outgoing from the system, while the sums in Eq. (5.2.6) contain the waves propagating in both positive and negative directions of the Y axis. Since the dispersion relation for electromagnetic wave in vacuum space is $\omega^2 = \left(\mathbf{q}_n^{\pm}\right)^2 c^2$, we can write

$$q_{ny} = \sqrt{\frac{\omega^2}{c^2} - q_{nx}^2} = \sqrt{\frac{\omega^2}{c^2} - \left(k_x + n\chi\right)^2}. \tag{5.2.8}$$

The solution of Maxwell equations in the form of Eqs. (5.2.5) and (5.2.6) is complete, since the sums present both propagating electromagnetic and surface waves. For propagating electromagnetic waves, we find that $\mathbf{q}_0^{\pm} = \mathbf{k}^{\pm}$, where $\mathbf{k}^{\pm} = \left(k_x, \pm k_y\right)$. All waves with a plus sign propagate to the positive direction of Y axis, while waves with a minus sign propagate in the

direction of the negative value on the Y axis. It means that the non-propagating surface waves are

damped modes in the direction of their propagation, i.e. $\mathrm{Im}\, q_{ny} > 0$. The solution (5.2.5)-(5.2.8) describes the case when the waves incoming from infinity are absent, and, therefore, the solution (5.2.5)-(5.2.8) satisfies the radiated boundary condition named as the Sommerfeld boundary condition.

There are only three non-zero components of electromagnetic field E_x, E_y and B_z. From the Maxwell equations for vacuum space we find

$$\begin{aligned} \left(\mathbf{E}_n \mathbf{q}_n^+\right) = 0, \mathbf{B}_n = \frac{c\mathbf{q}_n^+}{\omega} \times \mathbf{E}_n, \\ \left(\mathbf{E}_n^\pm \mathbf{q}_n^\pm\right) = 0, \mathbf{B}_n^\pm = \frac{c\mathbf{q}_n^\pm}{\omega} \times \mathbf{E}_n^\pm. \end{aligned} \tag{5.2.9}$$

Using these relations we can express the partial amplitudes of two components in terms of the partial amplitudes of the third component. For example, we can write the partial amplitudes of E_y and B_z in terms of the partial amplitudes of E_x: $E_{ny} = -(q_{nx}/q_{ny})E_{nx}$, $B_{nz} = -(\omega/q_{ny}c)E_{nx}$, $E_{ny}^\pm = \mp(q_{nx}/q_{ny})E_{nx}^\pm$, $B_{nz}^\pm = \mp(\omega/q_{ny}c)E_{nx}^\pm$. Since this operation breaks the symmetry between the field components and will cause problems later during analytical calculations, we will take a different approach and introduce the potential P:

$$P = \begin{cases} \sum_n P_n e^{-i\omega t + \mathbf{q}_n^+ \mathbf{r}}, y > b; \\ \sum_n \left(P_n^+ e^{i\mathbf{q}_n^+ \mathbf{r}} + P_n^- e^{i\mathbf{q}_n^- \mathbf{r}}\right) e^{-i\omega t}, y < b. \end{cases} \tag{5.2.10}$$

Equations (4.2.10) hold if the field components are determined by relations:

$$E_x = \frac{\partial P}{\partial y}, E_y = -\frac{\partial P}{\partial x}, B_z = \frac{1}{c}\frac{\partial P}{\partial t}. \tag{5.2.11}$$

Equation (5.2.11) determines fields in the regions $y > b$ and $y < b$ separately. To connect the partial amplitudes P_n with P_n^+ and P_n^- we have to use the boundary condition on the beam sheet. For the beam sheet we can write:

$$\begin{aligned} \delta\mathbf{j} &= \delta\mathbf{j}_s\delta(y-b) = (\delta j_{sx}, 0, 0)\delta(y-b), \\ \delta\rho &= \delta\rho_s\delta(y-b), \end{aligned} \tag{5.2.12}$$

where $\delta\rho_s$ and $\delta\mathbf{j}_s$ are the surface densities of the disturbed charge and the disturbed current, respectively. Integrating the Maxwell's equations with $\delta\rho$ and $\delta\mathbf{j}$ given by Eq. (5.2.12) over y in the infinite vicinity of point $y = b$ we find the boundary conditions on the sheet beam:

$$\begin{aligned} &E_x(b+0) = E_x(b-0), \\ &E_x(b+0) - E_x(b-0) = 4\pi\delta\rho_s, \\ &B_z(b+0) - B_z(b-0) = \frac{4\pi}{c}\delta j_s. \end{aligned} \tag{5.2.13}$$

We assume that current and charge densities can be written as

$$\begin{aligned} \delta j_s &= \sum_n \delta j_{ns} e^{-i\omega t + i\mathbf{q}_n^+\mathbf{r}}, \\ \delta\rho_s &= \sum_n \delta\rho_{ns} e^{-i\omega t + i\mathbf{q}_n^+\mathbf{r}}. \end{aligned} \tag{5.2.14}$$

Then we can derive relations for the amplitudes P_n, P_n^+ and P_n^-:

$$\begin{aligned} &P_n^+ e^{iq_{ny}b} - P_n^- e^{-iq_{ny}b} = P_n e^{iq_{ny}b}, \\ &P_n^+ e^{iq_{ny}b} - P_n^- e^{-iq_{ny}b} = P_n e^{iq_{ny}b} - 4\pi i\frac{\delta\rho_{ns}}{q_{nx}} e^{iq_{ny}b}, \\ &P_n^+ e^{iq_{ny}b} - P_n^- e^{-iq_{ny}b} = P_n e^{iq_{ny}b} - \frac{4\pi i}{\omega} e^{iq_{ny}b}. \end{aligned} \tag{5.2.15}$$

The second and the third equations are the same if the continuity equation for the Fourier components holds: $\omega\delta\rho_{ns} = q_{nx}\delta j_{ns}$. Solutions of Eqs. (5.2.15) are

$$P_n^+ = P_n - 2\pi i\frac{\delta\rho_{ns}}{q_{nx}},$$
$$P_n^- = -2\pi i\frac{\delta\rho_{ns}}{q_{nx}}e^{2iq_{ny}b}. \qquad (5.2.16)$$

In order to find the density $\delta\rho_{ns}$ we linearize Eqs. (5.2.3) and (5.2.4) using small perturbations. We assume that $\mathbf{v} = \mathbf{u} + \delta\mathbf{v}$, where $\delta\mathbf{v} = (\delta v_x, 0, 0)$ and $\rho = \rho_0 + \delta\rho$ with $\rho_0 = e\Delta_b n_{b0}\delta(y-b)$. The linearized equation of motion

$$\left(\frac{\partial}{\partial t} + \mathbf{u}\nabla\right)\delta v_x = \frac{eE_x}{m\gamma_0^3} \qquad (5.2.17)$$

has solution

$$\delta v_x = \sum_n \delta v_{nx} e^{-i\omega t + i\mathbf{q}_n^+\mathbf{r}}, \qquad (5.2.18)$$

Where

$$\delta v_{mx} = \frac{ie}{m\gamma_0^3}\frac{E_{nx}}{\omega - (\mathbf{q}_n^+\mathbf{u})}. \qquad (5.2.19)$$

The linearized continuity equation

$$\left(\frac{\partial}{\partial t} + \mathbf{u}\nabla\right)\delta\rho = -\rho_0 \operatorname{div}\delta\mathbf{v} \qquad (5.2.20)$$

gives a solution for the Fourier components $\delta\rho_n$:

$$\delta\rho_n = \rho_0\frac{q_{nx}\delta v_{nx}}{\omega - (\mathbf{q}_n^+\mathbf{u})}. \qquad (5.2.21)$$

Then we find

$$\delta\rho_{ns} = -\frac{\Delta_b \omega_b^2}{4\pi\gamma_0^3} \frac{q_{nx} q_{ny} P_n}{(\omega - (\mathbf{q}_n^+ \mathbf{u}))^2}, \tag{5.2.22}$$

where $\omega_b = (4\pi e^2 n_{b0} / m)^{1/2}$ is the Langmuir beam frequency.

The partial field amplitudes determined by Eq. (5.2.16) are

$$\begin{aligned} P_n^+ &= [1 + K(\mathrm{n})] P_n, \\ P_n^- &= K(\mathrm{n}) e^{2iq_{ny}b} P_n. \end{aligned} \tag{5.2.23}$$

Here we introduced the following notation

$$K(n) = \frac{i}{2} \Delta_b \omega_b^2 \gamma_0^{-3} \frac{q_{ny}}{(\omega - (\mathbf{q}_n^+ \mathbf{u}))^2}. \tag{5.2.24}$$

5.3. Dispersion equation: particular case

The solutions obtained in the previous section define the amplitudes of the field but do not determine its frequency and the growth rates of SP instability. In order to get the frequency we have to consider the boundary condition on the grating surface.

As a first step, we consider the simplest model of the grating, when the equation of metal surface is defined as

$$y(x) = h \sin(\chi x) = h \sin\left(\frac{2\pi}{d} x\right). \tag{5.3.25}$$

The vector tangential to the surface is $\mathbf{r}_0 = (1, h\chi\cos(\chi x))$. The boundary condition $(\mathbf{r}_0\mathbf{E}(x, y(\mathrm{x}))) = 0$ takes the form

$$E_x(x, y(\mathrm{x})) + h\chi\cos(\chi x)E_y(x, y(\mathrm{x})) = 0. \qquad (5.3.26)$$

Here E_x and E_y are given by (5.2.11). Substituting the solutions of Maxwell equations given by (5.2.10) and (5.2.23) in boundary condition (5.3.26), multiplying by $exp(-ip\chi x)$, where $p = 0; \pm 1; \pm 2; \pm 3, \ldots$, and integrating then over coordinate x within the interval $(0, d)$ we obtain an infinite system of algebraic equations for the partial amplitudes P_n (see Appendix A):

$$\sum_n \left(q_{ny} + (n-p)\chi\frac{q_{nx}}{q_{ny}} \right)\left(J_{n-p}(-q_{ny}h) + K(n)\left[J_{n-p}(-q_{ny}h) - J_{n-p}(q_{ny}h)e^{2iq_{ny}b} \right] \right) P_n = 0 \qquad (5.3.27)$$

Here $J_\alpha(x)$ are a Bessel functions.

a). 3-waves approximation

In order to cut the infinite system we assume that the amplitude of the grating h is vary small. Since the Bessel function of the small variable x drops as $J_\alpha(x) \approx (x/2)^\alpha / \alpha!$ with α increasing, the assumption that h is a small parameter permits us to consider 3-waves approximation. We suppose that there are only three non-zero partial amplitudes, namely, P_{n-1}, P_n and P_{n+1}. Other amplitudes are assumed to be zero. Then we get three algebraic equations

$$\mathbf{MV} = 0 \qquad (5.3.28)$$

where $\mathbf{V}$ is a column vector with components P_{n-1}, P_n and P_{n+1}, $\mathbf{M}$ is a 3×3 matrix expressed as

$$\begin{Vmatrix} q_{n-1y}\alpha_{n-1}, \beta_n^+, ,,,,,,\gamma_{n+1}^+ \\ \beta_{n-1}^-, ,,,,q_{ny}\alpha_n, ,,,,\beta_{n+1}^+ \\ \gamma_{n-1}^-, ,,,,,,\beta_n^-, ,,,q_{n+1y}\alpha_{n+1} \end{Vmatrix}. \tag{5.3.29}$$

Here the coefficients are

$$\begin{aligned} \alpha_n &= 1+K(n)\left(1-e^{2iq_{ny}b}\right), \\ \beta_n^{\pm} &= \mp\frac{h}{2}\left(q_{ny}^2 \mp \chi q_{nx}\right)\left[1+K(n)\left(1+e^{2iq_{ny}b}\right)\right], \\ \gamma_n^{\pm} &= \frac{h^2}{8}q_{ny}\left(q_{ny}^2 \pm 2\chi q_{nx}\right)\alpha_n. \end{aligned} \tag{5.3.30}$$

The nontrivial solution of the finite system of equations (5.3.28) takes place if its determinant equals zero. This dispersion equation describes both the spectrum of frequencies and the growth rates of the stimulated Smith-Purcell radiation. Neglecting the small terms proportional to h^p with $p\geq4$, we obtain the following simple dispersion equation:

$$D(\omega,\mathbf{k}) = q_{n-1y}q_{ny}q_{n+1y}\alpha_{n-1}\alpha_n\alpha_{n+1} - q_{n-1y}\alpha_{n-1}\beta_n^-\beta_{n+1}^+ - \beta_{n-1}^-\beta_n^+q_{n+1y}\alpha_{n+1} = 0 \tag{5.3.31}$$

The question is which the zero-order approximation for dispersion equation is. In the absence of the beam, when $\omega_b = 0$, we find from Eq.(5.2.16) that $P_n^- = 0$ and $P_n^+ = P_n$, which means that $\mathbf{E}_n^- = 0$ and $\mathbf{E}_n^+ = \mathbf{E}_n$. Substituting this amplitudes in the boundary condition we find that $\mathbf{E}_n = 0$. Since all amplitudes are zero, the determinant of the system is not equal to zero. Indeed, substituting $\omega_b = 0$ in equation (5.3.31) we get

$$D(\omega,\mathbf{k},\omega_b=0)=q_{n-1y}q_{ny}q_{n+1y}$$
$$+\frac{h^2}{4}\left\{q_{n-1y}\left(q_{ny}^2-\chi q_{nx}\right)\left(q_{n+1y}^2+\chi q_{n+1x}\right)+q_{n+1y}\left(q_{n-1y}^2-\chi q_{n-1x}\right)\left(q_{ny}^2+\chi q_{nx}\right)\right\}\neq 0. \tag{5.3.32}$$

It has a simple physical explanation. In the absence of the beam, the electromagnetic field in the system is absent too, because the grating does not emit the waves.

Therefore we can not use the condition of $\omega_b=0$ as a zero-order approximation to solve the dispersion equation. Instead we use as zero-order approximation condition of $h=0$, which gives

$$D(\omega,\mathbf{k},h=0)=q_{n-1y}q_{ny}q_{n+1y}\alpha_{n-1y}\alpha_{ny}\alpha_{n+1y}=0. \tag{5.3.33}$$

In the general case for an arbitrary angle θ the product of $q_{n-1y}q_{ny}q_{n+1y}$ does not equal zero, therefore we can write

$$D_0(\omega,\mathbf{k})=\alpha_{n-1y}\alpha_{ny}\alpha_{n+1y}=0 \tag{5.3.34}$$

Without loss of generality we assume that the n-mode of electromagnetic spectrum excites in the system. It means that α_n, which gives the following equation

$$(\omega-(k_x+n\chi)u)^2+\frac{i}{2}\Delta_b\omega_b^2\gamma_0^{-3}q_{ny}\left(1-e^{2iq_{ny}b}\right)=0. \tag{5.3.35}$$

We seek the solution of the equation in the form

$$\omega=\omega_n\pm\Omega_{bn}, \tag{5.3.36}$$

where ω_n satisfies the equation (5.3.35) in the limit $\omega_b\to 0$:

$$\omega_n=(k_x+n\chi)u, \tag{5.3.37}$$

which is the dispersion relation for longitudinal beam waves.

Taking into account the dispersion relation for electromagnetic wave in vacuum

$$k_x = \frac{\omega_n}{c}\cos\theta, \tag{5.3.38}$$

we find the frequency of the n-mode of the spectrum for the limit $\omega_b \to 0$ as the intersection point in the k_x, ω diagram shown in the Fig.8. :

$$\omega_n = \frac{n\chi u}{1-\beta\cos\theta}, \tag{5.3.39}$$

where $\beta = u/c$ is the dimensionless velocity of electron, θ is the angle between $\mathbf{k}^+$ vector and positive direction of x-axis, i.e. the angle of observation. Please do not confuse the n-mode in the spectrum of radiation with the n-mode in q_x-spectrum of surface wave E_n. With the help of Eq. (5.3.39), from Eq. (2.2.8) we find that

$$q_{ny} = i\frac{\omega_n}{u\gamma_0}, \tag{5.3.40}$$

So the n-mode of the surface wave E_n does not radiate, because it damps in the positive direction of the y-axis.

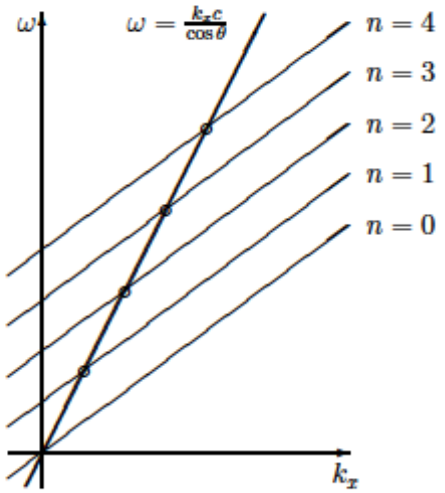

Fig.14. The dispersion relations for the electromagnetic wave $\omega = k_x c / \cos\theta$ and the beam waves with $\omega_n = (k_x + n\chi)u,$ are shown in k_x, ω plane. The intersection points determine the spectrum of frequency of Eq. (5.3.39).}.

Considering the presence of beam as perturbation and substituting the value of q_{ny} from Eq. (5.3.40) in Eq. (5.3.35) we can derive the beam frequency Ω_{bn}:

$$\Omega_{bn} = \omega_b \gamma_0^{-2} \sqrt{\frac{\Delta_b \omega_n}{2u}\left(1 - e^{-2\frac{\omega_n b}{u\gamma_0}}\right)}. \qquad (5.3.41)$$

Here we give the physical interpretation of the solutions obtained. The condition h=0 means that there is a flat mirror in the plane y. The fluctuations of charge and current densities of the electron beam produce fluctuations of the electromagnetic field, the plane wave of which is reflected from the mirror. The resonant condition (5.3.39) is the crossing point of the dispersion lines for the beam wave and the reflected electromagnetic plane wave. The boundary condition yields a discrete spectrum, the modes of

which contain two coupled frequencies: "high" frequency with $\omega = \omega_n + \Omega_{bn}$ and "low" frequency with $\omega = \omega_n - \Omega_{bn}$. The beam frequency Ω_{bn} depends on the height of the beam above the surface of $y = 0$ and has the following asymptotes:

$$\Omega_{bn} = \begin{cases} \omega_b \gamma_0^{-2} \sqrt{\dfrac{\Delta_b \omega_n}{2u}}, , , , , , b \to \infty \\ \omega_b \gamma_0^{-5/2} \dfrac{\omega_n}{2u} \sqrt{\Delta_b b}, , , , b \to 0. \end{cases} \tag{5.3.42}$$

Now we shall consider the presence of grooves on the mirror ($h \neq 0$) as a perturbation and formulate the solution of the dispersion equation near the synchronism point (5.3.36) as:

$$\omega = \omega_n \pm \Omega_{bn} + \delta\omega, \tag{5.3.43}$$

where $\delta\omega = \delta\omega_n' + i\delta\omega_n''$ is a complex number, and the imaginary part $\delta\omega_n''$ is the growth rate of the induced Smith-Purcell instability. Substituting solution (5.3.43) in Eq. (5.3.31) and neglecting the small terms under the realistic condition of $\{\omega_b, \Omega_{bn}, |\delta\omega|\} << \chi u$ we obtain the dispersion equation for small shift of frequency:

$$\delta\omega^2 \pm 2\Omega_{bn}\delta\omega = \frac{h^2}{4} \frac{\Delta_b \omega_b^2}{\gamma_0^5} \left(\frac{\omega_n}{u} \right)^3 e^{-2\frac{\omega_n b}{u\gamma_0}} \left[X_n(\theta, u) + iY_n(\theta, u) \right]. \tag{5.3.44}$$

For $\omega = \omega_n$ the wave number q_{n+1y} is always an imaginary value. We rewrite $q_{n+1y} = ig_{n+1}$,

Where $g_{n+1} = \dfrac{\omega_n}{nu} \sqrt{(n+1-\beta\cos\theta)^2 - n^2\beta^2}$. The wave number q_{n-1y} can be both real and imaginary for $\omega = \omega_n$. Under the condition

$$\frac{1-\beta\cos\theta}{1+\beta} < n < \frac{1-\beta\cos\theta}{1-\beta} \tag{5.3.45}$$

the wave number q_{n-1y} is real and then the coefficients

$$\begin{aligned} X_n &= \left(1+\frac{\chi u\gamma_0^2}{\omega_n}\right)\left(\frac{\chi}{g_{n+1}}\left(1+\frac{\chi u}{\omega_n}\right)-\frac{g_{n+1}u}{\omega_n}\right), \\ Y_n &= \left(1-\frac{\chi u\gamma_0^2}{\omega_n}\right)\left(\frac{q_{n-1}u}{\omega_n}-\left(1-\frac{\chi u}{\omega_n}\right)\frac{\chi}{q_{n-1y}}\right). \end{aligned} \tag{5.3.46}$$

The other case is real under the condition

$$n \notin \left(\frac{1-\beta\cos\theta}{1+\beta}, \frac{1-\beta\cos\theta}{1-\beta}\right), \tag{5.3.47}$$

when the wave number $q_{n-1y} = ig_{n-1}$ is imaginary and then the coefficients

$$\begin{aligned} X_n &= \left(1+\frac{\chi u\gamma_0^2}{\omega_n}\right)\left(\frac{\chi}{g_{n+1}}\left(1+\frac{\chi u}{\omega_n}\right)-\frac{g_{n+1}u}{\omega_n}\right)-\left(1-\frac{\chi u\gamma_0^2}{\omega_n}\right)\left(\frac{g_{n-1}u}{\omega_n}-\left(1-\frac{\chi u}{\omega_n}\right)\frac{\chi}{g_{n-1}}\right), \\ Y_n &= 0. \end{aligned} \tag{5.3.48}$$

here $g_{n-1} = \frac{\omega_n}{nu}\sqrt{(n+1+\beta\cos\theta)^2 - n^2\beta^2}$.

The quadratic equation (5.3.44) has simple solutions. Here we consider two interesting cases. First, we shall consider the Thompson type of excitation in a single-particle approximation, when the electron beam radiates as a single particle or a bunch.

In this case the beam waves can be neglected and the condition of generation is $|\delta\omega| >> \Omega_{bn}$. Under this condition we can omit the second term in the left-hand side of the dispersion equation and obtain the solution:

$$\delta\omega_n = \frac{h\omega_n}{2u}\sqrt{\frac{\Delta_b\omega_n}{u}}\frac{\omega_b}{\gamma_0^{5/2}}e^{-\frac{\omega_n b}{u\gamma_0}}\left(X_n+iY_n\right)^{1/2}. \tag{5.3.49}$$

The growth rate of instability of the n-mode (5.3.39) ($\delta\omega = \delta\omega_n' + i\delta\omega_n''$) in this case is

$$\delta\omega_n'' = \pm\frac{h\omega_n}{2u}\frac{\omega_b}{\gamma_0^{5/2}}\sqrt{\frac{\Delta_b\omega_n}{u}}e^{-\frac{\omega_n b}{u\gamma_0}}\left(X_n + iY_n\right)^{1/4}\sin\left|\frac{\psi}{2}\right|, \qquad (5.3.50)$$

where angle ψ is defined as $\psi = \arccos\left(X_n / \sqrt{X_n^2 + Y_n^2}\right)$.

For sufficiently large value of the relativistic factor γ_0, when the inequality $\gamma_0 >> \omega_n b / u$ holds, the growth rate of instability is proportional to the square root of inverse $\delta\omega'' = .\gamma_0^{-1/2}$. The condition of the Thompson regime excitation does not depend on the beam current; it has the following form:

$$\frac{h\omega_n}{2u}\frac{\left|X_n + iY_n\right|}{\sqrt{2\gamma_0\left(e^{2\frac{\omega_n b}{u\gamma_0}} - 1\right)}} >> 1. \qquad (5.3.51)$$

This inequality holds for $b \to 0$ and for large values of the grooves depth h of the grating.

The second case is the Raman (or collective) regime of generation, when the influence of beam waves is appreciable and $|\delta\omega| << \Omega_{bn}$. For the Raman regime we obtain

$$\delta\omega = \pm\frac{h^2\omega_n^{\,2}}{4u^2}\frac{\omega_b}{\gamma_0^3}\sqrt{\frac{\Delta_b\omega_n}{2u}}\frac{e^{-2\frac{\omega_n b}{u\gamma_0}}}{\sqrt{1 - e^{-2\frac{\omega_n b}{u\gamma_0}}}}\left(X_n + iY_n\right). \qquad (5.3.52)$$

The growth rate of instability is

$$\delta\omega_n'' = \pm\frac{h^2\omega_n^{\,2}}{4u^2}\frac{\omega_b}{\gamma_0^3}\sqrt{\frac{\Delta_b\omega_n}{2u}}\frac{e^{-2\frac{\omega_n b}{u\gamma_0}}}{\sqrt{1 - e^{-2\frac{\omega_n b}{u\gamma_0}}}}Y_n(\theta, u). \qquad (5.3.53)$$

If $Y_n(\theta,u)$, then the high-frequency branch with $\omega=\omega_n+\Omega_{bn}$ excites. In the opposite case the low-frequency waves with $\omega=\omega_n-\Omega_{bn}$ generate.

For sufficiently large value of the relativistic factor γ_0, when the inequality $\gamma_0 \gg \omega_n b/u$ holds, the growth rate of instability is proportional to inverse γ_0: $\delta\omega'' \propto \gamma_0^{-1}$. The condition for the Raman type of excitation is

$$\frac{h^2\omega_n^{\,2}}{4u^2\gamma_0}\frac{|Y_n|}{e^{2\frac{\omega_n b}{u\gamma_0}}-1}<<1. \qquad (5.3.54)$$

It does not depend on Langmuir beam frequency (or beam current), but it depends on the beam height b above the grating.

The mechanism of light radiation is as follows. The surface wave with mode number n acting on the beam electrons perturbs the trajectories of the latter. Electrons, oscillating near the equilibrium point of $\mathbf{r}=\mathbf{r}_0+\mathbf{u}t$, emit electromagnetic waves. As, the amplitude of oscillation is proportional to the magnitude of the surface wave at the beam height b, the value of the growth rate depends on the beam height above the grating surface.

b). 5-waves approximation

In the previous subsection we considered the 3-waves approximation. When $q_{n-1y}=0$ the 3-waves approximation does not work. It can be when $n\approx(1-\beta\cos\theta)(1\pm\beta)$, for example, for $n=1$ and $\theta=0$. In this case we have to include additional surface modes and consider 5-waves approximation; we assume that there are only five non-zero amplitudes: E_{n-2x}, E_{n-x}, E_{nx} and E_{n+x}

and E_{n+2x}. Other amplitudes are assumed to be zero. Taking into account that h is a small parameter and neglecting small terms as above, we obtain the following dispersion equation:

$$\begin{aligned} D(\omega,\mathbf{k}) = (&q_{n-2y}\alpha_{n-2}q_{n-1y}\alpha_{n-1}q_{n+1y}\alpha_{n+1}q_{n+2y}\alpha_{n+2} - q_{n-1y}\alpha_{n-1}\beta_n^-\beta_{n+1}^+ \\ &-q_{n-2y}\alpha_{n-2}q_{n-1y}\alpha_{n-1}\beta_{n+1}^-\beta_{n+2}^+ - \beta_{n-2}^-\beta_{n-1}^+q_{n+1y}\alpha_{n+1}q_{n+2y}\alpha_{n+2})q_{ny}\alpha_n \\ &-q_{n-2y}\alpha_{n-2}\beta_{n-1}^-\beta_n^+q_{n+1y}\alpha_{n+1}q_{n+2y}\alpha_{n+2} - q_{n-2y}\alpha_{n-2}\beta_n^-\beta_{n+1}^+q_{n-1y}\alpha_{n-1}q_{n+2y}\alpha_{n+2} = 0 \end{aligned} \tag{5.3.55}$$

Considering the solution of Eq. (5.3.55) near the synchronism point (5.3.43), we can rewrite the equation for $\delta\omega$ as

$$\delta\omega^2 \pm 2\Omega_{bn}\delta\omega = \frac{i}{2}h\frac{\Delta_b\omega_b^2\omega_n^2}{u^2\gamma_0^5}\frac{A}{B}e^{-2\frac{\omega_n b}{u\gamma_0}} = 0, \tag{5.3.56}$$

where

$$A = q_{n-2y}q_{n+2y}\left\{\left(1+\frac{\chi u\gamma_0^2}{\omega_n}\right)q_{n-1y}\beta_{n+1}^+ - \left(1-\frac{\chi u\gamma_0^2}{\omega_n}\right)q_{n+1y}\beta_{n-1}^+\right\} \tag{5.3.57}$$

and

$$A = q_{n-2y}q_{n-1y}q_{n+1y}q_{n+2y} - q_{n-2y}q_{n-1y}\beta_{n+1}^-\beta_{n+2}^+ - \beta_{n-2}^-\beta_{n-1}^+q_{n+1y}q_{n+2y}. \tag{5.3.58}$$

For $q_{n-1y} = 0$ the shift of frequency $\delta\omega$ does not depend on the small parameter h. This example shows that high orders of the surface modes can play a significant role for the SP instability and, therefore, they should be taken into account.

5.4. Dispersion equation: General form

Now, when we know the form of the dispersion equation for the SP instability, we can consider the general case. We assume that the surface of grating is described by an arbitrary periodic function

$y = y(x)$ wrere $y(x) = y\left(x + \frac{2\chi}{n}\right)$ and n is an integer. The metal grating is assumed to have ideal conductivity. This approach excludes the cases of rectangular grating and other gratings in which the form of the surface cannot be described by a function. But the results of this approach can be used for the

case of an arbitrary profile of the grating. Below we will show how this approach can be used for the case of a rectangular grating. Substituting the solutions of Maxwell equations in the general boundary condition for metal surface

$$E_x(x, y(x)) + y'(x)E_y(x, y(x)) = 0, \tag{5.4.59}$$

multiplying by $\exp(-ip\chi x)$, where $p = 0; \pm 1; \pm 2; \pm 3, \ldots$ and then integrating over coordinate x within the interval $(0, d)$ we obtain an infinite system of algebraic equations for the partial amplitudes P_n (see Appendix A):

$$\sum_{n=-\infty}^{n=\infty} T_{np} P_n = 0, \tag{5.4.60}$$

with the following coefficients

$$T_{np} = \left(q_{ny} + (n - p)\chi \frac{q_{nx}}{q_{ny}}\right)\left(G_{np}^{+}[1 + K(n)] - G_{np}^{-}K(n)e^{2iq_{ny}b}\right). \tag{5.4.61}$$

Here

$$G_{np}^{\pm} = \int_0^{2\pi} e^{i(n-p)\xi \pm q_{ny} y(\xi)} d\xi, \qquad (5.4.62)$$

and $\xi = \chi x$ is a dimensionless coordinate.

For a non-zero solution of Eqs. (5.4.60) to exist, the determinant of the system must be zero:

$$D(\omega, \mathbf{k}) = det \left\| T_{np} \right\| = 0. \qquad (5.4.63)$$

This is the most general form of the dispersion equation for the Smith-Purcell instability without resonator. Its roots give the spectrum of frequency and the growth rates. As above, the zero-order approximation for dispersion equation, giving the SP frequency spectrum, corresponds to the case with the plane mirror boundary of $y(x) = 0$, when $G_{np}^{\pm}(h = 0) = 2\pi\delta_{np}$, and the dispersion equation takes the following form:

$$D_0(\omega, \mathbf{k}) = \prod_n q_{ny} \prod_n \alpha_n = 0. \qquad (5.4.64)$$

The value α_n has been early defined in (5.3.30). The solutions of $\alpha_n = 0$ give the spectrum of resonant frequencies (5.3.36). Without loss of generality, we assume that the mode of SP-spectrum with n excites. Then, expanding the determinant on the sum over column n, Eq. (5.4.63) can be rewritten as:

$$D(\omega, \mathbf{k}) = \sum_{p=-\infty}^{p=\infty} T_{np} \hat{M}^{np} = 0, \qquad (5.4.65)$$

where $\hat{M}^{np}$ is the main minor, corresponding to the matrix coefficient T_{np}:

$$T_{np}\left(\omega-\omega_n\right)^2=\left(q_{ny}+(n-p)\chi\frac{q_{nx}}{q_{ny}}\right)G_{np}^{+}\left(\left(\omega-\omega_n\right)^2-\Omega_{bn}^2\right)$$
$$-\frac{\Delta_b\omega_b^2\omega_n}{2u\gamma_0^4}e^{-2\frac{\omega_n b}{u\gamma_0}}\left(q_{ny}+(n-p)\chi\frac{q_{nx}}{q_{ny}}\right)\left(G_{np}^{+}-G_{np}^{-}\right). \tag{5.4.66}$$

Introducing the value

$$Z_n=\frac{\sum_{p=-\infty}^{p=\infty}\left(q_{ny}+(n-p)\chi\frac{q_{nx}}{q_{ny}}\right)\left(G_{np}^{+}-G_{np}^{-}\right)\hat{M}^{np}}{\sum_{p=-\infty}^{p=\infty}\left(q_{ny}+(n-p)\chi\frac{q_{nx}}{q_{ny}}\right)G_{np}^{+}\hat{M}^{np}}, \tag{5.4.67}$$

we rewrite Eq. (5.4.65) as:

$$D(\omega,\mathbf{k})=\left(\omega-\omega_n\right)^2-\Omega_{bn}^2-Z_n\frac{\Delta_b\omega_b^2\omega_n}{2u\gamma_0^4}e^{-2\frac{\omega_n b}{u\gamma_0}}=0. \tag{5.4.68}$$

For frequency ω given by Eq. (5.3.43) we find $\left(\omega-\omega_n\right)^2-\Omega_{bn}^2=\delta\omega^2\pm2\Omega_{bn}\delta\omega$.

Introducing the following notation

$$\mu=\frac{Z_n}{e^{-2\frac{\omega_n b}{u\gamma_0}}-1}, \tag{5.4.69}$$

we obtain the final form of the dispersion equation for $\delta\omega$:

$$D(\omega,\mathbf{k})=\delta\omega^2\pm2\Omega_{bn}\delta\omega+\mu_n\Omega_{bn}^2=0. \tag{5.4.70}$$

The upper plus sign corresponds to the branch $\omega=\omega_n+\Omega_{bn}$, while the lower minus sign corresponds to the branch $\omega=\omega_n-\Omega_{bn}$. The solutions of Eq. (5.4.70) are $\delta\omega=\pm\Omega_{bn}\left(1\pm\sqrt{1-\mu_n}\right)$. The complex frequency of SP instability is

$$\omega=\omega_n\pm\Omega_{bn}\sqrt{1-\mu_n},\quad n=1,2,3,... \tag{5.4.71}$$

The growth rate of instability is $\delta\omega'' = \Omega_{bn}\,\mathrm{Im}\sqrt{1-\mu_n}$. If $|\mu_n| << 1$, we obtain the collective regime of generation, when $|\delta\omega| >> \Omega_{bn}$, with $\delta\omega \approx \pm\frac{i}{2}\Omega_{bn}\mu_n$. The growth rate is $\delta\omega'' = \pm\frac{1}{2}\Omega_{bn}\,\mathrm{Im}(\mu_n)$.

For $|\mu_n| >> 1$, we obtain the Thompson regime of generation, when $|\delta\omega| >> \Omega_{bn}$, with $\delta\omega \approx \pm i\Omega_{bn}\sqrt{\mu_n}$. The growth rate for the single-particle type is $\delta\omega'' = \pm\Omega_{bn}\,\mathrm{Re}\left(\sqrt{\mu_n}\right)$.

If one branch of coupled frequencies, for example, the branch with high frequency, increases, then the other branch decreases and vice versa.

5.5. Rectangular grating

In this section, as an important example of application of the obtained results, we present the small signal gain of a SP FEL in the case of a rectangular grating.

In spite of the fact that our approach excludes the case of a rectangular grating on the face of it, the obtained equation (5.4.60) can describe that case. One of the ways is to calculate the coefficients in Eq. (5.4.60) with the methodused in [128,132,134,138,]. The solution of Maxwell equations is expressed as series of the cavity modes for the grooves space y < h . To sew the solutions for y > h and for y < h gives the coefficients for Eq. (5.4.60). In our paper we offer another method. In order to find the coefficients G_{np} we consider the grating with trapezoid form

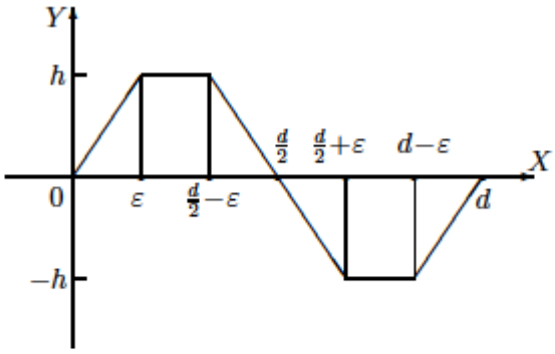

Fig.15. The function of f(x) given by Eq. (5.5.72).

$$f(x)=\begin{cases}\dfrac{h}{\varepsilon}x, & 0<x<\varepsilon\\ h, & \varepsilon<x<\dfrac{d}{2}-\varepsilon\\ -\dfrac{h}{\varepsilon}x+\dfrac{hd}{2\varepsilon}, & \dfrac{d}{2}-\varepsilon<x<\dfrac{d}{2}+\varepsilon\\ -h, & \dfrac{d}{2}+\varepsilon<x<d-\varepsilon\\ \dfrac{h}{\varepsilon}x-\dfrac{hd}{\varepsilon}, & d-\varepsilon<x<d\end{cases} \tag{5.5.72}$$

Substituting the function (5.5.72) in formula (5.4.62) and then integrating we find

$$G_{nn}^{\pm}=2(\pi-2\eta)\cos\left(q_{ny}h\right)+\frac{4\eta}{q_{ny}h}\sin\left(q_{ny}h\right), \tag{5.5.73}$$

$$G_{np}^{\pm}=\frac{2\eta}{(n-p)\eta\pm q_{ny}h}\sin[(n-p)\eta\pm q_{ny}h]+\frac{2\eta(-1)^{n-p}}{(n-p)\eta\mp q_{ny}h}\sin[(n-p)\eta\mp q_{ny}h]$$
$$-\frac{2}{n-p}\left\{\sin[(n-p)\eta\pm q_{ny}h]+(-1)^{n-p}\sin[(n-p)\eta\mp q_{ny}h]\right\}. \tag{5.5.74}$$

Here $\eta=\chi\varepsilon$ is a dimensionless length.

For the triangular form of grating $\eta = \pi/2$ and we get

$$G_{nn}^{\pm} = \frac{2\pi}{q_{ny}h}\sin\left(q_{ny}h\right), \tag{5.5.75}$$

$$G_{np}^{\pm} = \frac{\pi}{(n-p)\frac{\pi}{2} \pm q_{ny}h}\sin[(n-p)\frac{\pi}{2} \pm q_{ny}h] + \frac{\pi(-1)^{n-p}}{(n-p)\frac{\pi}{2} \mp q_{ny}h}\sin[(n-p)\frac{\pi}{2} \mp q_{ny}h]$$
$$-\frac{2}{n-p}\left\{\sin[(n-p)\frac{\pi}{2} \pm q_{ny}h] + (-1)^{n-p}\sin[(n-p)\frac{\pi}{2} \mp q_{ny}h]\right\}. \tag{5.5.76}$$

For the rectangular profile of the grating $\eta = 0$ and we find

$$\begin{aligned} G_{nn}^{\pm} &= 2\pi\cos\left(q_{ny}h\right), \\ G_{np}^{\pm} &= \pm\frac{2}{n-p}\left[(-1)^{n-p} - 1\right]\sin(q_{ny}h). \end{aligned} \tag{5.5.77}$$

With $|n|$ rising the coefficients T_{np} increase. In order to remove the overfull data in numerical calculations we have to re-normalize the coefficients T_{np}:

$$\begin{aligned} T_{nn} &= \alpha_n, \\ T_{np} &= \frac{(-1)^{n-p} - 1}{\pi}\left(\frac{1}{n-p} + \chi\frac{q_{nx}}{q_{ny}^2}\right)\frac{\sin(q_{ny}h)}{\cos(q_{ny}h)}\left(1 + K(n)\left(1 + e^{2iq_{nb}}\right)\right). \end{aligned} \tag{5.5.78}$$

for imaginary q_{ny}.

We can not make the analytic estimation of the upper limit for the absolute value of the term. Instead we made a numerical test. We took into account the (2N+1) surface modes, or in other words, we calculated the growth rate using (2N+1) x (2N+1) matrix. The results of calculations are shown in Fig.16

for the following parameters: mode of SP-radiation n=2, relativistic factor gamma_0=2, beam current I_b=2A/cm, period of the grating d=1cm, amplitude of the grating h=1cm and height of the beam b=1cm.

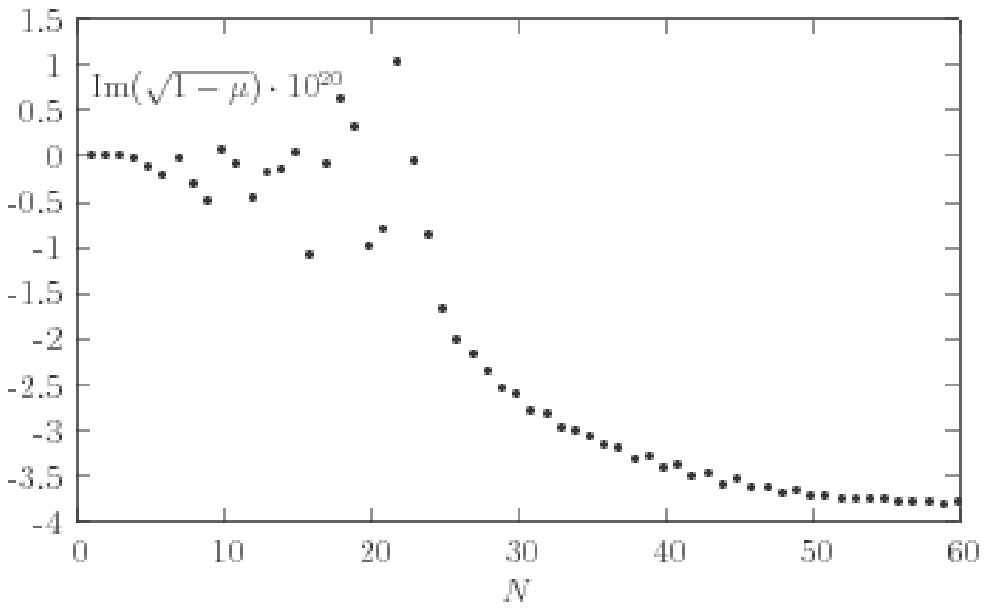

Fig.16. The dimensionless growth rate as a function of the matrix size (2N+1) x (2N+1) for theta =0.5rad. The calculation parameters are: mode of frequency n=2, gamma=2, beam current I_b=2A/cm, period of grating d=1cm, amplitude of grating h=1cm, and height of the beam b=1cm.

We can see that the results depend weakly on N for N > 48. Therefore, in our calculation we have used N = 50.

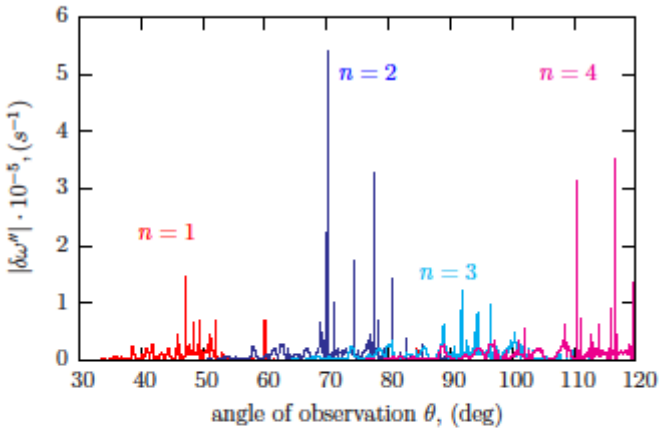

Fig.17. The growth rate as a function of the observation angle θ for different n modes of SP-radiation. The calculation parameters are: relativistic factor $\gamma = 4$, beam current I_b=10A/cm, period of grating d=1cm, amplitude of the grating h=1cm, and height of the beam b=1cm.

In Fig.17 the dependence of the growth rate on the observation angle θ is shown for the first four modes of the SP-spectrum for the following parameters of calculation: relativistic factor $\gamma = 4$, beam current I_b=10A/cm, period of grating d=1cm, amplitude of the grating h=1cm, and height of the beam b=1cm. The growth rate has got several high narrow peaks, the width of which is about 0.001~ rad. In real experiments this feature can be observed only if the real electron beams have narrow spread of electrons velocity. For the constant frequency ω_n the vagueness of the velocity $\delta\beta$ corresponds to the vagueness of the observation angle defined by the formula

$$\delta\theta = \frac{\delta\beta}{\beta^2 \sin\theta} \qquad (5.5.79)$$

For $\delta\beta = .0.01rad$ and $\beta \approx 1$, $\theta \approx 50\deg.$ we find that $\delta\theta = .0.01rad$. This means that the peaks will be smoothed. So, the peaks of growth rate are realized when the velocity spread of the beam is smaller than $\delta\beta = .0.01rad$.

The maximal values of the growth rate for the first mode localize within the range of 37deg.< θ <60deg.. With the number of the SP spectrum mode increasing, the region, where the instability can excite, shifts to the large values of the observation angle θ. For n=2 the maximal values of the growth rate are localized in the range of 55deg.< θ <100deg.. The maximum values of the growth rate for n=3 are in the interval of 70deg.< θ <110deg., while for n=4 are within the range of 90deg.< θ <120deg..

Fig.18 shows the growth rate as a function of the observation angle for parameters close to those of the Dartmouth experiment [35]: the Lorentz factor $\gamma = 1.068493$ (the corresponding electron energy E=35keV), and the distance between the beam and the top of grating $y_0 = 20\mu m$ (the corresponding height of the beam b = 70 μm).

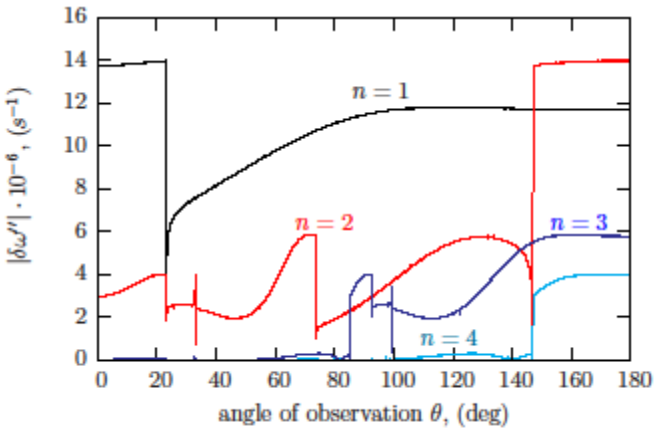

Fif.18. The growth rate as a function of the observation angle θ for different n modes of SP-radiation for parameters which are close to the parameters of the Dartmouth

experiment [35]. The calculation parameters are: relativistic factor $\gamma = 1.068493$ (the corresponding electron energy E=35keV), beam current I_b=10A/cm, period of grating d=173 μm, amplitude of the grating h=50 μm, and height of the beam b=70 μm (the corresponding gap between beam and top of grating $y_0 = 20\mu m$).

Other parameters are beam current I_b=10A/cm, period of grating d=173, $y_0 = 20\mu m$, and amplitude of grating h=50, $y_0 = 20\mu m$. In this case the narrow peaks are absent. The first mode n=1 dominates in the range of 0deg.< θ<147deg., while the second mode n=2 dominates within the interval of 147deg.< θ <180deg.. So the mode with n=1 will excite first of all at θ=90deg.. Our calculation well agrees with the results of the Dartmouth experiment, where only first mode was observed [35].

Fig. 19 shows the dependence of the growth rate on the beam current I_b for n=1 mode of SP-radiation and observation angle θ = 38.75 deg. The parameters of calculation are relativistic factor γ =10, period of grating d=1 cm, amplitude of the grating h=1 cm, and height of the beam b=1cm. One can see that within wide range of current values the growth rate places under the law $\delta\omega'' = .\sqrt{I_b}$.

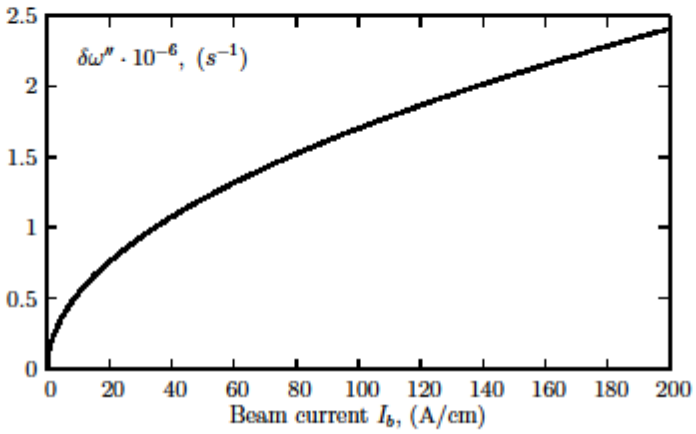

Fig.19. The growth rate as a function of the beam current I_b for n=1 mode of SP-radiation and observation angle θ=38.75deg. The calculation parameters are: relativistic factor γ=10, period of grating d=1cm, amplitude of the grating h=1cm, and height of the beam b=1cm.}

Fig. 20 shows the dependence of the growth rate on therelativistic factor gamma for the first three modes of of SP-spectrum for the following parameters of calculation: beam current I_b=10A/cm, period of grating d=1cm, amplitude of the grating h=1cm, and height of the beam b=1cm.

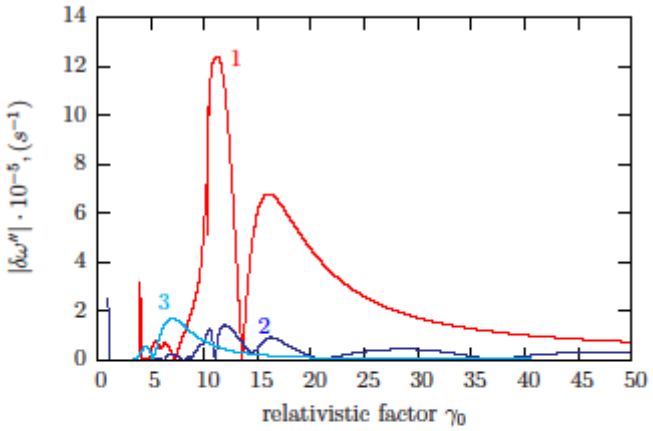

Fig.20. The growth rate as a function of the relativistic factor γ_0. (1) for n=1 mode of SP-radiation and observation angle θ =38.75deg, (2) for n=1 mode of SP-radiation and observation angle θ =32.83deg, (3) for mode n=3 of SP-radiation and observation angle θ = 80.21deg. The parameters of calculation are: beam current I_b=10A/cm, period of grating d=1cm, amplitude of the grating h=1cm, and height of the beam b=1cm.}

The growth rate dependence on relativity marks a complicated form; function $\delta\omega''(\gamma)$ oscillates and decreases with the relativity rising. The maximum rate for the first mode corresponds to the high narrow peak.

Our preliminary calculations show that the growth rate has of a complicated nature.

5.6. Discussion

We have used the framework of the dispersion equation to study coherent Smith-Purcell (SP) radiation induced by a relativistic magnetized electron beam in the absence of a resonator. We have found that the dispersion equation describing the induced SP instability is a quadratic equation for frequency; and the zero-order approximation for solution of the equation, which gives the SP spectrum of frequency, corresponds to the mirror boundary case, when the electron beam propagates above plane metal surface (mirror). It was found that the conditions for both the Thompson and the Raman regimes of excitation do not depend on beam current and depend on the height of the beam above the grating surface. The growth rate of the instability in both cases is proportional to the square root of the electron beam current. No feedback is needed to provide the coherent emission. As an important example of the application of the obtained results in [126] the growth rate of SP FEL in the case with a rectangular grating was calculated. The calculated results are consistent with the experimental data obtained by Urata [35].

We have presented a theoretical treatment of the small signal gain regime of a SP FEL. Considering an electron beam of infinite thickness being at a finite height above the grating, we have established the dispersion relation for the electromagnetic waves excited. An arbitrary grating is described with

metal boundary condition. The dispersion relation has been studied considering amplification of the surface as well as radiation modes. An analytical expression for the growth rate of SP instability has been derived. The gain dependence on the beam relativity factor and the beam height above the grating and the angle of observation has also been analyzed. We have examined various limits of the growth rate depending on the electron beam and grating parameters. Our calculations provided for rectangular grating are in good agreement with the results of the Dartmouth experiment, where only first mode of coherent emission by non-bunching beam was observed [40].

We have obtained the equation (4.4.60), which connects $\mathbf{E}_n^-$ and $\mathbf{E}_n^+$ waves, using general form of boundary condition for metal surface. Other authors [128,132,134,138] have used an approach in terms of an impedance matrix. Our approach yields an equation which has a more general form. Indeed, in the particular case when $\Pi_p = \Pi_p^*$ and $G_{np}^+ = -G_{np}^-$, equation (4.4.60) reduces to equation (40) in ref.[134].

We have found that the zero-order approximation for the solution of the dispersion equation of SP-generation corresponds to the plane mirror boundary case, when the electron beam propagates above a plane metal surface (mirror). We found that the "mirror" boundary condition gives a discrete spectrum, the modes of which contain two coupled frequencies: "high" frequency with $\omega = \omega_n + \Omega_{bn}$ and "low" frequency with $\omega = \omega_n + \Omega_{bn}$. The growth rates for both Thompson and Raman types of waves excitation are proportional to the Langmuir frequency ω_b or square root of the beam

current $I_b^{1/2}$. The conditions for both Thompson and Raman types of excitations do not depend on the Langmuir beam frequency (or beam current), but depend on the beam height b above the grating. It is essential that there is a distinction between the Vavilov-Cherenkov and the Smith-Purcell instabilities. But there are a parallels between the Cherenkov and the Smith-Purcell instabilities. The first of them is that no feedback is needed to provide coherent emission. The second parallel is the following. The operating frequencies and wavelengths for SP-spectrum are determined as intersection points of the dispersion line for the electromagnetic wave $\omega = k_x \mathrm{c}/\cos\theta$ with the lines of the longitudinal waves $\omega = k_x + n\chi u$. We can consider the longitudinal waves as beam waves, which excite in the beam propagating in the vicinity of a surface with a periodic structure. Then the Smith-Purcell instability is a specific case of the Cherenkov effect. Indeed, the solution (4.2.19) of motion equation contains the pole

$$\frac{1}{\omega - (k_x + n\chi)u}$$

which corresponds to excitation of eigenmodes in system quasi the Vavilov-Cherenkov instability is.

The SP instability can excite only for radiative waves, when k_y is real, and therefore $k_x < \omega/c$, and the condition (4.3.37) takes place. Recently Brau and co-workers [128] have suggested that there is a nonradiative mode with imaginary k_y, which propagates along the grating incoming from infinity and the wave number of which satisfies the condition of $k_x > \omega/c$, so that the Vavilov-Cherenkov effect condition can take place. They have considered the

Cherenkov instability of the evanescent mode of a rectangular grating as a candidate for the induced Smith-Purcell radiation. They suppose that the operating frequency and wavelength are defined by the intersection of the dispersion curve of evanescent mode with the beam line $\omega = (\mathbf{ku})$. In Phys. Rev. STAB there have recently appeared two articles [139,140] reporting experiments that do confirm the Andrews and Brau theory.

The induced Smith-Purcell and Andrews-Brau (AB) effects are similar. But there are differences between them. One of them is that the dispersion curve of the surface evanescent mode depends on the profile of grating. In particular, the dispersion curve depends on the depth and width of the groove on a rectangular grating. Andrews and Brau have obtained the coefficient of the reflection matrix $C_{mn} = R_{mn} + \chi_0 S_{mn}$ for the case, when uniform cold electron plasma moves with constant velocity above a rectangular grating. The first term R_{mn} of does not depend on the plasma density (beam current) and is given by Equation (31) in Ref. [128]. We rewrite here this term in the form of $R_{mn} = \tanh(\chi_n H) f(A,L)$, where H denotes the groove depth, A the groove width, and L the period of the grating; $\chi_n = \left((\pi n / A)^2 - \omega^2 / c^2\right)^{1/2}$ denotes the wave number. Under condition, when H tends to zero, the coefficients R_{mn} are proportional to H and tend to zero too. We find that the dispersion relation of $|R_{mn} - \delta_{mn}| = 0$ (equation (33) in Ref. [128]) does not hold for shallow depth H. This means that there is a threshold value for the groove depth, below which a grating cannot have a dispersion relation in the absence of a beam. Note that we have obtained the same result in Eq. (4.3.32). Thus, the Cherenkov instability of evanescent mode does not excite in case of gravity with moderate depth below the

threshold, while, as our analysis shows, the induced SP instability has not such threshold in case of an ideal metal grating, with no Ohmic losses. The second distinction between the SP and the AB effects is that there is a threshold value for the beam velocity, above which the operating point defined as the intersection of the dispersion curve of evanescent mode with the beam line $\omega = (\mathbf{ku})$ is absent. For the parameters used in [139] the threshold value of velocity is about v=0.94c (Fig. 2 in [139]). Therefore, only induced SP instability will excite in a SP FEL based on a relativistic electron beam.

Donohue and Gardelle [140] have performed a simulation of generation of SP radiation at terahertz frequencies using 2D code MAGIC for a configuration similar to the Dartmouth experiment. They have found that the first mode of SP-radiation excites first of all, which supports our results for the generation of coherent SP-radiation; and then oscillations with frequency corresponding to the Cherenkov instability of evanescent mode excite during non-linear regime. They found also that non-radiated surface waves propagating along the grating surface reflect and transform to radiated mode from the ends of the grating. In this case the grating with finite size is an open resonator. The growth rates of SP instability may slightly depend on the grating length. The four-wave radiative Pierce instability, which does not demand a resonant condition between the phase velocity of the wave and velocity of particle, can excite [141,142]. But the growth rate of such non-resonant instability will be noticeably small with respect to the growth rate of the resonant SP instability. Therefore, the SP instability will dominate.

The amplification problem for SP-system, when incoming waves are, may expect to correspond the Cherenkov case. If the dispersion equation tends to equal zero as beam current vanishes, the solutions of dispersion equation assume to get another forms, and the growth rate may be proportional to the cube root of beam current $I_b^{1/3}$. These phenomenon can be the subjects of separate studies.

Chapter 6.

Gamma Radiation Production Using Channeled Positrons Annihilation in Ionic Crystals

The Chapter based on 3 publications [157,169,170,172]

6.1. Overview

The search for short-wave coherent radiation generation always was an essential problem of science due to its wide applied significance. The author of paper [143] is one of the first to suggest the mechanism of radiation of relativistic electrons at their movement in periodic structures (see also [143]); later such structures were named undulators. This at the first sight imperceptible paper has later essentially accelerated the process of creation of such modern devices as synchrophasotrons and the lasers on free electrons (see for example [112], [43]). There are many articles and reviews on the short wavelength region of radiation. The overview [145] is devoted to X -ray optics and future prospects. In spite of the fact that the technology of generation of undulator radiation is being steadily developed and the successes are obvious ([145], [147]) the problems are obvious too and which remain unresolved up to now.

The frequency of undulator radiation is defined by the length of its periodic element, which in FELs and undulators devices is macroscopic. The drawback of undulators is that they are large and use high-energy electrons.

After the discovery of electrons (positrons) channeling in crystals [148-150] accompanied by its short-wave radiation [151], there appeared a hope that all the aforementioned problems can be solved. However, these hopes up to now are justified only partially. In particular, the problem of generation of short-wave radiation (X-ray) from less energetic electrons (of order of several MeV) at very small distances (of order of several micron) has been solved. Now a new problem arises. The point is, that in the regime of channeling the particles (electrons and positrons) usually live very short time $\sim 10^{-14} \div 10^{-15}$ sec.

However, this time is very short for the conversion of an appreciable part of particle energy to energy of radiation. The short lifetime as well does not conduce to use of external factors for control by beam of channeling particles and improving of spectral characteristics of radiation.

The quantum theory of channeling for electrons and positrons has been elaborated by many authors [151,152,62]. It is important to note that an electron in a crystal can commit both planar and axial channeling. At the same time only one type of real channeling for the positrons is known, the regime where a particle is localized between two adjacent planes. The possibility of axial channeling of positive particles has not been investigated seriously up to now, because the crystallographic axes, irrespective of grade of the crystal are been charged positively. However, investigation of possibilities of axial channeling of positrons and, hence, formation of metastable relativistic positron systems (PS) is a problem of utmost importance for a radiation physics.

Different methods have been proposed for generation of coherent gamma rays based on the effect of channeled positron annihilation with the electrons of media [153].

A scheme of an intense coherent gamma-ray source based on the spontaneous radiation of positronium atoms in a Bose-Einstein condensate (BEC) due to two-photon collective annihilation decay is investigated analytically arising from the second quantized formalism [154].

Macroscopic channeling in magnetic systems and in an intense electromagnetic wave is studied in [155].

In earlier studies [156] the possibilities of ionic crystals of type CsCl have been investigated; it was shown, that at channeling of positrons around the axes of negatively charged ions of Cl^- the main factor of dechanneling - the scattering of particles on phonons subsystem is absent. However, there are such channels for positrons, as shows the analysis, also in other more realistic crystals, for example, in crystal of SiO_2.

In this paper the annihilation processes in the expansion of energy levels of relativistic Positron Systems (PS) is analyzed and shown that PSs are metastable.

6.2. Formation of relativistic positron system (PS)

In the previous paper [157] we have shown, that if a low-energy relativistic positrons (5 - 20 MeV) are scattering under a small angles ϑ_L (where ϑ_L is a Lindhard angle) on the axis <100> of chlorine ions Cl^-, then they fall into

the regime of axial channeling. Moreover, the motions of positrons concentrate between two cylinders with cross section circles 1 and 2 in Fig.21 , which is very important from the point of view of movement stability. In particular, the effective 2D potential of channeling does not depend on temperature of media in a broad range of temperatures, as it was shown, and has a depths of potential of an order of -10eV , which is sufficient for the formation of several quantum states of transverse motion. Recall, that this type of effective potential can be in other crystals too. For example, the effective potential of negatively charged ions of O_2 axes often used in experiments with SiO_2 crystal is such.

In other words, the relativistic positrons in described regime of channeling do not interact with phonons subsystem. This means, that the main factor of dechanneling of particles in considered case is absent. Taking into account the symmetry of effective potential for positrons around negative ions axis (see Fig.21) we can write the following analytical formula:

$$U(\rho) = U_0\left(e^{-2\alpha\bar{\rho}} - 2e^{-\alpha\bar{\rho}}\right), \qquad \bar{\rho} = (\rho - \rho_0)/\rho_0, \quad \rho = \sqrt{x^2 + y^2}, \tag{6.2.1}$$

where the parameters for usual crystals are being found into intervals D_0=5 - 10 eV , $\alpha = 0.5 \div 0.8$ and $\rho_0 \approx 0.5d$, and d is a lattice constant.

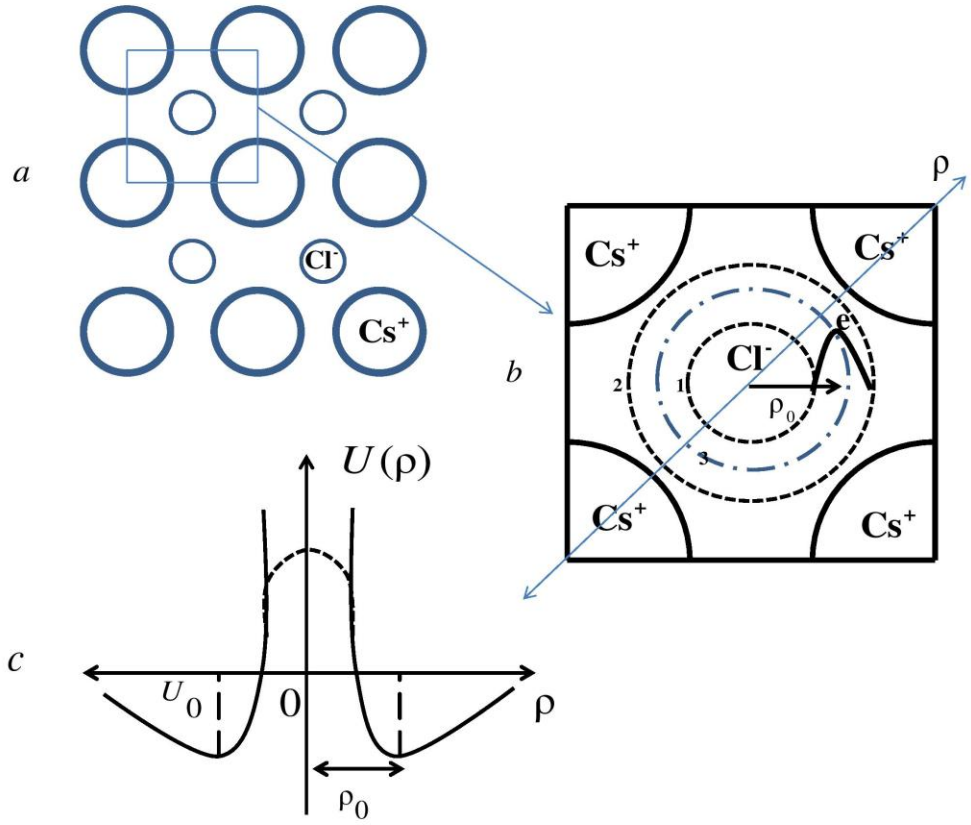

Fig.21. The lattice of $CsCl$ crystal, b) the lattice cell, c) the effective potential of axial canneling for positron around the axis of negatively charged ions of Cl^- is shown along radius ρ, which in region of positron localization is described very well by Morse potential.}

Potential (6.2.1) was obtained and discussed in details in [156]. An analytical expression is received for the effective interaction potential of a fast charged particle with the ionic crystal of CsCl near the direction of axis <100> as a function of the temperature of the medium in Ref.[157]. By numerical analysis it is shown that the effective potential of axial channeling of positrons along the axis <100> of negatively charged ions of Cl^- practically does not depend on the temperature of the media.

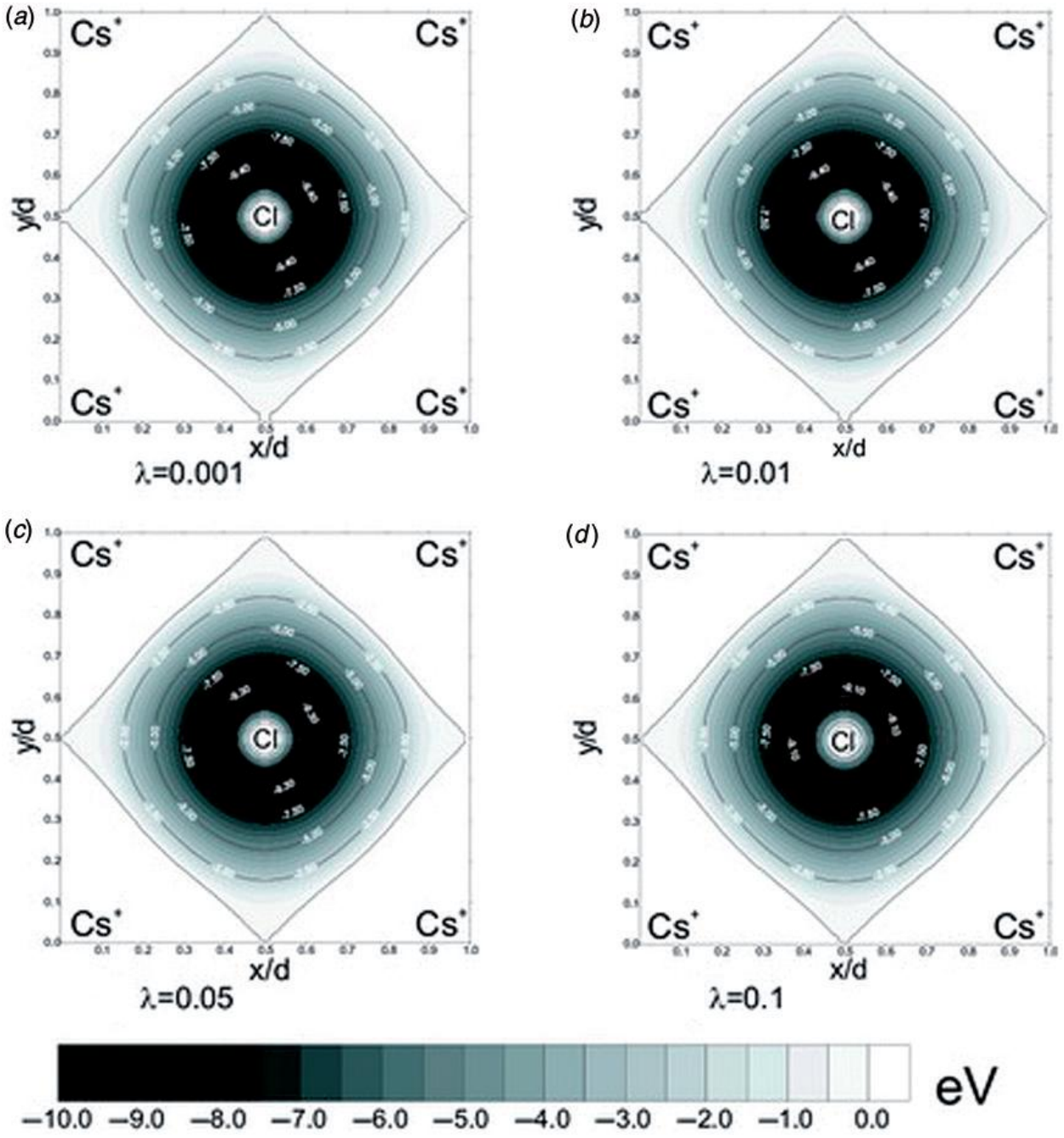

Fig.22. Profile of the effective potential for the axial channeling of a positron along the <100> axis of Cl_ ions at various temperatures.

As one can see from Figures 22(a) - 22(d) of [157], for positively charged fast particles around the <100> axis of ions there exists a rather broad potential (width $\Delta d \approx 0.25d$) with the depth of order of - 10 eV , which remains constant for a large range of thermal vibrations , $\lambda = u_0 / d = 0.001 - 0.1$ (u_0 are the thermal vibration amplitudes), i.e. for a broad range of temperatures. In other words, a relativistic positively charged particle, at scattering under a small angle on the <100> axis of Cl^- ions,

can be captured in the regime of axial channeling, during which the scattering of a positron on the phonon's subsystem does not occur. Based on the symmetry of the resulting effective potential (Figures 22(a) - 22(d) of [157] and Figure 21 b), the effective potential conveniently may be fitted by the function (5.2.1).

It is important to note that the potential (5.2.1), as we have shown, well enough approximates the exact effective field (6) of [157]. It is enough to say, that in the regions where the potential U < - 4 eV , the approximation error is below 1\%.

The full wavefunction of positron in the potential (5.2.1) in atomic units $\hbar$=c=1 is solved exactly and represented as [157]:

$$\Psi(\mathbf{r}) = \frac{1}{\sqrt{2\pi d}} e^{ip_z z} \Phi(\rho, \varphi), \quad \mathbf{r} = \mathbf{r}(z, \rho, \varphi), \tag{6.2.2}$$

where $\Phi(\rho,\varphi)$ describes the wavefunction of localized state of positron system (PS) with relativistic mass μ and is characterised by quantum numbers of vibration n and rotation m correspondingly [158]:

$$\Phi(\rho,\varphi) = \frac{1}{\sqrt{2\pi\rho}} e^{im\varphi} y^s exp\left(-\frac{y}{2}\right) {}_1F_1(a,b,y), \quad m = 0, \pm 1, \pm 2, ..., \tag{6.2.3}$$

where the following notations are made: $y = 2\gamma_2 \alpha^{-1} exp\left(-\alpha\bar{\rho}\right)$ and $s = \beta\alpha^{-1}$, in addition:

$$\begin{aligned} &a = \frac{1}{2}\left(1 + \frac{2\beta}{\alpha}\right) - \frac{1}{\alpha}\left(\frac{\gamma_1}{\gamma_2}\right)^2, \quad b = 1 + \frac{2\beta}{\alpha} \\ &\beta^2 = 2\mu\varepsilon\rho_0^2 + Mc_0, \quad \gamma_1^2 = 2\mu D_0\rho_0^2 - \frac{M}{\alpha}\left(2 - \frac{3}{\alpha}\right), \\ &\gamma_2^2 = 2\mu D_0\rho_0^2 - \frac{M}{\alpha}\left(1 - \frac{3}{\alpha}\right), \quad M = m^2 - 1/4. \end{aligned} \tag{6.2.4}$$

The localized state eigenvalues are presented by the following formula:

$$\varepsilon_{nm} = \frac{1}{2\mu\rho_0^2}\left\{-\gamma_0^2 + 2\alpha\gamma_0\left(n+\frac{1}{2}\right) - \alpha^2\left(n+\frac{1}{2}\right)^2\right\}$$
$$+\frac{1}{2\mu\rho_0^2}\left\{M - \frac{3(\alpha-1)}{\alpha\gamma_0}\left(n+\frac{1}{2}\right)M\right\} - \frac{1}{2\mu\rho_0^2}\frac{9}{4}\left(\frac{\alpha-1}{\gamma_0}\right)^2\frac{M^2}{\alpha^4}, \qquad (6.2.5)$$

where $\gamma_0 = \sqrt{2\mu D_0}\rho_0$,

6.3. Processes leading to decay of positron-systems

After exception of major factor of dechanneling there still remain two different processes, which lead to decay of PSs:

a) the annihilation of positron with electron of media on one gamma photon;

b) the annihilation of positron with electron of media on two gamma photons;

The main problem now is the investigation of the processes contributing to the lifetime of PSs.

A. Decay PA on One gamma Photon

It is obvious that PS may be illustrated as a system having zero total spin (like of parapositronium), because the skeleton of negatively charged ions axis does not possess spin and, accordingly, there is no spin-spin interaction between it and the positron. In other words, the interaction between positron and the axis is only an electromagnetic one. Another distinction between positronium and PS is the possibility of decaying of the last one on

one gamma photon. Note, that in this case the conservation laws of energy and momentum take place in view of presence of media.

This process is being defined by matrix element of first order [159]:

$$Q = \left\langle f \left| S^{(1)} \right| i \right\rangle = \frac{2\pi i e}{\sqrt{2\omega}} \int \Psi^{*}(\mathbf{r}) \mathbf{e} e^{-i\mathbf{qr}} \psi(\mathbf{r}) d^{3}r \delta\left(\varepsilon_{p} + \varepsilon_{e} - \omega\right), \tag{6.3.6}$$

where Ψ and ε_p are the wave function and the total energy of positron, ψ and ε_e designate the wave function and the energy of media's electron, $\mathbf{q}$-is the momentum of γ photon, ω-its frequency. Taking into account that the distribution of electrons in positive as well in negative ions is given by spherical model JMGR, we can write the wave function of electrons system in a factorized form:

$$\psi(\mathrm{r}) \equiv \psi(\rho, z, \varphi) = \frac{1}{\sqrt{d}} e^{i\eta(z)z} \chi(\rho), \tag{6.3.7}$$

where $\eta(z)$ is a momentum of media electron in the point z, it is supposed that the random function $\eta(z)$ has a zero average value. This means, that the statistical averaging of random term in (6.3.7) is equal to unity $\left\langle e^{i\eta z/\hbar} \right\rangle = 1$. In addition $\chi(\rho)$ is Gaussian function, which is normalized to unity:

$$\chi(\rho) = \frac{1}{(\pi)^{3/4} \rho_0} e^{-\bar{\rho}^{2}/2}. \tag{6.3.8}$$

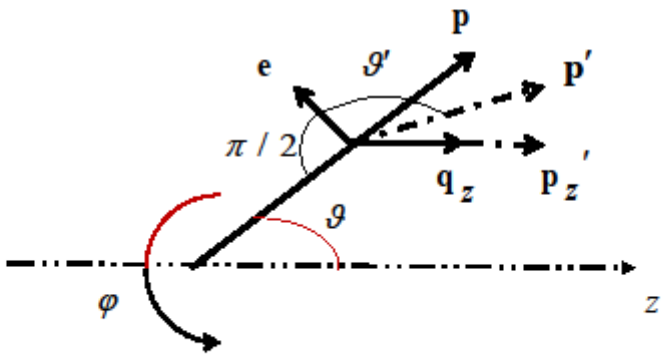

Fig.23. The kinematic schema of momenta and angles between them.

Channeling occurs along the axis of the negatively charged chlorine ions <100>, which are represented as negatively charged spheres with a radius of $\rho = \rho_0$. In the structure of CsCl , the nearest neighbors Cs^+ and Cl^- touch along the body diagonal [160]. $\rho = \rho_0$ is the radius of circle 3 (see Fig.21), which is the bottom of potential well and the top of electron wave function distribution as outer shell. Valence electron of Cl^- is situated on the outer shell of the sphere with radius $\rho = \rho_0$ on the circle 3 in fig.21.

The present research is devoted to the problem of formation of relativistic positron systems in medium. These systems can be stable, as was shown and hence, we can consider two different problems of radiation generation.

Since the main factor of dechanneling - the scattering of positrons on the phonons in the considered case is absent, then the positrons will be in the regime of channeling up to their decay. In this paper we have studied the problem of decay of positron systems for which level populations are not important.

As to the second problem connected with the radiation generated as a result of quantum transitions between the energy levels of positron systems, we are planning to investigate it in the nearest future.

We can write the following expression for the effective differential cross-section of annihilation:

$$d\sigma = \frac{e^2}{2(2\pi)^2 \omega} \sum_{\upsilon_e, \upsilon_p} |Q|^2 \delta(\varepsilon_p + \varepsilon_e - \omega) \omega^2 d\mathrm{o}_\gamma, \tag{6.3.9}$$

where $d\mathrm{o}_\gamma = \sin\theta d\theta d\varphi$ is the solid angle element in which is situated a photon momentum, υ_e and υ_p are summation indices of electron and positron spins in the initial state. However, for the considered problem, the electrons spin orientation does not play an important role and, correspondingly, later we will ignore the summation. In weakly relativistic case, the term Q in (5.3.9) is written in the following form:

$$Q = \int \Psi^*(\mathbf{r}) \mathbf{e} \hat{\mathbf{v}} e^{-i\mathbf{q}\mathbf{r}} \psi(\mathbf{r}) d^3 r, \quad \hat{\mathbf{v}} = \frac{1}{i\mu} \nabla_{\mathbf{r}}, \tag{6.3.10}$$

where $\hat{\mathbf{v}}$ is the operator of positron velocity, $\mathbf{e}$ - describes the unit vector of photon polarization. The expression (6.3.10) may be transformed to

$$Q = \frac{(2\pi)^3}{\mu} \int (\mathbf{e}\mathbf{p}') \hat{\Psi}^*(\mathbf{p}') \hat{\psi}(\mathbf{q} - \mathbf{p}') d^3 p',$$

where $\hat{\Psi}^*(\mathbf{p}')$ and $\hat{\psi}(\mathbf{q} - \mathbf{p}')$ are Fourier transforms of corresponding wave functions:

$$\begin{aligned} \hat{\Psi}^*(\mathbf{p}') &= \frac{1}{(2\pi)^3} \int exp(-i\mathbf{p}'\mathbf{r}) \Psi(\mathbf{r}) d^3 r, \\ \hat{\psi}(\mathbf{q} - \mathbf{p}') &= \frac{1}{(2\pi)^3} \int exp[-i(\mathbf{q} - \mathbf{p}')\mathbf{r}] \psi(\mathbf{r}) d^3 r. \end{aligned} \tag{6.3.11}$$

In (6.3.11) $\mathbf{p}'$-designates the momentum of positron, which in the considered case in toto coincides with its p_z projection. The analysis of expression for $\hat{\psi}(\mathbf{q}-\mathbf{p}')$ shows, that the transition amplitude is more probably if positron and photon momenta coincide i.e. $\mathbf{q}=\mathbf{p}'$.

Using the equality $(\mathbf{e}\,\mathbf{p}')=p'\sin\vartheta'$ and the above mentioned conclusion, we can write the expression (6.3.11) in the following form (see Fig 23):

$$Q=\frac{(2\pi)^3}{\mu}\hat{\psi}(0)\int p'\hat{\Psi}^*(p')\sin\vartheta' d^3p', \tag{6.3.12}$$

where $d^3p'=p'_\perp d\theta dp'_\perp dp'_z$.

The function $\hat{\Psi}(p')$ is calculated simply:

$$\begin{aligned}\hat{\Psi}(p')&=\frac{(-1)^m}{(2\pi)^2}\frac{e^{im\theta}}{\sqrt{d}}\delta\left(p_z-p'_z\right)\Theta_m\left(p'_\perp\right),\\ \Theta_m\left(p'_\perp\right)&=\int_0^\infty\Phi(\rho,0)J_m\left(p'_\perp\rho\right)\sqrt{\rho}d\rho.\end{aligned} \tag{6.3.13}$$

The calculation of cross-section we will begin with averaging of expression (6.3.12) by the photon polarization. It is obvious when we rotate the polarization vector $\mathbf{e}$ around photon's momentum $\mathbf{q}$ at an angle of π, then, as it can be shown, the angle ϑ' correspondingly changes within the limits $\pi/2-\left(\beta_q-\beta_{p'}\right)\le\vartheta'\le\pi/2+\left(\beta_q-\beta_{p'}\right)$, where $\beta_q=\arccos\left(q_z/q\right)$ and $\beta_{p'}=\arccos\left(p'_z/p'\right)$. After integration by angle ϑ' in Eq. (6.3.12) it is easy to find that

$$Q=-\frac{2(2\pi)^2}{\mu}\hat{\psi}(0)\int p'\hat{\Psi}^*(p')\sin\left(\beta_q-\beta_{p'}\right)d^3p'. \tag{5.3.14}$$

Now substituting (6.3.13) into (6.3.14) and making the elementary calculations we find:

$$Q = -\frac{2(2\pi)^2}{\mu d}\delta(p_z - q_z)\hat{\psi}(0) \times \int \bar{p}\,\Theta_0(p'_\perp)\sin(\beta_q - \beta_{\bar{p}})d^3p'_\perp, \tag{6.3.15}$$

where $\bar{p} = \sqrt{p_z^2 + p_\perp'^2}$, the δ - function shows the momenta conservation law on z - axis.

Finally, we analyze the amplitude Q forward, which is a more probable direction of PS decay on one γ photon, when the PS does not rotate. In this case, the equalities $\beta_q = 0$, $\beta_{\bar{p}} = \arccos(p_z / \bar{p})$ and $m=0$ take place with high accuracy.

We can substantially simplify expression (6.3.15) using these equalities:

$$Q = \frac{2(2\pi)^{5/2}}{\mu d}\delta(p_z - q_z)\hat{\psi}(0)p_z^{1/2}\int_0^\infty \Theta_0(p_\perp')p_\perp'^{3/2}dp_\perp', \tag{6.3.16}$$

Now using the expression (6.3.16) and standard connection between amplitude and transition probability [159] for the one-photon decay of PS we can write the following assessment:

$$P_\gamma \sim 10^6\,\mathrm{sec}^{-1}. \tag{6.3.17}$$

Note that in order to find assessment (6.3.17) we have used the parameters of a CsCl crystal with a lattice constant d=0.4123nm.

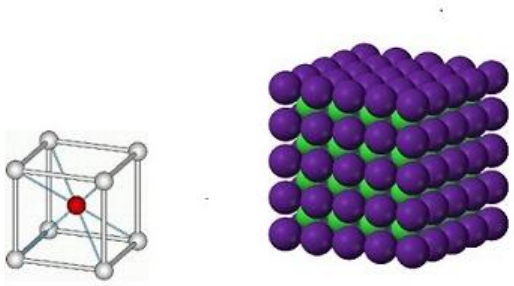

Figure 24. (Left) the cell of CsCl lattice, Cs+ ion is in the center of the cube (dark color) and Cl– ions are in vertexes, (right) CsCl lattice, Cl– ions are in dark color.

B. Decay PA on Two gamma Photons

It is easy to understand that the PA similar to positronium and, correspondingly the processes of their decaying should be similar too. This means, that the probability of annihilation of PA is similar to positronium annihilation and we can connect of PA decay with the probability of annihilation of free pair of positron and electron. It is obvious, that in the considered case the annihilation process does not depend on the orientation of electron and positron spins.

The analysis of Fourier image of PA wave function $\Theta_0(p_\perp)$ in a basic state shows, that the probability amplitude to find positron and electron with momenta $p_\perp$ and $-p_\perp$ is substantial for a momenta $p_\perp = .1/\rho_0$. Taking into account the last one, the cross-section of the process for a low-energy positron (namely such as the localization energies of positron) may be represented as (see for example)[172]:

$$\sigma = \pi r_0^2 / v_\perp, \qquad (6.3.18)$$

where r_0 is the electron's classical radius, $v_\perp = p_\perp / \mu$ is the positron speed on plane (x,y), where the positron's motion is localized between two circles 1 and 2 (see Fig 15, b).

Finally using (5.2.2) and (5.3.18), we can write the expression for probability of PA decay on two γ photons [159]:

$$P_{2\gamma} = \frac{1}{(2\pi)^2 \rho_0 d} \left|\Phi_{0,0}(\rho_0)\right|^2 (v_\perp \sigma)_{v_\perp \to 0} = \frac{r_0^2}{4\pi \rho_0 d} \left|\Phi_{0,0}(\rho_0)\right|^2 \square 10^6 \text{сек}^{-1}, \qquad (6.3.19)$$

where $\Phi_{n,m}(\rho_0)$ describes the radial part of wave function PS which in the "ground state" is written as $\Phi_{0,0}(\rho_0)$.

4.4. Conclusion

A possibility of channeling of low-energy (5 – 20 MeV) relativistic positrons in some ionic crystals with axial symmetry with coaxial symmetry around separate crystal axes of negative ions in some types of crystals, is shown. The annihilation processes of positrons with medium electrons are investigated in details. The lifetime of a positron in the regime of channeling is estimated; the existence of long relaxation lifetime has been shown, 10^{-6} sec, which on a $10^9 \div 10^8$ times is bigger than at usual cases.

Our investigations show, that problem connected with the short length of dechanneling is solved if we consider the channeling of positrons of energy 5 – 20 MeV, in particular, in CsCl type ionic crystals along the

chlorine ions axis <100>. In this case 2D relativistic positron systems are formed in crystal , which are practically not interacting with the phonons sub-system of lattice . All other types of influence on PS, collisions with electrons of media, the scattering on lattice discreteness etc, are perturbations of essentially small or similar to PS annihilation processes order. In other words, in the mentioned way, it is with higher probability possible to create 2D relativistic PSs in media with lifetimes bigger than 10^{-6}-10^{-7} sec. This means, that we solved the main problem of creation of nanoundulators, which have very large lifetimes and by which we can control.

7. SUMMARY

In conclusion we enumerate the main results obtained in the thesis.

1. Relativistic strophotron is investigated as an alternative scheme for Free Electron Laser. Spectral intensity of a spontaneous emission and the gain of an external wave in the strophotron are found by a superposition of contributions from emission or amplification at different (odd) harmonics of the main resonance frequency $\omega_{res}(x_0)$.
2. The main resonance frequency is shown to depend on the initial conditions of the electron, and in particular on its initial transversal

coordinate x_0. This dependence $\omega_{res}(x_0)$ is shown to give rise to a very strong inhomogeneous broadening of the spectral lines. The broadening can become large enough for the spectral lines to overlap with each other.

3. The spectral intensity of a spontaneous emission and the gain are averaged over x_0. The averaged spectral intensity is shown to have only a very weakly expressed resonance structure, whereas in the averaged gain, the resonance peaks are shown to be much higher than the nonresonant background. A physical nature of these resonances remaining after averaging is discussed. The maximum achieveable averaged gain and frequency of the strophotron FEL are estimated.
4. Estimates indicate a possibility of using the strophotron to construct such a FEL in the IR region. Probably both the gain G and the frequency $\omega = \omega_{res}$ can be increased with the help of an additional optirnization of the system [e.g., by the use of a "trough" with a varying field gradient g = g *(z)*] .
5. Comparision is done to indicate two features of the strophoton FEL differentiating this device from the usual undulator FEL. *1)* The frequency $\omega = \omega_{res}$ linearly depends on the angle α under which the electron enters the system. Hence, $\omega = \omega_{res}$ can be easily varied by a variation of α. *2)* The value of the "undulator" parameter K in the strophotron can be rather large. For example, the parameters used above for the estimates correspond to $\Omega \approx 2.2\times10^{10}\,s^{-1}$, $\alpha \approx 0.7$, $\alpha\gamma \approx 7$, $K(x_0 = 0) \approx 7$, and $s_{\max} \equiv \omega_{\max} / 2\omega_{res}(x_0 = 0) = \frac{3}{8}\left[K^3(x_0 = 0)\right] \approx 130$.

6. The nonlinear theory of radiation and amplification is developed.
7. Quantum-mechanical equations are derived for the amplitudes of the probabilities of transitions in a free-electron laser when transverse electron oscillations are due to a static potential, which is homogeneous in the direction of motion of the beam, but has a transverse gradient.
8. A quantum-mechanical description of the motion of an electron in classical fields is not in conflict with the fact that the final results obtained here do not contain the Planck constant $\hbar$. It is natural to expect the main results also in the classical approach [79].
9. Channeling of electrons moving across an intense standing light wave is described. This effect is proposed to be used for the creation of Free Electron Laser. Its linear gain is calculated and estimated. Estimates indicate that the gain should be sufficient for the construction of a free-electron laser operating in the infrared range.
10. We have shown that as a result of the allowance for magnetic field inhomogeneity, some additional peaks appear in the spectral distribution of spontaneous radiation and in the gain. Out of the multitude of these peaks one can obtain ultrashort pulses using the well-known mode-locking method. The peaks in the spectral distribution of spontaneous radiation and of the gain are localized at combinated frequencies of the odd harmonics of $(2n+1)\omega_{res,und}$ undulator resonant frequency and even harmonics of $2m\omega_{res,str}$ strophotronic resonance frequency. In case of an undulator with constant magnetic

field the peaks are localized at odd harmonics of undulator resonant frequency $\omega_{res,und} = \frac{2\gamma^2 q_0}{1+\gamma^2 \Omega^2/q_0^2}$, and in case of a strophotron they are localized at odd harmonics of strophotronic resonant frequency $\omega_{res,str} = \frac{2\gamma^2 \Omega}{1+\gamma^2 \Omega^2/q_0^2}$. One may conclude thus, that due to the presence of inhomogeneity in the magnetic field in the plane wiggler these two systems (wiggler with the constant magnetic field and the strophotron) are integrated in one unit and there appear peaks in the spectral distribution of spontaneous radiation and in the gain at combined (odd undulator and even strophotronic) resonant frequencies.

11. Taking into account the finite sizes of the beams, the value of the threshold laser power at the entry of the first undulator of FELWI, above which the selection of electrons via the transverse velocity in the drift region is possible, have been obtained for an FEL without inversion (FELWI). We find that an FELWI cannot operate under a weak-amplification Thompson regime, for which the spatial amplification is small: $k''L_e << 1$. Only a large-amplification regime, $k''L_e >> 1$, should be used to build an FELWI. It can be either the anomalous Thompson or the Raman regime of amplification, using an electron beam with overdense current density. For an FELWI operation, the optimal angle $\alpha + \theta$ between the electron and light beams is shown to depend on the the widths of the electron r_b and the laser r_L beams. The mechanism of an FELWI can be realized in scheme of a ring laser.

12. We have used the framework of the dispersion equation to study coherent Smith-Purcell (SP) radiation induced by a relativistic magnetized electron beam in the absence of a resonator. We have found that the dispersion equation describing the induced SP instability is a quadratic equation for frequency; and the zero-order approximation for solution of the equation, which gives the SP spectrum of frequency, corresponds to the mirror boundary case, when the electron beam propagates above plane metal surface (mirror). It was found that the conditions for both the Thompson and the Raman regimes of excitation do not depend on beam current and depend on the height of the beam above the grating surface. The growth rate of the instability in both cases is proportional to the square root of the electron beam current. No feedback is needed to provide the coherent emission. As an important example of the application of our obtained results in [126] the growth rate of SP FEL in the case with a rectangular grating was calculated. The calculated results are consistent with the experimental data obtained by Urata et. al. [35].
13. A possibility of channeling of low-energy (5 - 20 MeV) relativistic positrons in some ionic crystals with axial symmetry with coaxial symmetry around separate crystal axes of negative ions in some types of crystals, is shown. The annihilation processes of positrons with medium electrons are investigated in details. The lifetime of a positron in the regime of channeling is estimated; the existence of long relaxation lifetime has been shown. 10^{-6} sec which on a $10^{9}-10^{8}$ times is bigger than at usual cases. This means, that we solved the main

problem of creation of nanoundulators, which have very large lifetimes and by which we can control.

Acknowledgments

I am grateful to my co-authors, A.A. Akopyan , A.I. Artemyev, E.A. Ayryan, M.V. Fedorov, A.S. Gevorkyan, C.K. Hu, N.Sh. Izmailyan, R.V. Karapetyan, D.N. Klochkov, G. Kurizki, E.A. Nersesov, M.L. Petrosyan, A.M. Prokhorov, Yu.V. Rostovtsev, M.O. Scully, D.F. Zaretsky for fruitful collaboration.

REFERENCES

INTRODUCTION

1. Madey, John, "Stimulated emission of bremsstrahlung in a periodic magnetic field". J. Appl. Phys. 42, 1906 (1971)
2. P.Emma et al., “First Lasing and Operation of an Ångstrom-Wavelength Free-Electron Laser,” Nature Photonics 4, 641 - 647 (2010)
3. J.Stohr, “The Scientific Revolution Enabled by X-ray Free Electron Lasers,” this conference
4. P. Schmüser, M. Dohlus, J. Rossbach, “Ultraviolet and Soft X-Ray Free-Electron Lasers,” Vol. 229 of Springer Tracts in Modern Physics, 2008
5. W. Ackermann et al., Operation of a free-electron laser from the extreme ultraviolet to the water window,” Nature Photonics 1, 336 - 342 (2007)
6. S. Schreiber, “First Lasing in the Water Window with 4.1nm at FLASH,” proc. FEL’11, Shanghai, 2011
7. H.Tanaka, “The SPring-8 Angstrom Compact Free Electron Laser (SACLA),” this conference
8. M. Altarelli et al. (ed), “The European X-ray Free Electron Laser Technical Design Report,” DESY 2006-091, 2006
9. H. Braun, The future of X-ray FELs, Proceedings of IPAC 2012, New Orlean, Louisianna, USA, FRIAP01.

10. 3. A. I. Artemyev, M. V. Fedorov, J.K. McIver, and E. A. Shapiro, IEEE J. of Q. Electr., v. 34, no. 1, pp.24-31 , 1998
11. 4. V. V. Apollonov, A. I. Artemyev, M. V. Fedorov, E. A. Shapiro, J. K. McIver, " Free-electron laser exploiting a superlattice-like medium" 31 August 1998 / Vol. 3, No. 5 / OPTICS EXPRESS 162
12. 5. A. E. Kaplan and S. Datta," Extreme-ultlaviolet X –ray emission and amplification by nonrelativistic ectron beams traversing a superlattice"' Appl. Phys. Lett., v.44, pp.661-663. 1984
13. 6. A. P. Apanasevich and V. A Yarmolkevich "Resonance transition radiation and its observation in multilayer interference structures", Zh. Tech. Fiz., vol.62, no. 4, pp. l20-l25, 1992; also Sov Phys. Tech. Phys. v. 37. no.4 , pp 423-428, 1992
14. 7.. E. Kaplan, C. T. Law and P. L Shkolnikov, "X-ray narrow line transition radiation source based on low-energy electron beams traversing a multilayer nanostructure", Phys. Rev.E , v. 52, pp. 6795-6808,1995
15. 8. C. J. Pincus, M . A. Piestrup, D . G. Boyers, Q Li, J. L. Harrjs X. K. Maruyama, D. M. Skopik, R . M. Silzer, H . S. CaPlana, nd G. B. Rothbart, "Measuremenots of X-rave mission from photoabsorbtion-edge transition radiation", J. Appl. Phys, v. 72, pp 4300-4307, 1992
16. 9. M. A. Piestrup and P. F. Finman." The prospects of an X- ray free electron laser using stimulated resonance transition radiation" , IEEE J. Quantum Electr. QE-19, pp 357-364, 1983
17. 10. M. A. Piestrup, M. J. Moran, D. J. Boyers, C. L Pincus, J. O. Kephart, R. A. Gearhart, and X. K. Maruyama," Generation of hard X-

rays from transition radiation using high-density foils and moderate energy electrons,Phys.Rev A, v. 43, pp. 2387-2396, I 99I.

18. 11. K. R. Chen and J . M. Dawson, " Amplification mechanism of ion ripple lasers and its possible applications", I EEE Trans. Plasma Sci., v. 21, pp. I5I-155, 1993
19. 12. M.V. Fedorov and E . A. Shapiro "Free-elecrtron lasers based on media with periodically modulated refractive index", Laser Phys., v. 5, pp. 135-139, 1995.
20. 1. S. P. Mickan and X.-C. Zhang, Int. J. High Speed Electron. Syst. **13**, 601 (2003);
21. 2. E. Brundermann, et al.,. Infrared Phys. Technol. **40**, 141 (1999);
22. 3. J. R. Pierce, *Traveling-Wave Tubes* (D. Van Nostrand Company, New York, 1950);
23. 4. A. Dobroiu, et al., Appl. Opt. **43**, 5637 (2004);
24. 5. M. Abo-Bakr, et al., Phys. Lett., **88**, 254801 (2002);
25. 6. G. P. Williams, Rev. Sci. Instrum. **73**, 1461 (2002);
26. 7. G. Ramian, NIM Phys. Res., Sect. A **318**, 225 (1992);
27. 8. N. A. Vinokurov, et al., in *Proceedings of the International FEL Conference, Trieste, 2004*, http://accelconf.web.cern.ch/accelconf/f04/ index.html.;
28. 9. H. Koike, et al., NIM Phys. Res., Sect. A **507**, 242 (2003);
29. 10. Y. U. Jeong, et al., NIM Phys. Res., Sect. A **507**, 125 (2003);
30. 11. A. Doria, et al., Phys. Rev. Lett. **93**, 264801 (2004).
31. 12. S.J. Smith, and F.M. Purcell, Phys. Rev. **92**, p.1069, 1953
32. 13. Yariv, and C.C. Shih, Opt. Comm., **50**, p.223, 1978; J.M. Watchell, J. Appl. Phys., **50**, p.49, 1979; J.M. Watchell, J. Appl. Phys.,

50, p.49, 1979; J.E. Walsh et al., IEEE J. Quant. Electron., **QE-21**, p.920, 1981; F.J. Crowne, et al, Phys. Rev. A, **24**, p.1154, 1981; L. Shrichter, and H. Ron, Rev. A, **40**, p.876, 1988; D.B. Chang, J.C. McDaniel, Phys.Rev.Lett., **63**, p.1066, 1989, A.R. Mkrtchyan, et al., Acustica, **75**, p.184, 1991, A.R. Mkrtchyan, et al., NIM B **145**, p. 67, 1998, NIM B **173**, p. 211, 2001.

33. 14. J. E. Walsh, et al. , Phys. Rev. Lett. **74**, 3808 (1995); K. Ishi, et al., Phys. Rev. E **51**, R5212 (1995); Y. Shibata et al., Phys. Rev. E **57**, 1061 (1998); G. Kube et al., Phys. Rev. E **65**, 056501 (2002); S. E. Korbly, et al., Phys. Rev. Lett. **94**, 054803 (2005); Amit S. et al., Phys. Rev. ST Accel. Beams **9**, 022801 (2006).

34. 15. M. C. Lampel, NIM Phys. Res., Sect. A **385**, 19 (1997); D. C. Nguyen, NIM Phys. Res., Sect. A **393**, 514 (1997); J. E. Walsh et al. , NIM Phys. Res., Sect. A **474**, 10 (2001); A. Doria, et al., NIM Phys. Res., Sect. A **483**, 263 (2002); G. Doucas, M. F. Kimmitt, A. Doria, G. P. Gallerano, E. Giovenale, G. Messina, H. L. Andrews, and J. H. Brownell, Phys. Rev. ST Accel. Beams **5**, 072802 (2002).

35. 16. J. Urata, M. Goldstein, M. F. Kimmitt, A. Naumov, C. Platt, and J. E. Walsh, Phys. Rev. Lett. 80, 516 (1998).

36. 17. Bakhtyari, J. E.Walsh, and J. H. Brownell, Phys. Rev. E 65, 066503 (2002).

37. 18. G. Doucas, M. F. Kimmitt, A. Doria, G. P. Gallerano, E. Giovenale, G. Messina, H. L. Andrews, and J. H. Brownell, Phys. Rev. ST Accel. Beams 5, 072802 (2002), D. V. Karlovets and A. P. Potylitsyn, Phys. Rev. ST Accel. Beams 9, 080701 (2006), M. Wang, P. Liu, G.

Ge, and R. Dong, Optics & Laser Technology 39 (2007) 1254–1257, K.-J. Kim and S.-B. Song, NI M Phys. Res., Sect. A 475, 158 (2001).

38. 19. H. L. Andrews and C. A. Brau, Phys. Rev. ST Accel. Beams 7, 070701 (2004), H. L. Andrews, C. H. Boulware, C. A. Brau, and J. D. Jarvis, Phys. Rev. ST Accel. Beams 8, 050703 (2005), H. L. Andrews, C. H. Boulware, C. A. Brau, J. T. Donohue, J. Gardelle, and J. D. Jarvis, New J. Phys. 8, 289 (2006), V. Kumar and K.-J. Kim, Phys. Rev. E 73, 026501 (2006), J. T. Donohue and J. Gardelle, Phys. Rev. STAccel. Beams 8, 060702 (2005), D. Li, Z. Yang, K. Imasaki, and Gun-Sik Park, Phys. Rev. ST Accel. Beams 9, 040701 (2006), G. F. Mkrtchian, Phys. Rev. ST Accel. Beams 8, 080701 (2007)

39. 1. N.K.Zhevago, *A FEL Based on the Excitation of Local Surface Plasmons,* NIM **A 331,** 581-583, 1993

40. 2. N.K. Zhevago and V.I. Glebov, *On the Origin of High-Optical Emission from Metal Surfaces under Electron Bombardmen*t, Europhys. Lett. 10 (1989) 353,

41. 3. N.K. Zhevago, *Stimulated Radiation and Absorbtion of Light by Local Plasmons Excited by Relativistic Electrons,* Europhys. Lett. 15 (1991) 277.

42. 2. C.A. Brau, Free Electron Lasers, Academic, Boston, 1990

43. 3. M.V. Fedorov, Atomic and Free Electrons in a Strong Light Field, World Scientific, Singapore, 1997.

44. 4. G.~Kurizki, M.O.~Scully, C.~Keitel, Phys.~Rev.~Lett. {\bf 70}, 1433 (1993).

45. 5. B.~Sherman, G.~Kurizki, D.E.~Nikonov, M.O.~Scully, Phys.~Rev.~Lett. {\bf75}, 4602 (1995).

46. 6. D.E.~Nikonov, B.~Scherman, G.~Kurizki, M.O.~Scully, Opt.~Commun. {\bf 123}, 363 (1996).
47. 7. D.E.~Nikonov, M.O.~Scully, G.~Kurizki, Phys.~Rev.~E {\bf 54}, 6780 (1996).
48. 8. D.E.~Nikonov, Yu.V.~Rostovtsev, G.~Sussmann, Phys.~Rev.~E {\bf 57}, 3444 (1998).
49. 9. O.A.~Kocharovskaya and Ya.I.~ Khanin, Pis'ma Zh. Eksp. Teor. Fiz. {\bf 48}, 630(1988); O.A.~Kocharovskaya, Physics Reports, 01/1992; S.E.~Harris, Phys.Rev.Lett. {\bf 62}, 1033(1989); M.O.~Scully, S.-Y..~Zhu, and A. .~Gavrielides, ibid., {\bf 62}, 2813 (1989); A.S.~Zibrov, M.D.~ Lukin, D.E.~Nikonov, L.W.~Hollberg, M.O.~Scully, V.L.~Velichansky, and H.G. .~Robinson, ibid, {\bf 7}5, 1499 (1995), G.G.~Patmabandu, G.R.~Welch, I.N.~Shubin, E.S.~Fry, D.E.~Niconov, M.D.~Lukin, and M.O.~Scully,ibid., {\bf 76}, 2053 (1996).
50. 10. Alexander I. Artemiev, Mikhail V. Fedorov, Yuri V. Rostovtsev, Gershon Kurizki, Marlan O. Scully, PRL {\bf 85}, 4510 (2000).
51. 11. Yu.~Rostovtsev, S.~Trendafilov, A.~Artemyev, K.~Kapale, G.~Kurizki, and M.~O.~Scully, Phys.~Rev.~Lett. {\bf 90}, 214802 (2003).
52. 12. M.V. Kuzelev, A.A. Rukhadze, {\it Plasma Free Electron Lasers}. Edition Frontier, Paris, 1995.
53. 13. D.N.~Klochkov, A.I. Artemyev, G.~Kurizki, Yu.V.~Rostovtsev, M.O.~Scully, Phys. Rev. E {\bf 74}, 036503 (2006)
54. 14. A.I. Artemyev, D.N.~Klochkov, **K. Oganesyan**, Yu.V.~Rostovtsev,M. V. Fedorov, Laser Physics {\bf 17},1213 (2007)

55. 15. **K.B. Oganesyan**, M.L. Petrosyan, M.V. Fedorov, A.I. Artemiev, Y.V. Rostovtsev, M.O. Scully, G. Kurizki, C.K. Hu, Physica Scripta {\bf 140}, 014058 (2010)
56. 16. http://sbfel3.ucsb.edu/www/vl_fel.html, http://wwwhasylab.desy.de/facility/fel/, http://www.vanderbilt.edu/fel/

Chapter 1,2

Strophotron

57. 57. [1] H. Alfren and D. Romell, "A new electron tube: The strophotron,"
58. 58. [2] B. Agdur, in *Crossed-Field Microwave Devices,* vol. 2 New York:Academic, 1961.
59. 59. [3]D. F. Zaretsky and E. A. Nersesov, "Stimulated radiation emission by ultrarelativistic electrons in strong electric and magnetic fields," *Zh. Eksp. Teor.* ***Fiz.,*** vol. 84, pp. 892-902, 1983.
60. 60. [4] Yu. A. Bashmakov, and E. G. Bessonov, "On certain features of particle radiation in natural undulator crystals," Preprint, FIAN 171,
61. [5] M. A. Kumakhov and Kh. G. Trikalinos, "High harmonics of the spontaneous radiation of ultrarelativistic channeled particles," *Zh.* ***Eksp.*** *Teor. Fiz.,* vol. 78, pp. 1623-163.5, 1980.
62. [6] V. A. Bazylev and N. K. Zhevago, "Production of intense electromagnetic radiation by relativistic particles," ***Uspekhi*** *Fiz. Nauk,* vol.

137,605 (1982) [Sov. Phys. Usp. 25, 565 (1982)].

63. [71] V. L. Bratman, N. S. Ginzburg, and M. I. Petelin, “Common properties of free electron lasers,” *Opt. Cornmud.,* vol. 30, pp. 409-412, 1979.

64.. [8] E. ***G.*** Bessonov, “Some aspects of theory of the undulator radiation sources and their possible applications,” in *Proc. 4th Gen. Con$,* York, England, 1978, pp. 471-479.

65. [9] D. F. Alferov, Yu. A. Bashmakov, and E. C. Bessonov, “On the theory of undulator radiation,” *Zh. Techn. Fiz.,* vol. 43, pp. 2126-2132, 1973.

66. [I0] D. F. Zaretsky, E. A. Nersesov, K. B. Oganesyan, and M. V. Fedorov, “Free-electron lasers with transverse gradients,” Kvantovaya Elektron. (Moscow) 13, 685 (1986); [Sov. J. Quantum Electron. 16,448 (1986).

67. [11] L. D. Landau and E. M. Lifshitz, The Classical Theory of Fields. New York: Pergamon, 197.5.

68. [12j E. G. Bessonov, “On the theory of sources of the undulator emission,” Preprint, FIAN 18, Moscow, USSR, pp. 1-30, 1982.

69. [13] I. S. Gradstein and **I.** M. Ryzik, *Tables **of** Integrals, Series and Products*. New York, Academic, 1966.

70. [14] J. M. J. Madey, “Relationship between mean radiated energy, mean squared radiated energy and spontaneous power spectrum in a freeelectron laser,” *Nuovo Cimento,* vol. SOB, pp. 64-88, 1979.

71. [15] C. C. Shin and M. Z. Caponi, “Theory of multicomponent wiggler free-electron lasers in the small-signal regime,” *Phys. Rev.,* vol. A26,

72. [16] E. G. Bessonov, “Free electron lasers,” Preprint, FIAN 229, Moscow, USSR, pp. 1-36, 1983.

73. [17] W. Becker, “Increasing the frequency of a free electron laser by means of a linearly polarized magnetic field,” *Zh. Physik,* vol. B42, pp. 87- 92, 1981

74. 74. . [18] R. Coison, “Energy-loss calculation of gain in a plane sinusoidal freeelectron laser,” *IEEE J. Quantum Electron.,* vol. QE-17, pp. 1409- 1410, 1981.

75. 75. [19] W. B. Colson, “Free-electron lasers operating in higher harmonics,” *Phys. Rev.,* vol. A24, pp. 639-641, 1981.

76. 76. [20] D. F. Zaretsky and E. A. Nersesov, “Multiphoton processes in free electron lasers,” *Zh. Eksp. Eor, Fiz.,* vol. 81, pp. 517-526, 1981.

77. 77. [21] N. Al-Abowi, G. T. Moore, and M. 0. Scully, “Harmonic generation in the free-electron laser. Theory of the quasiperiodic wiggler,”*Phys. Rev.,* vol. A24, pp. 3143-3149, 1981.

78. 78. [22] F. Ciocci, G. Dattoli, and **A.** Renieri, “Comments on the gain calculation of a FEL operating with a linearly polarized wiggler,” *Nuovo Cimento* ***Lett.,*** vol. 34, pp. 341-347, 1982.

79. 79. . [1] Fedorov, M.V. and **Oganesyan, K.B.,** IEEE J. Quant. Electr, vol. **QE-21**, 1059 (1985)

80. [3] M.V. Fedorov, Usp. Fiz. Nauk 135, 213 (1981) ; [Sov. Phys. Usp. 24, 801 (1981).

81. [4] W.H. Louisel, J.F. Lam, D.A. Copeland, W.B. Colson, Exact Classical Electron Dynamic Approch for FEL Amplifier, Phys. Rev. **A 19**, 288, (1979).

82. 1. D. A. G. Deacon, L. R. Elias, J. M. J. Madey, G. J. Ramian, H. A. Schwettman, and T. I. Smith, Phys. Rev. Lett. 38, 892 (1977).

83. 2. M. Billardon, P. Elleaume, J. M. Ortega, C. Bazin, M. Bergher, M. Velghe, Y. Petroff, D. A. G. Deacon, K. E. Robinson, and J. M. J. Madey, Phys. Rev. Lett. 51, 1652 (1983).
84. 3. J. A. Edighoffer, G. R. Neil, C. E. Hess, T. I. Smith, S. W. Fornaca, and H. A. Schwettman, Phys. Rev. Lett. 52, 344 (1984).
85. 4. "D. F. Zaretskii and E. A. Nersesov, Zh. Eksp. Teor. Fiz. 84, 892 (1983) [Sov. Phys. JETP57, 518 (1983)].
86. 5. V. L. Bratman and N. S. Ginzburg, in: *Encyclopedia Physics Dictionary* (ed. by A. M. Prokhorov) [in Russian], Sovet-skaya Entsiklopediya, Moscow (1983), p. 343.
87. 6. E. G. Bessonov, in: Trends in Physics 1978 (Proc. Fourth General Conf. of European Physical Society, York, 1978), Adam Hilger, Bristol (1979), p. 471.
88. 7. V. V. Beloshitskiland M. A. Kumakhov, Zh. Eksp. Teor. Fiz. 74, 1244 (1978) [Sov. Phys. JETP 47, 652 (1978)].
89. 8. V. A. Bazylev and N. K. Zhevago, Usp. Fiz. Nauk **137,**605 (1982) [Sov. Phys. Usp. 25, 565 (1982)].
90. 9. M. V. Fedorov, E. A. Nersesov, and K. B. Oganesyan, Zh. Tekh. Fiz. (in press) [Sov. Phys. Tech. Phys. (in press)].
91. 10. A. S. Davydov, Quantum Mechanics, Pergamon Press, Oxford (1965).
92. 11. 'V.S.Popov and A. M. Perelomov, Zh. Eksp. Teor. Fiz. 56,1375 (1969) [Sov. Phys. JETP 29, 738 (1969)].
93. 12. J. K. McIver and M. V. Fedorov, Zh. Eksp. Teor. Fiz. 76, 1996 (1979) [Sov. Phys. JETP 49, 1012 (1979)].

94. 13. Yu. A. Bashmakov and E. G. Bessonov, Preprint No. 171 [in Russian], Lebedev Physics Institute, Academy of Sciences of the USSR, Moscow (1981).

95. 14. W. Becker, Z. Phys. B 42, 87 (1981).

96. 15. R. Coisson, IEEE J. Quantum Electron. **QE-17,** 1409 (1981).

97. 16. W. B. Coisson, Phys. Rev. A 24, 639 (1981).

98. 17. D. F. Zaretskii and E. A. Nersesov, Zh. Eksp. Teor. Fiz. 81, 517 (1981) [Sov. Phys. JETP 54, 278 (1981)].

99. 18. H. Al-Abawi, G. T. Moore, and M. O. Scully, Phys. Rev. A 24, 3143 (1981).

100. 19. N. S. Ginzburg, Zh. Tekh. Fiz. 51, 764 (1981) [Sov. Phys. Tech. Phys. 26,454(1981)].

101. 20. F. Ciocci, G. Dattoli, and A. Renieri, Lett. Nuovo Cimento 34, 341 (1982).

102. 21. I. S. Gradshteyn and I. M. Ryzhik (eds.), *Table of Integrals, Series and Products,* Academic Press, New York (1965).

Chapter 3

Standing Light Wave

103. 1. 'M. Billardon, P. Elleaume, J. M. Ortega, C. Bazin, M. Bergher, M. Velghe, D. A. G. Deacon, and Y. Petroff, IEEE J. Quantum Electron. QE-21, 805 (1985); C. A. Brau, *ibid.,* p. 284; T. J. Orzechowski, E. T. Scharlemann, B. Anderson, V. K. Neil, W. M. Fawley, D. Prosnitz, S. M. Yarema, D. B. Hopkins, A. C. Paul, A. M. Sessler, and J. S. Wurtele, *ibid.,* p. 831. :

80. 2. 'M. V. Fedorov, Usp. Fiz. Nauk 135, 213 (1981) [Sov. Phys. Usp. 24, 801 (1981)l.

61. 3. M. A. Kumakhov and Kh. G. Trikalinos, Zh. Eksp. Teor. Fiz. 78, 1623 (1980) [Sov. Phys. JETP 51, 815 (1980).

62. 4. V. A. Bazylev and N. K. Zhevago, Usp. Fiz. Nauk 137,605 (1982) [Sov. Phys. Usp.25,565 (198211.

104. 5. V. L. Bratman, N. S. Ginzburg, and M. I. Petelin, Izv. Akad. Nauk SSSR Ser. Fiz . 44, 1593 (1980).

59. 6. D. F. Zaretskii and E. A. Nersesov, Zh. Eksp. Teor. Fiz. 84,892 (1983) [Sov. Phys. JETP 57,518 (1983).

66. 7. D. F. Zaretskii, E. A. Nersesov, K. B. Oganesyan, and **M.** V. Fedorov, Kvantovaya Elektron. (Moscow) 13, 685 (1986) [Sov. J. Quantum Electron. 16,448 (1986) 1.

79. 8. M. V. Fedorov and K. B. Oganesyan, IEEE J. Quantum Electron. QE- 21, 1059 (1985).

105. 9. E. A. Nersesov, K. B. Oganesyan, and M. V. Fedorov, Zh. Tekh. Fiz. 56, 2402 (1986) [Sov. Phys. Tech. Phys. 31, 1437 (1986)l.

106. 10. D. F. Zaretskii and Yu. A. Malov, Zh. Eksp. Teor. Fiz. 91, 1302 (1986) [Sov. Phys. JETP 64,769 (1986)l.

107. 11. M. V. Fedorov, Zh. Eksp. Teor. Fiz. 52, 1434 (1967) [Sov. Phys. JETP 25,952 (1967)l.

108. 12. K. B. Oganesyan, A. M. Prokhorov, and M. V. Fedorov, Preprint No. 276 [in Russian], Institute of General Physics, Academy of Sciences of the USSR, Moscow (1987).

109. 13. L. D. Landau and E. M. Lifshitz, Quantum Mechanics: Non-Relatiuistic Theory, 2nd ed., Pergamon Press, Oxford (1965) .

110. 1. Scholl, C. and Schaa, V., (eds.), *Proceedings of FEL-13*, New York, USA, 2013.

111. 2. Satogata, T., Petit-Jean-Genaz, C., and Schaa, V., (eds.), *Proceedings of NA PAC'13*, Pasadena, LA, USA, 2013.

112. 3. Brau, C.A., *Free-Electron Lasers*, Boston: Academic, 1990.

43. 4. Fedorov, M.V., *Atomic and Free Electrons in a Strong Light Field*, Singapore, World Scientific, 1997.

113. 5. Oganesyan, K.B. and Petrosyan, M.L., YerPHI-475(18) – 81, Yerevan, 1981.

79. 6. Fedorov, M.V. and Oganesyan, K.B., *IEEE J. Quant. Electr*, 1985, vol. QE-21, p. 1059.

66. 7. Zaretskij, D.F., Nersesov, E.A., Oganesyan, K.B., and Fedorov, M.V., *Quantum Electronics*, 1986, vol. 13, p. 685.

105. 8. Nersesov, E.A., Oganesyan, K.B., and Fedorov, M.V., *ZhTF*, 1986, vol. 56, p. 2402.

114. 9. **Oganesyan, K.B**. and Fedorov, M.V., *ZhTF*, 1987, vol. 57, p. 2105.

115. 10. Petrosyan, M.L., Gabrielyan, L.A., Nazaryan, Yu.R., Tovmasyan, G.Kh., and **Oganesyan, K.B**., *Laser Physics*, 2007, vol. 17, p. 1077.

116. 11. Fedorov, M.V., **Oganesyan, K.B**., and Prokhorov, A.M., *Appl. Phys. Lett.*, 1988, vol. 53, p. 353.

117. 12. **Oganesyan, K.B.,** Prokhorov, A.M., and Fedorov, M.V., *ZhETF*, 1988, vol. 94, p. 80.

118. 13. Sarkisyan, E.M., Petrosyan, K.G., Oganesyan, K.B., Saakyan, V.A., Izmailyan, N.Sh., and Hu, C.K., *Laser Physics*, 2008, vol. 18, p. 621.

119. 14. Petrosyan, M.L., Gabrielyan, L.A., Nazaryan, Yu.R., Tovmasyan, G.Kh., and Hovhannisyan, K.B., *J. Contemp. Phys.* (*Armenian Ac. Sci.*), 2007, vol. 42, p. 38.

120. 15. Jerby, E., *NIM*, 1988, vol. A27, p. 457.

67. 16. Landau, L.D. and Lifshits, E.M., *Teoriya polya* (Field Theory), M.: Nauka, 1988.

102. 17. Gradshtein, I.S. and Ryzhik, I.M., *Tablicy integralov, sum i proizvedeniy* (Tables of Integrals, Sums and Products), M.: Fizmat Publishers, 1963.

70. 18. Madey, J.M.J., *Nuovo Cimento*, 1979, vol. 50b, p. 64.

Chapter 4

FELWI

112. 1. C.A. Brau, Free Electron Lasers, Academic, Boston, 1990

43. 2. M.V. Fedorov, Atomic and Free Electrons in a Strong Light Field, World Scientific, Singapore, 1997.

44. 3. G.~Kurizki, M.O.~Scully, C.~Keitel, Phys.~Rev.~Lett. {\bf 70}, 1433 (1993).

45. 4. B.~Sherman, G.~Kurizki, D.E.~Nikonov, M.O.~Scully, Phys.~Rev.~Lett. {\bf75}, 4602 (1995).

46. 5. {Nikonov1}D.E.~Nikonov, B.~Scherman, G.~Kurizki, M.O.~Scully, Opt.~Commun. {\bf 123}, 363 (1996).

47. 6. D.E.~Nikonov, M.O.~Scully, G.~Kurizki, Phys.~Rev.~E {\bf 54}, 6780 (1996).

48. 7. D.E.~Nikonov, Yu.V.~Rostovtsev, G.~Sussmann, Phys.~Rev.~E {\bf 57}, 3444 (1998).

49. 8. O.A.~Kocharovskaya and Ya.I.~ Khanin, Pis'ma Zh. Eksp. Teor. Fiz. {\bf 48}, 630(1988); O.A.~Kocharovskaya, Physics Reports, 01/1992; S.E.~Harris, Phys.Rev.Lett. {\bf 62}, 1033(1989); M.O.~Scully, S.-Y..~Zhu, and A. .~Gavrielides, ibid., {\bf 62}, 2813 (1989); A.S.~Zibrov, M.D.~ Lukin, D.E.~Nikonov, L.W.~Hollberg, M.O.~Scully, V.L.~Velichansky, and H.G. .~Robinson, ibid, {\bf 7}5, 1499 (1995), G.G.~Patmabandu, G.R.~Welch, I.N.~Shubin, E.S.~Fry, D.E.~Niconov, M.D.~Lukin, and M.O.~Scully,ibid., {\bf 76}, 2053 (1996).

50. 9. Alexander I. Artemiev, Mikhail V. Fedorov, Yuri V. Rostovtsev, Gershon Kurizki, Marlan O. Scully, PRL {\bf 85}, 4510 (2000).

51. 10. Yu.~Rostovtsev, S.~Trendafilov, A.~Artemyev, K.~Kapale, G.~Kurizki, and M.~O.~Scully, Phys.~Rev.~Lett. {\bf 90}, 214802 (2003).

52. 11. M.V. Kuzelev, A.A. Rukhadze, {\it Plasma Free Electron Lasers}. Edition Frontier, Paris, 1995.

53. 12. D.N.~Klochkov, A.I. Artemyev, G.~Kurizki, Yu.V.~Rostovtsev, M.O.~Scully, Phys. Rev. E {\bf 74}, 036503 (2006)

54. 13. A.I. Artemyev, D.N.~Klochkov, K. Oganesyan, Yu.V.~Rostovtsev,M. V. Fedorov, Laser Physics {\bf 17},1213 (2007)

55. 14. K.B. Oganesyan, M.L. Petrosyan, M.V. Fedorov, A.I. Artemiev, Y.V. Rostovtsev, M.O. Scully, G. Kurizki, C.K. Hu, Physica Scripta {\bf 140}, 014058 (2010)

56. 15.http://sbfel3.ucsb.edu/www/vl_fel.html, http://wwwhasylab.desy.de/facility/fel/, http://www.vanderbilt.edu/fel/

Chapter 5

Smith-Purcell

121. I. M. Frank, Izv. Akad. Nauk SSSR, Ser. Fiz. {\bf 6}, 3 (1942).

31. {SP}S.J. Smith and E.M. Purcell, Phys. Rev. {\bf 92}, 1069 (1953).

122. G. Doucas, J.H. Mulvey, M. Omori, J. Walsh, M.F. Kimmitt, Phys. Rev. Lett. {\bf 69}, 1761 (1992).

123. K.J. Woods, J.E. Walsh, R.E. Stoner, H.G. Kirk, R.C. Fernow, Phys. Rev. Lett.{\bf 74}, 3808 (1995).

124. K. Ishi, Y. Shibata, T. Takahashi, S. Hasebe, M. Ikezawa, K. Takami, T. Matsuyama, K. Kobayashi, Y. Fujita, Phys. Rev. E. {\bf 51}, R5212 (1995).

125. A.I. Artemiev, M.V. Fedorov, and E.A.Shapiro, Laser Physics, {\bf 4}, no.6, pp.1114-1119 (1994).

126. D.N. Klochkov, A.I. Artemiev, **K.B.Oganesyan**, Y.V.Rostovtsev, C.K. Hu, Induced Smith-Purcell Radiation , J.Modern Optics, {bf 57}, Issue 20, 2060-2068, (2010).

20. S. P. Mickan and X.-C. Zhang, Int. J. High Speed Electron.{\bf 13}, 601 (2003).

35. J. Urata, M. Goldstein, M. F. Kimmitt, A. Naumov, C. Platt, and J. E. Walsh, Phys. Rev. Lett. {\bf 80}, 516 (1998).

127. K.-J. Kim and S.-B. Song, Nucl. Instrum. Methods Phys. Res., Sect. A {\bf 475}, 158 (2001).

128. H. L. Andrews and C. A. Brau, Phys. Rev. ST Accel. Beams {\bf 7},

129. H.L. Andrews, C. H. Boulware, C. A. Brau, and J. D. Jarvis, Phys. Rev. ST Accel. Beams {\bf 8}, 050703 (2005).

130. J. D. Jarvis, H. L. Andrews, and C. A. Brau, Phys. Rev. ST Accel. Beams {\bf 13}, 020701 (2010).

131. H.L. Andrews, C. H. Boulware, C. A. Brau, J. T. Donohue, J. Gardelle, and J. D. Jarvis, New J. Phys. {\bf 8}, 289 (2006).

132. Vinit Kumar and Kwange-Je Kim, Phys. Rev. E {\bf 73}, 026501 (2006).

133. J. T. Donohue, J. Gardelle, Phys. Rev. ST Accel. Beams {\bf 9}, 060701 (2006)

134. G. F. Mkrtchian, Phys. Rev. ST Accel. Beams {\bf 10}, 080701 (2007).

135. Zongjun Shi, Ziqiang Yang, Zheng Liang, Feng Lan, Wenxin Liu, Xi Gao, D. Li. , Nucl. Instrum. Methods Phys. Res., Sect. A {\bf 578}, 543 (2007).

136. D. Li, Z. Yang, K. Imasaki, Gun-Sik Park, Phys. Rev. ST Accel. Beams {\bf 9}, 040701 (2006).

137. L. Schachter and A. Ron, Phys. Rev. A 40, 876 (1989).

138. P. M. Van den berg, Appl. Sci. Res. {\bf 24}, 261 (1971).

139. H.L. Andrews, C.A. Brau, J.D. Jarvis, C.F. Guertin, A. O'Donnell, B. Durant, T.H. Lowell and M. R. Mross, Phys. Rev. ST Accel. Beams {\bf 12}, 080703 (2009).

140. J. Gardelle, L. Courtois, P. Modin and J. T. Donohue, Phys. Rev. ST Accel. Beams {\bf 12}, 110701 (2009).

141. D.N. Klochkov, M.Yu. Pekar, A.A. Rukhadze, Physics of Plasmas {\bf 7}, 4707 (2000)

142. D.N. Klochkov, A.A. Rukhadze, JETP {\bf 93}, 1209, (2001)

Chapter 6

Gamma Radiation Production

143. V. L. Ginzburg, Izv. AN SSSR, Ser. Fiz. \textbf{11} (2) 165 (1947).

144. G. A. Schott, Electromagnetic Radiation and the Mechanical Reactions Arising from It (Cambridge: Univ. Press, 1912)

112. C.A. Brau, Free-Electron Lasers, Acadenmic, Boston, 1990

43. M.V. Fedorov, Atomic and Free Electrons in a Strong Light Field, World Scientific, Singapore, 1997.

145. B.W. Adams, C. Buth, S.M. Cavaletto, J. Evers, Z. Harman, C.H. Keitel, A. Palffy, A. Picon, R. Rohlsberger, Y. Rostovtsev and K. Tamasaku, J. of Modern Optics, \textbf{60} 2-22 (2013).

146. Proceedings of FEL'13, New York, USA, 2013; Proceedings of FEL'14, Basel, Switzerland, 2014.

147. H.H. Braun, Future of X-ray FELs, Proceedings of IPAC 2012, FRAP01, pp. 4180-4184, New Orleans, USA

148. J. A. Davies, J. Friesen and J. D. McIntyre, Can. J. Chem., \textbf{38} 1526 (1960).

149. M. T. Robinson and O. S. Oen, Appl. Phys. Lett., \textbf{2}, 30 (1963).

150. J. Lindhard, Kgl. Dan. Viden. Sels. Mat. - Fys. Medd., \textbf{14}, 34 (1965).

151. M. A. Kumakhov, Phys. Lett. Ser. A., \textbf{57}, 17 (1976).

152. V. V. Beloshitsky and F. F. Komarov, Phys. Rep., \textbf{93}, 117 (1982)

62. V. A. Bazylev and N. K. Zhevago, Sov. Phys. Usp., \textbf{25}, 565 (1982).

153. G. Kurizki, A. Friedman, Phys. Rev. A \textbf{18}, 512, 1988.

154. H.K. Avetissian, A.K. Avetissian, G.F. Mkrtchian, Phys. Rev.Lett., \textbf{113},023904 (2014).

155. K.B. Oganesyan, M.L. Petrossyan, The magnetic fields of hellical wiggler, Yerevan 1981, YERPHI-475(18) - 81, M.V.Fedorov, E.A.Nersesov, K.B.Oganesyan, Potential laser realization on relativistic strophotron-type free-electrons, Zhurnal Tekhnicheskoi Fiziki, {\bf 56}, 2402-2404 (1986); Sov. J. Tech. Phys. {\bf 31}, 1437, (1986), Fedorov M.V., Oganesyan K.B., Classical theory of emission at high harmonics in the relativistic strophotron FEL, IEEE Journal of Quant. Electr. {\bf 21}, 1059-1068 (1985), D.F. Zaretsky, E.A. Nersesov, K.B. Oganesyan, M.V. Fedorov, A laser utilizing free-electrons moving in transverse-gradient fields,

Kvantovaya Elektronika, {\bf 13}, pp.685-692, (1986); Sov. J. Quant. Electr., {\bf 16}, 448, (1986), K.B. Oganesyan, M.V. Fedorov, Non-linear amplification theory in free-electron laser of the relativistic strophotron type, Zhurnal Tekhnichekoi Fiziki, {\bf 57}, 2105-2114, (1987), M.V. Fedorov, K.B. Oganesyan, A.M. Prokhorov, Free-electron laser based on the effect of channeling in an intense standing light-wave, Appl. Phys. Lett., {\bf 53}, 353-354 (1988), K.B. Oganesyan, A.M. Prokhorov, M.V. Fedorov, Transverse channeling and free-electron laser on intense standing wave, Zhurnal Eksperimentalnoi i Teoreticheskoi Fiziki, {\bf 53}, 80-86, (1988); Sov. Phys. JETP {\bf 68}, 1342 (1988), K.B. Oganesyan, Strophotron spontaneous radiation in the FEL with transversaly inhomogeneous %magnetic field in plane wiggler, Journal of Modern Optics, {\bf 61}, Issue 9, 763-765, (2014), K.B. Oganesyan, %The Gain in the Plane Wiggler with Inhomogeneous Magnetic Field, Journal of Modern Optics, {\bf 61}, Issue 17, 1398-1399, (2014)

156. A. S. Gevorkyan, Sov. Phys. Tech. Phys. \textbf{34}, 285 (1989).

157. A.I. Artemiev, M.V. Fedorov, A.S. Gevorkyan, N.Sh. Izmailyan, R.V. Karapetyan, K.B. Oganesyan, A.A. Akopyan, Yu.V. Rostovtsev, M.O. Scully, G. Kurizki, J. Mod. Optics, \textbf{56}, 18, 2148-2157, 2009,

158. Z. Fliigge, Practical Quantum Mechanics, (Springer-Verlag, Berlin, 1971).

159. A. I. Akhiezer and V. B. Berestetskii, Quantum Electrodynamics, (in Russian), Moscow Nauka 1969, 623.

160. P. Gambos, Statistical Theory of the Atom and Its Application; IL: Moscow, 1951; [Russian translation].

161. **K.B. Oganesyan**, Strophotron spontaneous radiation in the FEL with transversaly inhomogeneous magnetic field in plane wiggler, Journal of Modern Optics, **61**, Issue 9, 763-765, (2014),

162. **K.B. Oganesyan**, The Gain in the Plane Wiggler with Inhomogeneous Magnetic Field, Journal of Modern Optics, **61**, Issue 17, 1398-1399, (2014)

163. **К.Б. Оганесян**, О влиянии неоднородности магнитного поля плоского виглера на спектральное распределение спонтанного излучения и на коэффициент усиления, Изв. НАН Армении, Физика т.**50**, n. 2, 169-175 2015.

164. D.N. Klochkov, **K.B. Oganesyan**, Y.V. Rostovtsev, G. Kurizki, Threshold characteristics of free electron lasers without inversion / Laser Physics Letters, **11**, Number 12, 125001, 2014.

165. **K.B. Oganesyan**, FELWI Realization Difficulties, NIM **A 812,** 33 (2016)

166. D.N. Klochkov, A.I. Artemiev, **K.B.Oganesyan**, Y.V.Rostovtsev, M.O.Scully, C.K. Hu, The dispersion equation of the induced Smith–Purcell instability, Physica Scripta T, 2010, v.**140**, (2010) 014049

167. **K.B. Oganesyan**, Smith-Purcell Radiation Amplifier, Laser Physics Lett., **12**, Issue 11, 116002, 2015

168. **K.B. Oganesyan**, E.A. Ayryan, N.Sh. Izmailian, Induced Smith-Purcell radiation: Free electron laser in open system, J. of Modern Optics, **63**, Issue 7, 633, 2015.

169. A.S. Gevorkyan, **K.B. Oganesyan**, Y.V. Rostovtsev, G. Kurizki, Gamma Radiation Production Using Positron Channeling in Ionic Crystals, Laser Physics Letters, June, **12**, 076002, 2015

170. K.B. Oganesyan, Creation of Nanoundulators for Radiation Using Positron Annihilation in Ionic Crystals, J. of Modern Optics, , 62, Issue 11, pp. 933 - 936, 2015

171. Э.А. Нерсесов, **К.Б. Оганесян**, М.В. Федоров, О возможной реализации Лазеров на свободных электронах типа релятивистского строфотрона, ЖТФ, vol. **56**, p. 2105 **1986.**

172. **К.Б. Оганесян,** Каналированные позитроны как источник гамма излучения, Известия НАН Армении, Физика, **т.50**, №4, с.422-427 (2015).

173. **К.Б. Оганесян,** Некоторые особенности реализации Лазеров на свободных электронах без инверсии, Известия НАН Армении, Физика, **т.51**, №1, с.15-19 (2015)

174. D. N. Klochkov, A. I. Artemyev, **K. B. Oganesyan**, Y. V. Rostovtsev, M. O. Scully, Chin-Kun Hu, Generation of induced Smith-Purcell radiation in the absence of resonator, Journal of Physics: Conference Series **236,** (2010), 012022

Appendix

Boundary Condition for Dispersion Equation

Substituting electrical field in the form given by Eq. (5.2.6) into eq. (5.4.59), we find

$$\sum_n \left(E_{nx}^{+} e^{in\chi x + iq_{ny}y} + E_{nx}^{-} e^{in\chi x - iq_{ny}y} + E_{ny}^{+} y'(x) e^{in\chi x + iq_{ny}y} + E_{ny}^{-} y'(x) e^{in\chi x - iq_{ny}y} \right) = 0, \qquad \text{(A1)}$$

We multiply the equation by $exp(-ip\chi x)$, where $p = 0, \pm 1, \pm 2, \pm 3, \ldots$, and then integrate it over coordinate x within the interval (0;d). Introducing the dimensionless coordinate $\xi = \chi x$ we find that

$$\begin{aligned} &\int_0^{2\pi/\chi} y'(x) e^{i(n-p)\chi x \pm iq_{ny} y(x)} dx = \int_0^{2\pi} y'(\xi) e^{i(n-p)\xi \pm iq_{ny} y(\xi)} d\xi \\ &= \frac{1}{\pm iq_{ny}} \int_0^{2\pi} e^{i(n-p)\xi} d\left[e^{\pm iq_{ny} y(\xi)} \right] = \mp \frac{n-p}{q_{ny}} \int_0^{2\pi} e^{i(n-p)\xi \pm iq_{ny} y(\xi)} d\xi = \mp \frac{n-p}{q_{ny}} G_{np}^{+} \end{aligned} \qquad \text{(A2)}$$

Where

$$G_{np}^{\pm} = \int_0^{2\pi} e^{i(n-p)\xi \pm iq_{ny} y(\xi)} d\xi. \qquad \text{(A3)}$$

The latter is obtained assuming that $y(0) = y(2\pi)$, because the function y(x) is periodic. Substituting the relations $E_{nx}^{\pm} = \pm iq_{ny} P_n^{\pm}$ and $E_{ny}^{\pm} = \pm iq_{nx} P_n^{\pm}$ in the Eq.~\eqref{a:1} we can write

$$\sum_n \left(q_{ny} + (n-p)\chi \frac{q_{nx}}{q_{ny}} \right) \left(G_{np}^{+} P_n^{+} - G_{np}^{-} P_n^{-} \right) = 0. \qquad \text{(A4)}$$

Taking into account the relations (5.2.23) following from the beam model, we get

$$\sum_n \left(q_{ny} + (n-p)\chi \frac{q_{nx}}{q_{ny}} \right) \left(G_{np}^{+} \left[1 + K(n) \right] - G_{np}^{-} K(n) e^{2iq_{ny}b} \right) P_n = 0, \tag{A5}$$

which is Eq. (5.4.60).

For the surface described by Eq. (5.3.25), we find that

$$\begin{aligned} G_{np}^{\pm} &= \int_0^{2\pi} e^{i(n-p)\xi \pm iq_{ny}h\sin(\xi)} d\xi = 2\pi(-1)^{n-p} \frac{1}{2\pi} \int_{-\pi}^{\pi} e^{i[(n-p)t \pm iq_{ny}h\sin(t)]} dt \\ &= 2\pi(-1)^{n-p} J_{p-n}\left(\mp q_{ny}h \right) = 2\pi J_{n-p}\left(\mp q_{ny}h \right) \end{aligned} \tag{A6}$$

where $J_n(x)$ are the Bessel functions.